CHAPTER THIRTY ONE

# ACTINIDES IN ANIMALS AND MAN

Patricia W. Durbin



## 31.1 INTRODUCTION

Protection of workers and the public has been the main objective of actinide biology research since its beginning in early 1942. It was recognized even before the fission chain reaction was demonstrated that nearly all of the isotopes of the newly created elements heavier than radium would be radioactive and emit alpha particles, and that, if taken into the body, they would be as damaging in the tissues as radium (Stone, 1951). Biological research with the actinides concentrated on quantifying their uptake and retention in tissues after introduction into the body by ingestion, inhalation, or injection (biokinetics, metabolism); identifying the nature of the radiation and/or chemical damage in the tissues with the greatest initial uptake, concentration, and longest retention; defining the radiation dose-dependent relationships between toxicity and actinide intake to blood.

Actinide biokinetics studies now include many species and the actinide sequence from $^{227}Ac^{3+}$ to $^{253}Es^{3+}$. Whole-body retention of several actinides has been measured in long-lived animals, in some cases for life span. Microscopic localization of actinides in the tissues has been investigated autoradiographically. Significant advances in the methods of aerosol preparation and inhalation exposure allowed quantification of deposition and retention of inhaled actinide particles in the lungs. Most of the biological investigations of internally

deposited actinides were undertaken to define their dose-dependent chronic radiotoxicity, which is manifested mainly as functional impairment and/or cancer induction in bone, liver, kidneys, and lung (when actinide aerosols are inhaled). Many of the actinide biology studies have been summarized (Zirkle, 1947; Voegtlin and Hodge, 1949, 1953; Thompson, 1962, 1989; Stover and Jee, 1972; Thompson and Bair, 1972; Hodge *et al.*, 1973; Nenot and Stather, 1979; Stannard, 1988; Lloyd *et al.*, 1993, 1994). As they became available, the data generated by those investigations were used to set and refine protection limits for actinide intakes into the body, both for workers and the public (Chalk River, 1949; NBS, 1953; ICRP, 1959, 1979, 1980, 1986, 1993, 1995). An introduction to the actinide biology literature is provided as an Appendix.

The biokinetic and toxicological data have generally been considered sufficient for radiation protection purposes, and with the exception of uranyl ion, less attention was given to understanding the chemical reactions of the actinides in the special chemical environments of the blood, tissue fluid, and tissues of the mammalian body.

Some of the aspects of actinide chemistry relevant to their uptake, distribution, and retention in the tissues of mammals have been reviewed (Durbin, 1962, 1975; Gindler, 1973; Taylor, 1973a,b; Bulman, 1978, 1980; Raymond and Smith, 1981; Duffield and Taylor, 1986; Katz *et al.*, 1986).

The chemical reactions of actinide ions in warm (37°C), nearly neutral (pH 7.4), dilute saline fluids of the mammalian body are dominated by hydrolysis and complexation (ICRP, 1972, 1986; Durbin, 1975; Duffield and Taylor, 1986; Taylor, 1998). After intake of an actinide in solution into the blood, ligand competition and exchange, in some cases facilitated by changes in local pH, determine its distribution among the tissues, presumably favoring those tissues or structural elements that contain or display the most stably binding bioligands on their surfaces.

## 31.2 INITIAL DISTRIBUTION OF ACTINIDES IN MAMMALIAN TISSUES

Access of foreign metal ions, in this case actinides, is most likely to occur by absorption from inhaled particles deposited in the lungs and from ingested food and water. Less likely modes of intake are through a contaminated wound or the broken skin. Once solubilized and transported into the blood, deposition in tissues and excretion of the absorbed actinides are essentially independent of the route of entry, for example, tissue deposition is equivalent for injected, inhaled, or ingested $^{239}Pu^{4+}$ citrate (Ballou *et al.*, 1972) and for a wide variety of uranium compounds (Voegtlin and Hodge, 1949, 1953; Tannenbaum, 1951b; Durbin and Wrenn, 1975). Parenteral injection (intravenous, iv; intraperitoneal, ip; intramuscular, im; subcutaneous, sc) has been a useful tool for investigating the chemically related factors that determine the disposition of actinides in the animal body. By placing solutions of actinide salts or complexes directly into the

blood or tissue fluid the experimental variables introduced by the efficient lung and gastrointestinal (GI) tract barriers are avoided. Comparable studies of the same actinide in several animal species help to differentiate between the chemical factors that are common across species and the biological factors that are species- or age-specific.

The initial distribution and excretion of soluble forms of the first ten actinides (Th through Es) plus Ac have been defined, in some cases in several animal species. Those basic biological data are collected in Tables 31.1–31.6; seven trivalent actinides including $Pu^{3+}$ (rats, Table 31.1); five actinides injected in oxidation states greater than trivalent (rats, Table 31.2); actinide ions representing the four major oxidation states (mature female mice, Table 31.3); seven actinides considered to be long-term health hazards or with special radiological characteristics (young adult beagle dogs, Table 31.4); actinides in four major

**Table 31.1** *Initial distribution of injected trivalent actinides in rats.*[a]

| | | | *Fractions of absorbed actinide (%)*[b] | | | | |
|---|---|---|---|---|---|---|---|
| | | | *Tissues* | | | *Excreta* | |
| *Nuclide* | *Mass injected* ($\mu g\ kg^{-1}$) | *Time* (days) | *Skeleton* | *Liver* | *Other tissues*[c] | *Urine* | *Feces and GI tract* |
| $^{227}Ac^{3+}$[d] | 0.019 | 4 | 27 | 56 | 4 | 5 | 8 |
| $^{239}Pu^{3+}$[e] | 67 | 4 | 51 | 23 | 9 | 1 | 17 |
| $^{241}Am^{3+}$[f] | 0.12 | 4 | 35 | 42 | 3 | 10 | 10 |
| $^{242}Cm^{3+}$[g] | $1.6 \times 10^{-3}$ | 4 | 31 | 36 | 8 | 1 | 24 |
| $^{249}Bk^{3+}$[h] | $4 \times 10^{-3}$ | 5 | 54 | 16 | 9 | 15 | 6 |
| $^{249,252}Cf^{3+}$[i] | 0.02 | 4 | 64 | 14 | 4 | 7 | 11 |
| $^{253}Es^{3+}$[j] | $2.2 \times 10^{-3}$ | 7 | 69 | 7 | 2 | 11 | 11 |

[a] Investigators in the different laboratories used several strains of Wistar-derived albino rats. Ages at the time of injection were rarely stated; however, the reported body weights indicate a range of age from 60 to 150 days. For some incompletely reported studies, sex and body weight and/or age were obtained from archived data. Rats of both sexes are sexually mature at about 60 days, but this species does not achieve skeletal maturity. Because active growth centers remain at the ends of some long bones and vertebrae after 150 days of age, the skeletons of the rats used in these studies must be considered to be still growing (Simpson *et al.*, 1950).

[b] Data are normalized to 100% absorption and 100% material recovery; discrepancies are due to rounding.

[c] Includes kidneys, range 0.6 to 2.2%; $^{249}Bk$ and $^{253}Es$ studies also include full GI tract.

[d] Hamilton (1956); 180 g females; im injection of $^{227}Ac^{3+}$ in 0.1 M Na citrate (73% absorbed).

[e] Carritt *et al.* (1947); 225 g young males; iv injection of $^{239}Pu^{3+}$ in 0.14 M NaCl.

[f] Durbin *et al.* (1969); Durbin (1973); 240 g, 110-day-old females; im injection of $^{241}Am^{3+}$ in 0.1 M Na citrate (99% absorbed).

[g] Scott *et al.* (1949b); 190 g females; im injection of $^{242}Cm^{3+}$ in 0.14 M NaCl, pH 5 (92% absorbed).

[h] Hungate and Baxter (1972); 400 g males; iv injection of $^{249}Bk^{3+}$ in 0.01 M HCl.

[i] Durbin (1973); 250 g, 130-day-old females; im injection of $^{249,252}Cf^{3+}$ in 0.1 M Na citrate (98% absorbed).

[j] Smith (1972); 300 g females; iv injection of $^{253}Es^{3+}$ in $HNO_3$, pH 2.

**Table 31.2** *Initial distribution of injected tetravalent, pentavalent, and hexavalent actinides in rats.*[a]

| | | | *Fraction of absorbed actinide (%)*[b] | | | | | |
|---|---|---|---|---|---|---|---|---|
| | | | *Tissues* | | | | *Excreta* | |
| *Nuclide* | *Mass injected* ($\mu g\ kg^{-1}$) | *Time* (days) | *Skeleton* | *Liver* | *Kidneys* | *Other tissues* | *Urine* | *Feces and GI tract* |
| $^{227}Th^{4+}$[c] | $2 \times 10^{-4}$ | 8 | 66 | 4 | 3 | 10 | 9 | 7 |
| $^{233}Pa^{5+}$[d] | $5 \times 10^{-3}$ | 4 | 46 | 8 | 4 | 18 | 9 | 16 |
| $^{239}Np^{4+}$[e] | $3 \times 10^{-6}$ | 4 | 56 | 4 | 1 | 1 | 24 | 14 |
| $^{237,238}Pu^{4+}$[f] | 0.04 | 3 | 64 | 17 | 1 | 8 | 3 | 7 |
| $^{239}Pu^{4+}$[g] | 0.14 | 6 | 69 | 8 | 1 | 10 | 2 | 9 |
| $^{239}Pu^{4+}$[g] | 67 | 4 | 67 | 10 | 2 | 8 | 1 | 11 |
| $^{237}NpO_2^{+}$[h] | 360 | 3 | 45 | 5 | 3 | 6 | 36 | 5 |
| $^{230}UO_2^{2+}$[i] | $3 \times 10^{-5}$ | 4 | 11 | 0.2 | 12 | 0.9 | 76 | – |
| $^{233}UO_2^{2+}$[j] | 200 | 4 | 21 | 0.2 | 20 | 2 | 56 | – |
| $^{238}PuO_2^{2+}$[k] | 0.04 | 15 | 64 | 7 | 1 | 4 | 5 | 19 |
| $^{239}PuO_2^{2+}$[l] | 67 | 4 | 66 | 10 | 2 | 8 | 8 | 6 |

[a] Investigators in the different laboratories used several strains of Wistar-derived albino rats. Ages at the time of injection were rarely stated; however, the reported body weights indicate a range of age from 60 to 150 days. For some incompletely reported studies, sex and body weight and/or age were obtained from archived data. Rats of both sexes are sexually mature at about 60 days, but this species does not achieve skeletal maturity. Because active growth centers remain at the ends of some long bones and vertebrae after 150 days of age, the skeletons of the rats used in these studies must be considered to be still growing (Simpson *et al.*, 1950).

[b] Data are normalized to 100% absorption and 100% material recovery; discrepancies are due to rounding.

[c] Hamilton (1953); 215 g females; im injection of $^{227}Th^{4+}$ in 0.05 M Na citrate (94% absorbed).

[d] Hamilton (1948a); 190 g females; im injection of $^{233}Pa^{5+}$ in 0.14 M NaCl, pH 1.9 (42% absorbed).

[e] Lanz *et al.* (1946); 270 g males; im injection of $^{239}Np^{4+}$ in 0.14 M NaCl, pH 2.6 (64% absorbed).

[f] Talbot *et al.* (1990); 300 g, 140-day-old males; iv injection of $^{237}Pu^{4+}$ plus 30 Bq of other alpha-emitting Pu isotopes, 'impure $^{237}Pu$', in citrate buffer.

[g] Carritt *et al.* (1947); 225 g, young males; iv injection of $^{239}Pu^{4+}$ in citrate buffer.

[h] Morin *et al.* (1973); 275 g, sex not specified; im injection of $^{237}NpO_2^{+}$ in $HNO_3$, pH 1.5 (43% absorbed).

[i] Hamilton (1948b); 190 g females; im injection of $^{230}UO_2^{2+}$ in 0.14 M NaCl (94% absorbed).

[j] Hamilton (1947a); 180 g males; im injection of $^{233}UO_2^{2+}$ in 0.14 M NaCl (97% absorbed).

[k] J. G. Hamilton (unpublished data); 200 g females; im injection of $^{238}PuO_2^{2+}$ in 0.1 M Na citrate and 0.01 M Na bromate (71% absorbed).

[l] Carritt *et al.* (1947); 225 g, young males; iv injection of $^{239}PuO_2^{2+}$ in dilute $HNO_3$.

oxidation states (mature Macaque monkeys, Table 31.5; mature Kenya baboons, Table 31.6); isotopes of industrially important $Pu^{4+}$ and $UO_2^{2+}$ and results from a $^{241}Am^{3+}$ accident case (adult human males, Table 31.7).

The data sets selected for inclusion in Tables 31.1–31.7 met the following criteria: The actinide studied was injected as an ultrafilterable citrate complex or a chloride or nitrate solution sufficiently acidic to avoid hydrolysis and colloid

**Table 31.3** *Initial distribution of intravenously injected actinides in mice.*[a]

| | | *Fraction of injected actinide at 1 day (%)*[b] | | | | | |
|---|---|---|---|---|---|---|---|
| | | *Tissues* | | | | *Excreta* | |
| *Nuclide* | *Mass injected* ($\mu g\ kg^{-1}$) | *Skeleton* | *Liver* | *Kidneys* | *Other tissues* | *Urine* | *Feces and GI tract* |
| $^{241}Am^{3+}$[c] | 0.23 | 27 | 50 | 1 | 6 | 14 | 3 |
| $^{238}Pu^{4+}$[c] | 0.09 | 31 | 50 | 2 | 8 | 4 | 5 |
| $^{237}NpO_2^+$[d] | 200 | 37 | 14 | 2 | 6 | 39 | 2 |
| $^{232,234,235}UO_2^{2+}$[e] | 100 | 17 | 1 | 19 | 3 | 58 | 2 |

[a] Sexually and skeletally mature female Swiss-Webster mice 90 to 160 days old (35 g body weight) (Durbin *et al.*, 1992).
[b] Data are normalized to 100% material recovery; discrepancies are due to rounding.
[c] Durbin *et al.* (1994); $^{241}Am^{3+}$ or $^{238}Pu^{4+}$ in 0.008 M Na citrate and 0.14 M NaCl, pH 3.5.
[d] Durbin *et al.* (1994); $^{237}NpO_2^+$ in 0.14 M NaCl, pH 3.5.
[e] Durbin *et al.* (1994); $^{232}UO_2^{2+}$ plus $^{234,235}UO_2^{2+}$ in 0.14 M NaCl, pH 3.5.

**Table 31.4** *Initial distribution of intravenously injected actinides in beagle dogs.*[a]

| | | | *Fraction of injected actinide (%)*[b] | | | | | |
|---|---|---|---|---|---|---|---|---|
| | | | *Tissues* | | | | *Excreta* | |
| *Nuclide* | *Mass injected* ($\mu g\ kg^{-1}$) | *Time* (days) | *Skeleton* | *Liver* | *Kidneys* | *Other tissues* | *Urine* | *Feces* |
| $^{241}Am^{3+}$[c] | 0.54 | 1–21 | 31 | 52 | 0.7 | 5 | 10 | 1 |
| $^{243,244}Cm^{3+}$[d] | 0.042 | 6–20 | 44 | 38 | 0.7 | 6 | 8 | 4 |
| $^{249}Cf^{3+}$, $^{252}Cf^{3+}$[e] | 0.0005–0.7 | 1–21 | 49 | 18 | 1 | 10 | 16 | 7 |
| $^{253}Es^{3+}$[f] | $10^{-4}$ | 21 | 54 | 12 | 0.6 | 7 | 19 | 7 |
| $^{228}Th^{4+}$[g] | $3 \times 10^{-3}$ | 1–23 | 66 | 4 | 3 | 15 | 10 | 2 |
| $^{239}Pu^{4+}$[h] | 2.2 | 1–22 | 51 | 34 | 0.5 | 2 | 5 | 8 |
| $^{233}UO_2^{2+}$[i] | 300 | 7 | 8 | 1 | 7 | 2 | 83 | ~0 |

[a] Beagle dogs were bred and raised in the University of Utah colony (Rehfield *et al.*, 1972; Stover and Stover, 1972). Both sexes, 15 to 18 months old (mean body weight 10 kg), were sexually mature at the time of injection. Skeletal growth centers were united except in the ribs, but bone remodeling was still active in the spongy (trabecular) bone sites at the ends of some long bones and in the ribs and vertebrae (Dougherty, 1962).
[b] All actinides were injected iv in 0.08 M Na citrate buffer, pH 3.5; data are normalized to 100% material recovery.
[c] Lloyd *et al.* (1970); average dosage shown for dogs given 0.26 to 0.81 $\mu g\ kg^{-1}$.
[d] Lloyd *et al.* (1974).
[e] Lloyd *et al.* (1972a, 1976); Atherton *et al.* (1972); injected either $^{249}Cf^{3+}$ or $^{252}Cf^{3+}$.
[f] Lloyd *et al.* (1975).
[g] Stover *et al.* (1960), Lloyd *et al.* (1984a).
[h] Stover *et al.* (1959, 1972); average dosage shown for dogs given 0.25 to 4.85 $\mu g\ kg^{-1}$.
[i] Stevens *et al.* (1980).

**Table 31.5** *Initial distribution of injected actinides in Macaque monkeys.*[a]

| | | | *Fractions of absorbed actinide (%)*[b] | | | | | |
|---|---|---|---|---|---|---|---|---|
| | | | *Tissues* | | | | *Excreta* | |
| *Nuclide* | *Mass injected* ($\mu g\ kg^{-1}$) | *Time* (days) | *Skeleton* | *Liver* | *Kidneys* | *Other tissues* | *Urine* | *Feces and GI tract* |
| $^{241}Am^{3+}$[c] | 0.12 | 8 | 25 | 56 | 0.6 | 7 | 9 | 2 |
| $^{238}Pu^{4+}$[d] | 0.04 | 8 | 28 | 61 | 0.6 | 5 | 3 | 2 |
| $^{237}NpO_2^+$[e] | 42 | 4 | 42 | 10 | 1 | 3 | 43 | 0.5 |
| $^{233}UO_2^{2+}$[f] | 18 | 3 | 3 | 0.5 | 9 | 2 | 84 | 1 |

[a] Macaque monkeys (*Macaca mulatta*, *Macaca fasicularis*) were caught in the wild. Both sexes were used (about 80% were females), and injected at 5 to 15 years of age (2.5–11 kg body weight). They were sexually and skeletally mature; skeletal maturity was verified roentgenographically (Van Wagenen and Asling, 1958).
[b] Data are normalized to 100% absorption and 100% material recovery; discrepancies are due to rounding.
[c] Durbin (1973); im injection of $^{241}Am^{3+}$ in 0.08 M Na citrate buffer, pH 3.5 (98% absorbed); average dosage shown for monkeys given 0.03 to 0.17 $\mu g\ kg^{-1}$.
[d] Durbin *et al.* (1985); iv or im injection of $^{238}Pu^{4+}$ in 0.08 M Na citrate buffer, pH 3.5 (91% absorbed); average dosage shown for monkeys given 0.017 to 0.112 $\mu g\ kg^{-1}$.
[e] Durbin *et al.* (1987); im injection of $^{237}Np$ in 0.08 M Na citrate buffer, pH 3.5, probably a mixture of $NpO_2^+$ and $Np^{4+}$ (99% absorbed).
[f] P. W. Durbin and N. Jeung unpublished data; im injection of $^{233}UO_2^{2+}$ in 0.14 M NaCl (100% absorbed).

formation in the medium; values were reported for the actinide content of all soft tissues, the whole skeleton, and the separated urine and feces; the fraction retained at the wound site was reported for im injection studies.

The skeleton is a major deposition site for the actinides in all of the oxidation states that have been administered to animals. Liver is the most important soft tissue deposition site for all of the actinides except $UO_2^{2+}$. Shortly after intake to blood, the skeleton and liver (skeleton and kidneys in the case of $UO_2^{2+}$) account for about 90% of the actinide in the body (Tables 31.1–31.6; ICRP, 1972). It is clear that both bone and liver possess appropriate binding sites and ligands with high affinities for actinide ions, but the partitioning of the individual actinides between deposition in bone and liver varies with their chemical properties, most importantly electronic charge and ionic radius.

The initial partitioning of an actinide between deposition in bone and liver is likely to depend primarily on the relative affinities of the ligands on the anatomical surfaces of bone and on liver cell membranes for binding that actinide in competition with the ligands that transport it in the blood. The outcome of those competitions will be modulated by the relative abundances of ligands (binding sites) on the bone surfaces and hepatic cell membranes that are exposed

**Table 31.6** *Initial distribution of injected actinides in Kenya baboons.*[a]

| | | | *Fraction of injected actinide (%)*[b] | | | | | |
|---|---|---|---|---|---|---|---|---|
| | | | *Tissues* | | | | *Excreta* | |
| *Nuclide* | *Mass injected* ($\mu g\ kg^{-1}$) | *Time* (days) | *Skeleton* | *Liver* | *Kidneys* | *Other tissues* | *Urine* | *Feces and GI tract* |
| $^{241}Am^{3+}$[c] | 0.06 | 1 | 35 | 31 | 0.7 | 22 | 10 | 1 |
| $^{243,244}Cm^{3+}$[d] | $3 \times 10^{-3}$ | 16 | 43 | 26 | – | 12[e] | 17 | 3 |
| $^{239}NpO_2^{2+}$[f] | $4 \times 10^{-4}$ | 1 | 54 | 3 | 0.5 | 2 | 40 | ~0 |
| $^{237}UO_2^{2+}$[g] | $2 \times 10^{-6}$ | 4 | ~6 | 0.5 | 5 | 1 | 87 | 0.1 |

[a] Female Kenya baboons (*Papio anubis*, *Papio cynocephalus*) were caught in the wild. They were injected when 7 to 16 years old (12–15 kg body weight) and were sexually and skeletally mature. Skeletal maturity and ages were estimated from data on molar tooth eruption and wear, estrus cycles, and body weight (Guilmette *et al.*, 1980).
[b] Data are normalized to 100% absorption and 100% material recovery; discrepancies are due to rounding.
[c] Guilmette *et al.* (1980); iv injection of $^{241}Am^{3+}$ in 0.08 M Na citrate, pH 3.5.
[d] Lo Sasso *et al.* (1981); iv injection of $^{243,244}Cm^{3+}$ in 0.08 M Na citrate buffer, pH 3.5.
[e] Includes kidneys.
[f] Ralston *et al.* (1986); iv injection of $^{239}NpO_2^{2+}$ in 0.01 M $NaHCO_3$.
[g] Lipsztein (1981); iv injection of $^{237}UO_2^{2+}$ in $HNO_3$, pH 1.6.

to the circulating fluids, the relative rates of blood flow through those tissues, and the concentrations of the transport ligands.

### 31.2.1 Trivalent actinides

The initial distributions of $Am^{3+}$ in the tissues of the six mammals (Tables 31.1–31.7) agree well with one another, as do the overall distributions of $Cm^{3+}$ in the rats, dogs, and baboons (Tables 31.1, 31.4, and 31.6), and those of $Cf^{3+}$ and $Es^{3+}$ in the rats and dogs (Tables 31.1 and 31.4). Bone and liver are the major initial deposition sites. The larger animals (dog, baboon) retained more $Am^{3+}$, $Cm^{3+}$, $Cf^{3+}$, and $Es^{3+}$ in the bulk soft tissues, mainly muscle and pelt, than did the rats and mice. Renal excretion of the trivalent actinides is limited. It tended to be somewhat greater for the heavier than for the lighter members of the series, and to be greater for the dogs, who were given iv injections of actinide solutions containing large excesses of citrate buffer. Impeded filtration through the kidneys into urine indicates that uptake of the trivalent actinides in the target tissues is rapid and/or that the major fraction of circulating actinide is bound to nonfilterable protein.

In both the rats (Table 31.1) and the dogs (Table 31.4), and similarly to the behavior of the lanthanides, the initial skeletal deposition of the trivalent actinides increases and the partitioning between deposition in bone and liver

**Table 31.7** *Initial distribution of absorbed actinides in adult men.*

| | | | *Fraction of absorbed actinide (%)* | | | | | |
|---|---|---|---|---|---|---|---|---|
| | | | *Tissues* | | | | *Excreta* | |
| *Nuclide* | *Mass* ($\mu g\ kg^{-1}$) | *Time* (days) | *Skeleton* | *Liver* | *Kidneys* | *Other tissues* | *Urine* | *Feces* |
| $^{241}Am^{3+a}$ | ~0.04 | 4 | ~31 | ~69 | – | – | – | – |
| $^{237}Pu^{4+b}$ | $4 \times 10^{-8}$ | ~20 | ~32 | ~59 | – | ~6[c] | 2 | 2 |
| $^{234,235,238}U^{4+d}$ | 700 | 21 | 12 | 11 | 1 | 8 | 68 | – |
| $^{234,235,238}UO_2^{2+d}$ | 105 | 18 | 14 | 1 | 7 | 6 | 72 | – |

[a] Robinson *et al.* (1983); 64-year-old man; accidental high-level skin burns and abrasions contaminated with ~3 mCi of $^{241}Am$ in hot 7 M $HNO_3$; 10 μCi absorbed and retained as estimated from external photon measurements.
[b] Talbot *et al.* (1993); two male volunteers, average age 66 years, average body weight 73 kg; iv injection of $^{237}Pu^{4+}$ in 0.03 M Na citrate; tissue distribution estimated from collected excreta and external photon measurements.
[c] Includes kidneys.
[d] Original data of Bernard and Struxness (1957) normalized to 100% material recovery; bedridden terminally ill adult males with inoperable brain tumors; tissue distributions estimated from autopsy specimens. Case 6, iv injection of $UO_2(NO_3)_2$ enriched with $^{234,235}UO_2^{2+}$, age 60 years, body weight 57 kg. Case 8, iv injection of $UCl_4$ enriched with $^{234,235}U^{4+}$in in 0.2 M acetate buffer, pH 4.7, age 56 years, body weight 63 kg; most of the U detected in 'other tissues' was in the spleen (6.7%).

shifts from favoring liver to favoring bone with the decrease in ionic radius ($r$) that accompanies the addition of f-shell electrons (Durbin, 1962, 1973). Within each series, that is also the trend of increasing stability of complexes.

Within the lanthanide and actinide series, the stabilities of complexes with the same ligand increase with decreasing ionic radius (Cotton and Wilkinson, 1980), as illustrated for the actinide oxalate and citrate complexes in Table 31.8. It is reasonable to expect that the stabilities of their complexes with other biologically important ligands such as phosphate, for which stability constants are unavailable, will exhibit a similar trend. For the same ligand, complexes of the trivalent actinides tend to be more stable than those of their lanthanide analogs with the same ionic radii. For example, the EDTA complexes of the trivalent actinides are, on average, one to two orders of magnitude greater than those of the EDTA complexes with lanthanides of the same ionic radii (Sillen and Martell, 1964; Ahrland, 1986; Hulet, 1986).

For the purposes of this discussion, initial skeletal deposition is expressed as the skeletal fraction of the initial body burden ($BB_{0,\%}$ of injected amount), where $BB_0$=skeleton + soft tissue + $liver_{max}$=100% – $\Sigma$ (urine). Skeleton, soft tissue, and urine are the measured amounts of actinide in those specimens (Table 31.1), and $liver_{max}$ is the sum of the measured amounts of actinide in the liver, GI tract plus contents, and passed feces. Biliary excretion of liver actinide into the GI tract and feces will be discussed in the context of actinides in

**Table 31.8** *Ionic radii and stabilities of complexes of some actinides with the low molecular weight ligands in mammalian plasma and tissues.*

| | | *Stability constant* ($\log \beta_1$)[a] | | | | | |
|---|---|---|---|---|---|---|---|
| | *Ion radius* (nm)[b] | $OH^-$ | $CO_3^{2-}$ | $HPO_4^{2-}$ | *Acetate*[c] | *Oxalate* | *Citrate* |
| Trivalent actinides (CN6) | | | | | | | |
| $Ac^{3+}$[d] | 0.112 | (4.7) | (5.6) | | – | (4.7) | (7.6) |
| $Pu^{3+}$ | 0.100 | 6.7[e] | – | | 2.0[f] | 7.3[g] | 8.7[g] |
| $Am^{3+}$ | 0.098 | 7.9[e] | 5.8[e] | | 2.0[f] | 4.8[f] | 7.1[g] |
| $Cm^{3+}$ | 0.097 | 7.9[e] | – | | 2.1[f] | 4.8[f] | 7.7[h] |
| $Bk^{3+}$ | 0.096 | 8.2[e] | – | | 2.1[f] | 5.4[h] | 7.9[h] |
| $Cf^{3+}$ | 0.095 | 8.2[e] | – | | 2.1[f] | 5.5[h] | 7.9[h] |
| $Es^{3+}$ | 0.094 | 8.9[j] | – | | – | – | 11[i] |
| Tetravalent actinides (CN8) | | | | | | | |
| $Th^{4+}$ | 0.105 | 9.6[e] | – | 11[g] | 3.9[f] | 11[g] | 13[g] |
| $U^{4+}$ | 0.100 | 12[e] | | 12[g] | | 12[g] | |
| $Np^{4+}$ | 0.098 | 12[e] | – | 12[j] | – | 11[g] | 15[g] |
| $Pu^{4+}$ | 0.096 | 12[e] | – | 13[g] | 4.9[g] | 11[g] | 15[g] |
| Pentavalent actinides (CN8) | | | | | | | |
| $Pa^{5+}$ | 0.091 | 15 | | | | | |
| Actinide dioxo cations (CN6) | | | | | | | |
| $NpO_2^+$ | 0.075 | 4.2[k] | 4.5[l] | 3.0[l] | 1.9[g] | 3.7[f] | 3.7[g] |
| $UO_2^{2+}$ | 0.073 | 8.0[e] | 9.3[m] | 7.2[m] | 2.4[f] | 6.4[h] | 7.4[h] |
| $NpO_2^{2+}$ | 0.072 | 8.6[e] | | | 2.3[h] | 7.2[h] | |
| $PuO_2^{2-}$ | 0.071 | 7.8[e] | – | 8.2[g] | 2.3[f] | 9.4[h] | – |

[a] Where available, values used were determined at or corrected to 25°C, ionic strength 0.1 to match 0.14 M NaCl in mammalian body fluids; reported values rounded to two significant figures.
[b] Shannon (1976); Katz *et al* (1986).
[c] Acetate is included as a representative monocarboxylic acid.
[d] Stability constants of $La^{3+}$ complexes shown in parentheses are from Smith and Martell (1976, 1989) and Martell and Smith (1977). $Ac^{3+}$ complexes are expected to be somewhat less stable. Log $\beta$, for $HPO_4^{2-}$ complex from Kirby (1986a).
[e] Smith and Martell (1976).
[f] Ahrland (1986).
[g] Moskvin (1971).
[h] Martell and Smith (1977).
[i] Hulet (1986).
[j] Sillen and Martell (1971).
[k] Smith and Martell (1989).
[l] Lemire *et al.* (2001).
[m] Grenthe *et al.* (1992).

the liver. The initial skeletal fraction, skeleton/$BB_0$, normalizes the data by accounting for the somewhat variable early urinary excretion. Initial skeletal fractions of the trivalent lanthanides and actinides in rats are plotted vs ionic radius in Fig. 31.1. The straight-line segments were fitted by linear regression analysis to serve as eye guides. The initial skeletal fraction of $Pu^{3+}$ lies so far

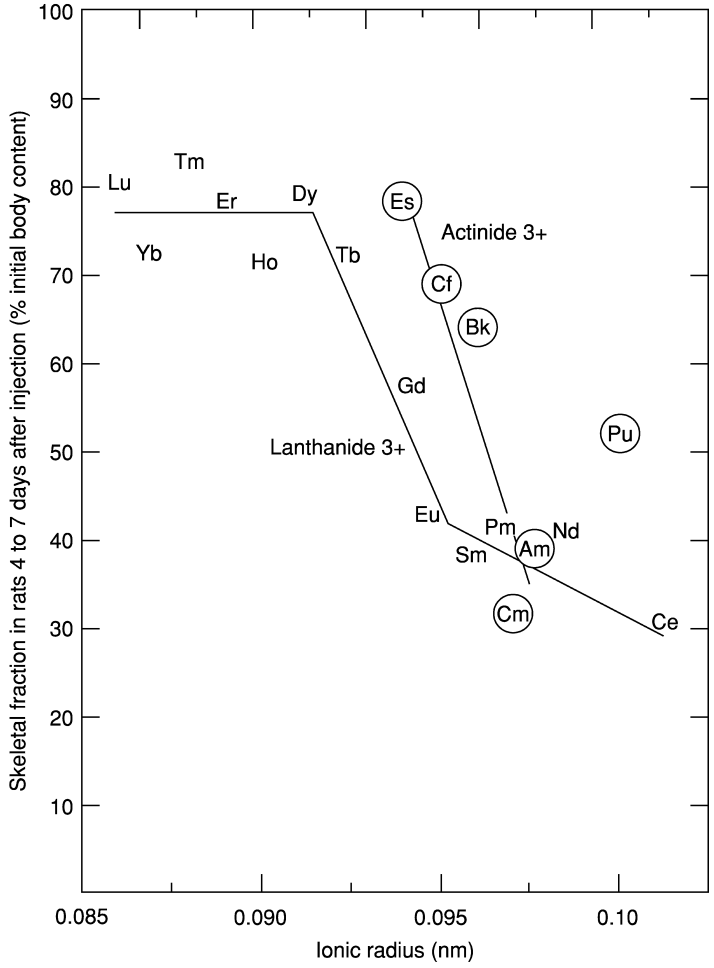


**Fig. 31.1** *Deposition of trivalent actinides and lanthanides in the skeleton of rats at* 4 *to* 7 *days after injection, expressed as percent of initial body content* (%$BB_0$), *and shown as functions of their six-coordinate ionic radii. Lanthanide data from Durbin* (1973); *actinide data from Table* 31.1; *ionic radii from Shannon* (1976) *and Katz* et al. (1986).

from the trend line for the other trivalent actinides that it was not included in determining the regression line for the trivalent actinides. The aberrant behavior of $Pu^{3+}$ supports the view that $Pu^{3+}$ will be oxidized to $Pu^{4+}$ *in vivo* (Carritt *et al.*, 1947; Scott *et al.*, 1948b).

The plot of initial skeletal fraction vs ionic radius for the trivalent actinides and lanthanides in rats (Fig. 31.1) is discontinuous. Six-coordinate ionic radii are those reported by Shannon (1976). Fig. 31.1 exhibits three distinct regions,

as follows: For the lanthanides, there is a plateau from $Lu^{3+}$ to $Tb^{3+}$ ($r < 0.0925$ nm), followed by a steeply declining region from $Tb^{3+}$ to $Eu^{3+}$ ($r = 0.0925$–$0.095$ nm), and a less steeply declining segment from $Eu^{3+}$ to $Ce^{3+}$ ($r \geq 0.095$ nm). For the trivalent actinides, $Es^{3+}$ to $Am^{3+}$ ($r = 0.094$–$0.0975$ nm), only the steeply declining central region was observed.

The initial skeletal fractions of $Am^{3+}$ and $Cm^{3+}$ in rats lie in the region defined by the larger lighter lanthanides; they resemble $Pm^{3+}$, which has about the same ionic radius, but two less f-shell electrons. The initial skeletal fraction of $Es^{3+}$ lies within the region defined by the smaller heavier lanthanides; the initial skeletal fractions of $Bk^{3+}$, $Cf^{3+}$, and $Es^{3+}$ most closely resemble the lanthanides, $Gd^{3+}$, $Tb^{3+}$, and $Dy^{3+}$, respectively, which have ionic radii 0.0025 nm smaller, on average, and one less f-shell electron.

If the increase in initial skeletal fraction with decreasing ionic radius found for the lanthanides and trivalent actinides depended only on their affinities for bone surface ligands (bone mineral and/or protein), a more gradual trend would be expected. The discontinuous pattern observed resembles the relationship between the size of a multivalent cation and its ability to occupy both of the similar but unequal metal-binding sites of transferrin (Tf), the iron-transport protein of mammalian blood plasma (Pecoraro *et al.*, 1981). The combined data for the skeletal deposition of the trivalent actinides and lanthanides in rats and metal binding to Tf suggest that the stabilities of their Tf complexes strongly influence the skeletal deposition of these trivalent metal ions.

Studies in several animal species show that a number of soft tissues other than liver accumulate radiologically significant concentrations of trivalent actinides (Lloyd *et al.*, 1970, 1974, 1975, 1976; Atherton and Lloyd, 1972; Durbin, 1973; Guilmette *et al.*, 1980). Autoradiographs of soft tissues of rats, dogs, monkeys, and baboons show that the initial actinide deposits are located extracellularly in the connective tissue components (Taylor *et al.*, 1969a,b, 1972a; Lloyd *et al.*, 1970; Durbin, 1973; Guilmette *et al.*, 1980). The connective tissue at most, but not all, of the sites of actinide deposition was shown histochemically to contain substances that react positively to the periodic-acid Schiff (PAS) stain for mucins, glycogen, and glycoproteins (Pearse, 1961; Taylor *et al.*, 1972a). The trivalent actinides were found deposited in the intertubular connective tissue of the kidneys of all of the species, and in the dogs, also in the capillary tufts and in or on the basement membrane of the glomerular capsule.

The most widely distributed deposition site identified in all of the tissues examined from all of the animals studied is the medial layer of the small arterioles, where the nuclides appeared to be localized in the connective tissue and not the smooth muscle layers. There was also some selective localization in specialized connective tissue components of the aorta, coronary arteries, and heart valves. Skeletal muscle and pelt contribute 43 and 14%, respectively, of the body weight of the study animals (Tables 31.1–31.6). Although the concentrations of the trivalent actinides in those tissues are low (0.5–2.5% per kg), most of the actinide in the body, apart from liver and skeleton, is associated with those

large tissue masses. Actinides in the walls of their abundant blood vessels can account for much of the early actinide content of these tissue masses.

All of the investigated trivalent actinides concentrated in the interfollicular connective tissue of the thyroid glands of the dogs, but not the primates. The stability of that binding was demonstrated by prolonged retention of $^{241}Am^{3+}$ (Lloyd *et al.*, 1970) and $^{249}Cf^{3+}$–$^{249}Bk^{3+}$ (Taylor *et al.*, 1972a) and by the recovery with the insoluble connective tissue fraction of 95% of $^{241}Am$ in a homogenate of the thyroid of a $^{241}Am^{3+}$ injected dog (Stevens *et al.*, 1969). Combined, all of these observations suggest that the trivalent actinides bind to glycoprotein in the connective tissue ground substance, a hypothesis supported by the affinity of purified bone glycoprotein for $^{241}Am^{3+}$ *in vitro* (Chipperfield and Taylor, 1968, 1972).

### 31.2.2 Tetravalent and pentavalent actinides

Thorium, protactinium, and plutonium were injected in animals as $Th^{4+}$, $Pa^{5+}$, and $Pu^{4+}$, respectively, their most stable states in biological systems (dilute saline solution, mild redox conditions, nearly neutral pH). The biological data indicate that $Np^{4+}$ and $U^{4+}$ tend to be unstable *in vivo* (Tables 31.2 and 31.7).

#### (a) $Th^{4+}$

Tracers of citrate complexes of two shorter-lived Th isotopes were injected im in rats ($^{227}Th^{4+}$, Table 31.2) and iv in dogs ($^{228}Th^{4+}$, Table 31.4). Absorption of $Th^{4+}$ from the im injection site in the rats was nearly complete in 8 days. There was no evidence of intravascular colloid formation in the iv-injected dogs. The initial distributions of $Th^{4+}$ in the rats and dogs agreed well. Bone is the predominant deposition site of $Th^{4+}$. Liver deposition is low, but soon after injection, kidneys and other soft tissues account for a substantial fraction of the body content (13 to 18% at 1 to 23 days). About 10% of the injected $Th^{4+}$ is excreted in the urine, mainly in the first 24 h. Fecal excretion is low for the rats and negligible for the dogs.

Autoradiographs were prepared from the soft tissues of a dog that died 10 days after sc injection of a lethal dose of $^{228}Th^{4+}$ (10 μCi $kg^{-1}$ of $^{228}ThCl_4$, pH 4–5) (Erleksova, 1960). The published autoradiographs are overexposed, and the distribution of the $^{228}Th^{4+}$ is obscured by tracks from the ingrown $^{224}Ra^{2+}$ and $^{220}Rn$ daughters. There is phagocytized radiation-damaged cell debris in many of the tissues. However, the general pattern of $Th^{4+}$ distribution in the soft tissues can be discerned, and it is nearly the same as that described above for $Am^{3+}$ and $Cf^{3+}$ in dogs (Taylor *et al.*, 1969b, 1972a; Lloyd *et al.*, 1970). Some $Th^{4+}$ in the liver was contained within hepatic cells. In the kidneys, $Th^{4+}$ was associated with the tubular epithelium and with cell debris in collecting tubules. Combined, these observations were taken as evidence for the intratubular dissociation of an ultrafilterable low molecular weight $Th^{4+}$ complex present

in the plasma. The $^{228}Th^{4+}$ alpha tracks appeared mainly, if not entirely, to be located in the connective tissue components of the organs examined, including thyroid, testis, and adrenal glands, and in the medial layers of arterioles. In the lungs, the $Th^{4+}$ was accumulated in the bronchiolar cartilages. Slow release of $^{228}Th^{4+}$ from the soft tissues of the dogs (Stover *et al.*, 1960) and the great affinity of bone glycoproteins for $Th^{4+}$ *in vitro* (Chipperfield and Taylor, 1972) suggest that $Th^{4+}$ can bind stably to PAS-positive proteins in connective tissue.

### (b) $U^{4+}$

The initial distribution of U after iv injection of $U^{4+}$ has been reported for rats (Neuman, 1949) and an adult man (Bernard and Struxness, 1957). The details of the human study are given in Table 31.7. The rats (63 days old males and 112 days old females, 200 g body weight) were injected iv with natural $UCl_4$ in 0.2 M acetate buffer, pH 4.6, at doses ranging from 1.5 to 3 mg U per kg. Excreta and all tissues were analyzed for U by a fluorometric method (Flagg, 1949). In the female rats killed at 5 days, the injected U was distributed as follows [original data of Neuman (1949) normalized to 100% material recovery]: liver and spleen 59%, kidneys 4%, skeleton 7%, urine 21%, feces 6%.

The initial distributions of U injected iv as $U^{4+}$ in the rats and the man can be compared with those of soluble $Pu^{4+}$ and $UO_2^{2+}$ (Tables 31.2 and 31.7). The initial urinary excretion of the U was much greater than for $Pu^{4+}$, but much less than for $UO_2^{2+}$. Deposition of the U in bone was much less than for $Pu^{4+}$ and about the same as for $UO_2^{2+}$. Deposition of the U in the kidneys was much less than would be expected for $UO_2^{2+}$. The U retained in the liver and spleen of the man was less than for $Pu^{4+}$, but much greater than for $UO_2^{2+}$; in the rats, retention of the U in liver and spleen was much greater than would be expected for either soluble $Pu^{4+}$ or $UO_2^{2+}$.

Several U compounds, including $UCl_4$, are unstable *in vivo*, and are slowly oxidized to $UO_2^{2+}$ in 0.025 M $HCO_3^-$ pH 7.4 (Dounce, 1949). If, similarly to $Th^{4+}$ and $Pu^{4+}$, $U^{4+}$ circulated as a nonfilterable plasma protein complex that was cleared slowly from the plasma, only a small amount would be excreted by the kidneys. However, an important fraction of the U injected as $U^{4+}$ was excreted in the urine during the first day (14 and 24% by the rats and the man, respectively). The presence of filterable U in the circulation is evidence that some of the $U^{4+}$ was oxidized to $UO_2^{2+}$ within minutes after the injection. The rats excreted an additional 7% of the U in the urine in days 2 to 5 (Neuman, 1949), and the man excreted an additional 44% in the interval 2 to 21 days, (Table 31.7), providing evidence of slow continuous oxidation to $UO_2^{2+}$ of $U^{4+}$ initially sequestered in the tissues. Parenterally injected $UCl_4$ is only about one-tenth as toxic to the kidneys of rats as $UO_2(NO_3)_2$; the $LD_{50s}$ at 14 to 21 days are 25 and 2.5 mg U per kg body weight, respectively (Yuile, 1973). *In vivo* oxidation of $U^{4+}$ and release of $UO_2^{2+}$ into the circulation apparently proceed sufficiently slowly that the kidneys are not exposed to a toxic level of $UO_2^{2+}$.

### (c) $Np^{4+}$

Tetravalent $^{239}Np^{4+}$ and $^{237}Np^{4+}$ have been studied in rats (Table 31.2; Moskalev *et al.*, 1979; Paquet *et al.*, 1996; Ramounet *et al.*, 1998). The biological behavior of $Np^{4+}$ would be expected to resemble $Pu^{4+}$, based on similar chemical properties. Deposition of $Np^{4+}$ in the skeleton is about the same as that of $Pu^{4+}$ and within the range of values reported for initial skeletal $Pu^{4+}$ content of rats (ICRP, 1972). However, the $Np^{4+}$ content of the liver was well below that expected based on similarity to $Pu^{4+}$. Urinary excretion of $Np^{4+}$ was 24% in 4 days, more than 10 times that found for $Pu^{4+}$, but less than the early urinary excretion of $NpO_2^+$ (36% in 3 days, Table 31.2). Uptake of iv-injected $^{237}Np^{4+}$ citrate in the skeleton was significantly faster than for $^{238}Pu^{4+}$, but significantly slower than for $^{237}NpO_2^+$ (Ramounet *et al.*, 1998).

### (d) $Pu^{4+}$

Most of the biological studies of Pu have been performed with $^{239}Pu^{4+}$, however, other Pu isotopes have been used to take advantage of their special physical properties – the photon emissions of $^{237}Pu^{4+}$, the greater specific radioactivity of $^{238}Pu^{4+}$, and the beta particle emissions of $^{241}Pu$. In addition to the numerous studies of injected $Pu^{4+}$, various chemical forms of $Pu^{4+}$ have been administered to animals by inhalation to measure absorption into the body and assess the local radiotoxicity of the Pu alpha particles in the tissues of the respiratory tract, and by mouth to measure absorption from the GI tract. Chemical forms of Pu that have been investigated in those studies range from soluble complexes to insoluble $PuO_2$ particles. In addition to the animal species represented in Tables 31.1–31.7, distribution, retention, and toxicity of injected $Pu^{4+}$ have also been studied in rabbits, chinchillas, swine, and sheep (Buldakov *et al.*, 1969; Taylor, 1969; ICRP, 1972, 1986; Bair *et al.*, 1973; Vaughan *et al.*, 1973).

Overall, the initial distributions of injected $Pu^{4+}$ in rats, mice, dogs, monkeys, and human adults are similar (Tables 31.1–31.5 and 31.7). On average, skeleton plus liver accounts for 85% of the injected $Pu^{4+}$, and soft tissues other than liver and early urinary and fecal excretion, for 7, 4, and 5%, respectively. The initial $Pu^{4+}$ distributions in the rats and dogs are nearly the same as those of the heavier trivalent actinides, $Bk^{3+}$, $Cf^{3+}$, and $Es^{3+}$, whereas the $Pu^{4+}$ distributions in the mice, monkeys, and human adults closely resemble $Am^{3+}$. The combined data for the initial $Pu^{4+}$ distributions in the five species may be compared to those for the trivalent actinide(s) they resemble most closely. The $Pu^{4+}$ contents of the soft tissues other than liver, as well as the early fecal $Pu^{4+}$ excretion are nearly the same as the best matched trivalent actinide(s). About 10% more of the injected $Pu^{4+}$ is deposited in the skeleton plus liver (85%) than is found for the matched trivalent actinide(s) (75%), and that difference is accounted for by the smaller amount of early $Pu^{4+}$ excretion in urine (4%, on average) compared with an average early excretion of 15% for the matched trivalent actinides.

Although the initial $Pu^{4+}$ content of skeleton plus liver is nearly the same for all five species, the partitioning of the $Pu^{4+}$ between those two tissues favors skeletal deposition in the rats and dogs, and liver in the mice, monkeys, and human adults. That species difference may be attributed in part to the less mature and/or more reactive skeletons of the rats and dogs at the time of $Pu^{4+}$ injection (Durbin, 1975). The male rat skeleton grows slowly until late in life (Simpson *et al.*, 1950). In dogs, the degree of skeletal maturity (age at the time of $Pu^{4+}$ injection) alters the proportions of Pu in the skeleton and liver in a reciprocal manner, favoring deposition in bone of juvenile dogs (3 months old) and young adult dogs (18 months old) and in the liver in older dogs (5 years old) (Bruenger *et al.*, 1983).

Autoradiographs of soft tissues of several species show that initially, soluble $Pu^{4+}$ is prominently deposited in hepatic cells and to a lesser degree in the renal papillae, on nonskeletal mineralized structures both physiological (calcifying tracheal cartilages) and ectopic (calcified renal stones and scar tissue), and occasionally in involuting ovarian follicles and corpora lutea. Low concentrations are seen in the medial layer of arteries and arterioles and in the connective tissue of all tissues and organs examined, including bronchiolar cartilages, heart, testis, and thyroid gland (Painter *et al.*, 1946; Bloom, 1948; Erleksova, 1960; Cochran *et al.*, 1962; Jee and Arnold, 1962; Durbin, 1975; Green *et al.*, 1977; Miller *et al.*, 1980; Durbin *et al.*, 1985). Concentrations of $Pu^{4+}$ in connective tissue are much less than those found for the heavier trivalent actinides. Those observations suggest that $Pu^{4+}$ complexes with connective tissue glycoproteins are not as stable as the circulating $Pu^{4+}$ complexes with plasma proteins, particularly Tf, or the complexes that $Pu^{4+}$ forms at binding sites on the surfaces of hepatic cells and bone.

Carritt *et al.* (1947) studied groups of rats injected iv with $^{239}Pu^{4+}$ citrate at doses ranging from 0.14 to 231 μg $kg^{-1}$ (data for the 0.14 and 67 μg $kg^{-1}$ groups are included in Table 31.2), and Talbot *et al.* (1990) injected rats iv with 0.04 μg $kg^{-1}$ of $^{237,238}Pu^{4+}$ citrate. The results are essentially the same over the entire range of iv-injected $Pu^{4+}$ doses indicating that, although limited in quantity, a sufficient number of Tf-binding sites were available to accommodate the largest amount of $^{239}Pu^{4+}$ (0.97 μmo1 $kg^{-1}$) injected.

### (e) $Pa^{5+}$

The stable state of this poorly studied actinide appears to be $Pa^{5+}$ *in vivo*. The eight-coordinate ionic radius of $Pa^{5+}$, 0.091 nm (Shannon, 1976), is smaller and the charge/radius ratio is larger than those of its quadrivalent neighbors, and it is more acidic and hydrolyzes at a lower pH (Smith and Martell, 1976; Katz *et al.*, 1986). Stability constants are not available for $Pa^{5+}$ complexes with the low molecular weight ligands shown in Table 31.8, but complexes with those ligands and with Tf and tissue and bone glycoproteins should be as stable, if not more stable, than those formed by $Pu^{4+}$. Complete distribution and excretion

studies of $Pa^{5+}$ have been conducted only in rats (Table 31.2). Distribution of the absorbed fraction of im-injected $^{233}Pa^{5+}$ in the tissue of rats – predominant deposition in the skeleton and low uptake in liver – closely resembles that of $Th^{4+}$. These results in rats are similar to those reported by others for im-injected $^{233}PaCl_5$ (Lanz *et al.*, 1946) or iv-injected, ultra filtered $^{233}Pa^{5+}$ citrate (Schuppler *et al.*, 1988).

There are incomplete data for the tissue distribution in baboons of iv-injected $^{233}Pa^{5+}$ ($10^{-6}$μg $kg^{-1}$) in 0.08 M citrate buffer, pH 3.2 (Ralston *et al.*, 1986). Initial excretion in urine was low (6% in 24 h). At 24 h, the $Pa^{5+}$ content of the skeleton is estimated to be about 50% of the amount injected. Because plasma clearance of the $Pa^{5+}$ is slow (Cohen and Ralston, 1983), much of the $Pa^{5+}$ associated with soft tissue at early times can be accounted for by contained blood. By 21 days, when the plasma $Pa^{5+}$ has been reduced to about 2% of the amount injected, measurements of excreta and *in vivo* γ-ray counting of the whole body indicate the following distribution of $Pa^{5+}$ in this large animal: cumulative urine and feces 15 and 3%, respectively, skeleton 65%, all soft tissue 13%.

Ralston *et al.* (1986) reported that they also prepared an injection solution similar to the $^{233}Pa^{5+}$ described above, in which Pa was in the 6+ oxidation state. There is no evidence for the existence of a stable state of Pa higher than $Pa^{5+}$ (Kirby, 1986b; Katz *et al.*, 1986), so it is reasonable to conclude that the procedures used to prepare the second solution made no change, and the oxidation state was $Pa^{5+}$ in both injection media. Furthermore, the plasma clearances and whole-body retentions of the two preparations were identical, indicating that the oxidation state was the same, $Pa^{5+}$, in both cases.

### 31.2.3 The dioxo ions

#### (a) $UO_2^{2+}$

Hexavalent uranium, $UO_2^{2+}$, is the most stable state of U in the animal body. Many U compounds with broad ranges of composition and solubility have been fed to or inhaled by animals, and U metal fragments have been implanted in wounds. The fractions of the U that dissolve and are absorbed to blood are distributed in the tissues (skeleton and kidneys) and excreted in the urine similarly to injected $UO_2(NO_3)_2$ (Hodge, 1949; Maynard and Hodge, 1949; Stokinger *et al.*, 1949; Stradling *et al.*, 1985a,b, 1987, 1988; Hahn *et al.*, 2002).

Kidney is the only organ in which histopathological changes are seen consistently in U-poisoned animals. The nature and location of the renal injury (predominantly in the last third of the proximal tubules) are diagnostic of intake of $UO_2^{2+}$ to blood (Voegtlin and Hodge, 1949, 1953; Hodge, 1949; Yuile, 1973). All of the U compounds studied that have any degree of dose-dependent toxicity exhibit the renal injury typical of $UO_2^{2+}$. The similarities to $UO_2^{2+}$ (tissue distribution, urinary excretion, and kind and site of renal pathology) led to

the conclusion that the absorbed fractions of U compounds are converted to $UO_2^{2+}$ under physiological conditions (Hodge, 1949; Dounce and Flagg, 1949).

The initial tissue distributions of U injected as $UO_2^{2+}$ in the six mammalian species shown in Tables 31.2–31.7 agree well with one another, even though the sampling (postinjection) time ranged from 1 to 7 days and the $UO_2^{2+}$ dose ranged from $2 \times 10^{-6}$ μg $kg^{-1}$ of $^{237}UO_2^{2+}$ (baboon) to 300 μg $kg^{-1}$ of $^{233}UO_2^{2+}$ (dog). Skeleton and kidneys are the main sites of $UO_2^{2+}$ deposition. They each contain about 12% at 4 days, on average, 3.5% is present in all other soft tissues; about 73% has been excreted, almost entirely in the urine. Linear regression analysis indicates weak correlations of tissue deposition and urinary excretion with $UO_2^{2+}$ dosage; weakly positive for U deposition in skeleton and kidneys and weakly negative for urinary excretion. Linear regression analysis of tissue deposition and urinary excretion with time after injection predicts that at 24 h after a $UO_2^{2+}$ injection, the U will be distributed, as follows: skeleton 15%, kidneys 18%, other tissues 5%, and urine 63%. That predicted distribution is in essential agreement with the parameters of the biokinetic model for U most recently adopted by the ICRP (1995).

The U initially deposited in the kidneys passes into the urine with a half-time of about 7 days (ICRP, 1995), until nearly all of the original U deposit has been eliminated. Nearly all of the long-retained U in the body is in the skeleton (Neuman, 1949; Yuile, 1973; Stevens *et al.*, 1980; Wrenn *et al.*, 1985).

In young rapidly growing rats, $UO_2^{2+}$ is less toxic to the kidneys than in adults, and it is less toxic in adult male rats than in females of the same age (Haven and Hodge, 1949). Neuman (1949) observed that growing rats stored more U administered as $UO_2^{2+}$ in their skeletons than adults and that the incomplete skeletons of adult male rats took up more U than adult females. The relative proportion of the U dose deposited in the kidneys varied inversely with U storage in bone; the kidneys of the growing rats and adult male rats were spared by diversion of larger fractions of the injected U to the skeleton.

### (b) $NpO_2^+$, $NpO_2^{2+}$

The initial distributions in the tissues of im- or iv-injected $^{237}NpO_2^+$ in rats, mice, and monkeys agree well with one another (Tables 31.2, 31.3, and 31.5). Skeleton is the main site of Np deposition. Filtration into urine is the main excretory pathway, but little Np is deposited in the kidneys. At 1 to 4 days after injection, on average, 41% of the Np is in the skeleton, and the remainder is distributed as follows: liver 10%, kidneys 2%, other soft tissues 5%, urine 39%, and feces 2%. The initial distribution of circulating $NpO_2^+$ in the animals appears to be the result of competition between skeletal uptake and urinary excretion.

The initial distribution of Np in the tissues of a baboon-injected iv with $^{239}NpO_2^{2+}$ in 0.01 M $NaHCO_3$ was reported by Ralston *et al.* (1986), and those data are included in Table 31.6. The initial distributions of tracer quantities of $^{239}NpO_2^{2+}$ and $^{237}UO_2^{2+}$ in the baboon can be compared directly; the early

urinary excretion of the Np is much less, the skeletal deposition of Np is much greater, and Np deposition in the kidneys is much less than $UO_2^{2+}$. Distributions in the tissues and early urinary excretion of the dioxo Np ions are nearly the same regardless of the animal (rat, mouse, monkey, baboon), the reported valence state of the Np ($NpO_2^+$, $NpO_2^{2+}$), the injected dose of Np (range, $4 \times 10^{-7}$ μg $kg^{-1}$ of $^{239}NpO_2^{2+}$ or $^{239}NpO_2^+$ in baboons to 360 μg $kg^{-1}$ of $^{237}NpO_2^+$ in rats), or the chemical composition of the injection medium (dilute nitric acid, isotonic saline, or citrate or bicarbonate buffer). Combined, these observations indicate that $NpO_2^{2+}$ is unstable *in vivo* with respect to reduction to $NpO_2^+$.

Under the conditions of poorly oxygenated, slowly flowing tissue fluid at an im wound site in rats, 200 μg $kg^{-1}$ of $^{233}UO_2^{2+}$ was rapidly and quantitatively absorbed (Table 31.2). In contrast, absorption of 360 μg $kg^{-1}$ of $^{237}NpO_2^+$ injected im was slow (22% at 1 day and 62% at 30 days, Morin *et al.*, 1973). Those results suggest some reduction to $Np^{4+}$ at the wound site.

### (c) $PuO_2^{2+}$

In several early studies of Pu distribution in animal tissues, mice, rats, rabbits, and dogs were injected iv or im with $^{239}PuO_2^{2+}$ (Finkle *et al.*, 1946; Painter *et al.*, 1946; Van Middlesworth, 1947; Carritt *et al.*, 1947; Kisieleski and Woodruff, 1948, Scott *et al.*, 1948b). Complete data sets are available only for rats, and those shown in Table 31.2 are representative for rats injected im with $^{238}PuO_2^{2+}$ citrate or iv with $^{239}PuO_2(NO_3)_2$. The deposition pattern of $PuO_2^{2+}$ in rats (Table 31.2) can be compared with data for both $Pu^{4+}$ and $UO_2^{2+}$ in several animal species (Tables 31.2–31.7). The initial tissue distribution of Pu given as $PuO_2^{2+}$ does not resemble that of its analog $UO_2^{2+}$, but is nearly the same as that of $Pu^{4+}$.

The early association of about 5% of iv-injected $PuO_2^{2+}$ with red blood cells (Painter *et al.*, 1946) resembles $UO_2^{2+}$ (Lipsztein, 1981), but not $Pu^{4+}$ (Stover *et al.*, 1959). Urinary excretion of $PuO_2^{2+}$ in the first 24 h was much less than for $PuO_2^{2+}$ and only somewhat greater than for $Pu^{4+}$. Retention of Pu in the kidneys after injection of $PuO_2^{2+}$ was much less than for $UO_2^{2+}$ and about the same as that of $Pu^{4+}$. Absorption of Pu after im injection of $^{239}PuO_2Cl_2$ was slower and much less efficient than for $UO_2^{2+}$, but faster than for the same mass of im-injected $^{239}PuCl_4$ (Scott *et al.*, 1948b). Combined, these results indicate that $PuO_2^{2+}$ is unstable *in vivo* with respect to reduction to $Pu^{4+}$.

## 31.3 ACTINIDE TRANSPORT IN BODY FLUIDS

### 31.3.1 Composition of mammalian plasma and tissue fluid

The concentrations of the major electrolytes in normal human blood plasma listed in Table 31.9 include cations that compete with actinide ions for circulating bioligands and low molecular weight anions with the potential for actinide

**Table 31.9** *Concentrations of low molecular weight electrolytes in human plasma and urine, and estimated concentrations in fluid entering last third of proximal ural tubules.*

| | *Concentration* (mM) | | |
|---|---|---|---|
| *Electrolyte* | *Plasma and tissue fluid* | *Late proximal tubule fluid*[a] | *Bladder urine*[b] |
| $Na^+$ | 140[b] | 140 | 130 |
| $K^+$ | 5[b] | 5 | 44 |
| $Ca^{2+}$ | 1.5[c] | 2 | 4 |
| $Cl^-$ | 110[b] | 110 | 140 |
| $HCO_3^-$ | 25[b] | 8.8 | 1.6 |
| $HPO_4^{2-}$[d] | 1[d] | 0.5 | 20 |
| Citrate | 0.1[d] | 0.1[e] | 4 |
| pH | 7.4 | 6.5[e] | 6.0 |

[a] Calculated from human plasma concentrations and data of Wong *et al.* (1986) for electrolyte concentrations at last accessible micropuncture site in proximal tubules of *Cercopithicus aethiops* monkey kidneys.
[b] Altman and Dittmer (1971); Gamble (1954).
[c] Ultrafilterable fraction of plasma $Ca^{2+}$ (Neuman and Neuman, 1958; Bronner, 1964).
[d] Total phosphate; distribution in plasma is 81% $HPO_4^{2-}$ and 19% $HPO_4^-$ (Neuman and Neuman, 1958; Youmans and Siebens, 1973).
[e] Estimated.

complexation. The concentrations of the major electrolytes in the plasma of the laboratory animals used in the studies of tissue distribution (Tables 31.1–31.7) differ little from each other or from those in human plasma (Altman and Dittmer, 1971; Loeb and Quimby, 1999).

Table 31.10 lists the fluid volumes (plasma, interstitial fluid) and the concentrations of proteins and iron in the plasma of the laboratory animals and human adults. Even though there is a 2000-fold range of body weight from mouse to man, their fractional plasma and tissue fluid volumes are similar. The mean fractional plasma and tissue fluid volumes of the animals are $43 \pm 8$ and $210 \pm 39$ mL $kg^{-1}$ body weight, respectively, similar to those of human adults. The concentrations of albumin, globulins, and Tf, the iron-transport protein of mammalian plasma, do not vary greatly among the animals and man. However, the concentration of plasma iron and the numbers of Tf-binding sites normally occupied by iron (saturation) differ among the species. Tf Fe-saturation, which ranges from 33 to 44% for the larger animals (beagle, nonhuman primates, man) and from 59 to 74% for the small rodents, is inversely correlated with body weight (Table 31.10) and directly correlated with metabolic rate (Brody, 1945).

### 31.3.2 Circulation of extracellular fluid

Foreign ions taken into the mammalian body are transported in the circulating extracellular fluid (ECF), which is actually two communicating compartments. The plasma is the fluid phase of the blood, and it is confined within the blood

**Table 31.10** *Fluid volumes and protein and iron concentrations in plasma of mature laboratory animals and human adults.*

| | *Mouse* | *Rat* | *Beagle dog* | *Macaque monkey* | *Human adult* |
|---|---|---|---|---|---|
| Body weight (kg)[a] | 0.035[b] | 0.25 | 10 | 6.2 | 70[c] |
| Plasma (mL $kg^{-1}$) | 50[b] | 36[d] | 49[e] | 36[f] | 43[c] |
| Interstitial water (mL $kg^{-1}$) | 180[b] | 250[g] | 230[g] | 170[g] | 200[c] |
| Serum albumen (mM $L^{-1}$)[a] | 0.56 | 0.60 | 0.52 | 0.64 | 0.65[g] |
| Serum globulins (mM $L^{-1}$)[a] | 0.14 | 0.22 | 0.19 | 0.25 | 0.21[g] |
| Transferrin (mM $L^{-1}$)[h] | 0.036 | 0.033 | 0.032 | 0.040 | 0.027 |
| Serum iron (mM $L^{-1}$)[a] | 0.053[i] | 0.039 | 0.025 | 0.032 | 0.018[j] |
| Transferrin saturation (%)[k] | 74 | 59 | 39 | 40 | 33[i] |

[a] Loeb and Quimby (1999). Body weights and serum protein and iron concentrations for all animals unless otherwise noted.
[b] Durbin *et al.* (1992).
[c] ICRP (1974). Reference man.
[d] Everett *et al.* (1956).
[e] Stover *et al.* (1959).
[f] Gregerson *et al.* (1959).
[g] Altman and Dittmer (1971).
[h] LeBoeuf *et al.* (1995).
[i] Fairbanks and Beutler (1995).
[j] Transferrin concentration calculated from total iron binding capacities of mouse (Durbin *et al.*, 1992); human adult (Fairbanks and Beutler, 1995); other animals (Loeb and Quimby, 1999).
[k] Calculated from serum iron and transferrin concentrations, assuming 2 moles iron bound by 1 mole transferrin.

vessels. The interstitial (tissue) fluid is outside the vascular system, and it bathes the body cells and their supporting connective tissue.

Mammalian plasma is a steadily flowing, well-mixed, nearly neutral (pH 7.4), dilute saline solution containing numerous solutes (electrolytes and proteins) at closely regulated concentrations. The plasma water and filterable (low molecular weight, nonprotein constituents) are in steady-state exchange with the tissue fluid by outward diffusion though the arterial ends of the capillaries and inward diffusion at the venous ends, at a rate in human adults of about one plasma volume per min. The capillary walls are not completely impermeable, and between 50 and 100% of plasma proteins escape through the capillaries and reenter the blood via the lymphatic circulation daily (Cronkite, 1973). The composition of the tissue fluid approximates an ultrafiltrate of the plasma. It contains small molecules and electrolytes at about the same concentrations as the plasma, but the protein concentration is less than 20% of that in the plasma. The tissue fluid is the medium that transports the filterable dissolved solutes of the plasma to the body cells, and it transports cell products and wastes back into the plasma.

More tissue fluid is produced at the arterial ends of the capillaries than is withdrawn by diffusion back into the venous capillaries. That excess fluid and

the escaped protein are drained away and returned to the plasma by colocated lymph capillaries. The concentration of protein in lymph is somewhat greater than that in the tissue fluid.

### 31.3.3 Loose connective tissue

Tissue fluid does not flow freely; it penetrates and is confined within the loose connective tissue that fills the spaces between the capillaries and the cells of most tissues and organs. Loose connective tissue is composed of fine collagen and elastin fibers embedded in a colloidal gel hydrated by the tissue fluid. The solids of the gel are hydrated high molecular weight mucopolysaccharides (hyaluronic and chondroitin sulfuric acids) and glycoprotein. Both the structural proteins and the components of the connective tissue gel contain potential metal-binding sites – the carboxyl groups of the mucopolysaccharides, the carboxyl (aspartic and glutamic acid) and hydroxyl (tyrosine) side chains of the proteins, and the sialic acid side chains of the glycoproteins (Dounce and Lan, 1949; Passow *et al.*, 1961; Rothstein, 1961; Taylor, 1973a,b; Ham, 1974; Luckey and Venugopal, 1977; Pecoraro *et al.*, 1981).

### 31.3.4 Distribution of actinides in plasma

Trace quantities of multivalent cations circulate in the body fluids as complexes (Taylor, 1972, 1998; Luckey and Venugopal, 1977). Any complexing species such as citrate ion injected with a foreign cation is rapidly diluted and removed from the circulation, and the cation must form new complexes with the filterable low molecular weight plasma constituents (Table 31.9) or with nonfilterable plasma proteins (Table 31.10) or both.

Distribution of actinide ions among the constituents of mammalian blood plasma has been studied in plasma and serum (plasma minus fibrinogen and clotting factors) of rats and dogs injected iv with soluble actinides (*in vivo*) and in whole blood, plasma or serum of rats, dogs, and human adults and purified plasma constituents incubated with actinide solutions (*in vitro*).

The analytical techniques have included: ultrafiltration, electrophoresis, electrodialysis, size exclusion and ion-exchange chromatography, immunochromatography, immunoprecipitation, protein precipitation, and spectroscopy. The information provided by those studies is mainly semiquantitative, because each procedure tends to disturb the natural speciation of the system (reviewed by Taylor, 1998). Furthermore, in the living animal competition for injected actinide ions among the plasma constituents and between the plasma constituents and the tissue ligands continually shifts the chemical speciation in the plasma compartment in favor of the most stable complex(es) (Dounce, 1949; Stevens *et al.*, 1968; Turner and Taylor, 1968a,b; Durbin *et al.*, 1972; Durbin, 1973; Ramounet *et al.*, 1998).

### (a) Filterable low molecular weight ligands

The stabilities of actinide complexes with a given ligand, including the OH of water, increase in the order: $MO_2^+ < MO_2^{2+} \sim M^{3+} < M^{4+}$. For actinides of the same electric charge, $e^-$, the stabilities of complexes with the same ligand generally increase with decreasing ionic radius, $r$. The net effect is increased stabilities of complexes with the increasing ratio of electric charge to ionic radius, $e/r$. The most stable complexes formed by the 'hard' actinide ions are those with ligands that contain oxygen as the electron donor group. In general, the stabilities of the actinide complexes with such groups are in the order: $SO_4^{2-} < CO_2^- < CO_3^{2-} \sim PO_4^{3-}$ (Ahrland, 1986).

Most of the actinide ions introduced into mammalian plasma *in vivo* or *in vitro* tend to associate predominantly with plasma proteins, but in all cases an ultrafilterable low molecular weight fraction has been identified, ranging from small (<10%) for the trivalent, tetravalent, and pentavalent actinides (Stevens *et al.*, 1968; Popplewell and Boocock, 1968; Turner and Taylor, 1968a,b; Bruenger *et al.*, 1971a) to large (≥50%) for $UO_2^{2+}$ and $NpO_2^+$ (Dounce, 1949; Bruenger *et al.*, 1971b; Stevens *et al.*, 1980; Guilmette *et al.*, 1982).

Stability constants (log $K_1$) of one-to-one complexes with several of the low molecular weight ligands present in mammalian plasma are shown in Table 31.8 for the actinides that have been studied in animals and humans (Tables 31.1–31.7). Table 31.8 also includes the ionic radii of those actinide species (Shannon, 1976), assigning coordination number 6 (CN 6) for the trivalent actinides and the dioxo actinide cations, $MO_2^+$ and $MO_2^{2+}$, and CN 8 for the tetravalent and pentavalent actinides. The ionic radii are included to emphasize the relationships among ionic charge and ionic radius (charge–radius ratio, $e/r$) and the tendencies of the metal ions to hydrolyze and form stable complexes. The first hydrolysis constants for the actinides are shown for comparison with the other ligands, because at the nearly neutral pH of mammalian plasma, in the absence of stable complexing ligands, all of the actinides that have been administered to animals, with the possible exception of $NpO_2^+$, would be expected to hydrolyze and form colloidal hydroxides intravascularly.

#### (*i*) *Citric and other alpha-hydroxy dicarboxylic acids*

Citrate ion is the only low molecular weight ligand in mammalian plasma that is competitive with $OH^-$ for all of the actinides studied (Table 31.9), and it is the only competitive ligand for the trivalent actinides. Dicarboxylic acids and phosphate may also compete with $OH^-$ for the tetravalent actinides, and carbonate is competitive for the $MO_2^{2+}$ dioxo actinide ions.

In addition to citrate, other alpha-hydroxy 3- and 4-carbon dicarboxylic acids (malic, oxaloacetic, tartaric) stably bind $UO_2^+$. These tridentate ligands bind

metal ions through the alpha OH group as well as the two carboxylate groups, forming stable five- and six-membered chelate rings. Those ligands form $UO_2^{2+}$ complexes that are stable enough to prevent and to reverse the inhibitory binding of $UO_2^{2+}$ to protein enzymes (Singer *et al.*, 1951). Low concentrations of three alpha-hydroxy dicarboxylic acids (malic, oxaloacetic, isocitric) are present in human plasma (Table 31.9), and their combined concentration is about the same as that of citrate ion. Those organic acids may also participate in actinide complexation in the plasma.

A small fraction of the filterable plasma $Ca^{2+}$ circulates as a citrate complex (concentration about $7 \times 10^{-5}$ M, Neuman and Neuman, 1958). The concentration of plasma citrate is about $10^{-4}$ M (Table 31.9), so nearly 70% of the circulating citrate ion is bound to $Ca^{2+}$. The stabilities of the citrate complexes with trivalent and tetravalent actinides (Table 31.8) are several orders of magnitude greater than that of Ca-citrate (log $K_f$=3.2, Martell and Smith, 1977), and they can be expected to compete with $Ca^{2+}$ for citrate *in vivo*.

When citrate complexes of the tri- and tetravalent actinides are injected iv, the subsequent behavior of the metal ion demonstrates that the injected complexes are transient and less stable than the complexes that the metal ions can form with plasma protein(s) and tissue ligands. In rats and dogs within 2 h after iv injection of the Pu–citrate complex, 90% of the $Pu^{4+}$ in the plasma was found by gel chromatography to be bound to nonfilterable protein(s); by 24 h after the injection less than 5% of the circulating $Pu^{4+}$ was associated with filterable low molecular weight species. Concurrently, excretion of $Pu^{4+}$ in the urine, which is a modified, concentrated ultrafiltrate of plasma, declined rapidly demonstrating the disappearance of the originally ultrafilterable citrate complex from the plasma (Stevens *et al.*, 1968; Turner and Taylor, 1968a; Durbin *et al.*, 1972).

The presence of low concentrations of ultrafilterable citrate complexes of $Pu^{4+}$, $Am^{3+}$, and $Cm^{3+}$ in plasma was shown indirectly through identification of their citrate complexes as the major, if not the only, species of those actinides in urine (Popplewell *et al.*, 1975; Stradling *et al.*, 1976). It is reasonable to assume that small amounts of other actinides and foreign metal ions circulate as citrate complexes that can be ultrafiltered by the kidneys and excreted in the urine.

Citrate ion, injected locally soon after $Pu^{4+}$ is deposited in an im wound, is capable of complexing and hastening $Pu^{4+}$ absorption (Volf, 1975).

### (*ii*) *Carbonate and bicarbonate*

Most carbonates are sparingly soluble, but the actinide dioxo ions form stable carbonate complexes at physiological pH (Smith and Martell, 1976; Ahrland, 1986). The special cases of *in vivo* transport of $UO_2^{2+}$ and $NpO_2^{+}$ as carbonate complexes are discussed below.

### 3.4.2 Nonfilterable plasma proteins

#### (a) Albumin and the globulins

Serum albumin and globulin are globular proteins that are soluble in dilute saline. In normal human plasma, albumin transports about 26% of $Ca^{2+}$ and globulins transport about 7%. $Ca^{2+}$ has low affinity for amino groups and monocarboxylic acids like acetate, but it is strongly chelated by polycarboxylic and hydroxycarboxylic acids like citrate (Neuman and Neuman, 1958). The serum proteins contain abundant amino acids with –COOH side chains (aspartic acid, glutamic acid, cystine), –OH side chains (serine, threonine, hydroxyproline), and phenolic side chains (tyrosine) (Hawk *et al.*, 1947). However, only carboxylate or hydroxyl side chains of the amino acids in close proximity to one another in the protein structure are able to bind $Ca^{2+}$ and other multivalent cations.

The affinities of the serum proteins for cations depend on both their amino acid composition and the spatial arrangement of those amino acids and the binding units of their residues. The globular structures of the serum proteins are determined and maintained by the continuous coiling, bending, and folding of the polypeptide chains, which provide close approach of amino acid side chains that are widely separated in the primary (elongated) structure. That folded lattice-like three-dimensional structure provides numerous carboxyl and hydroxyl groups positioned suitably for metal binding (Schwartz and Fien, 1973). Nonspecific binding to serum proteins has been described for $UO_2^{2+}$, the trivalent lanthanides, and other multivalent metal ions (Painter *et al.*, 1946; Dounce and Lan, 1949; Gurd and Wilcox, 1956; Clarkson, 1961; Passow *et al.*, 1961; Rothstein, 1961; Kyker, 1962; Stevens *et al.*, 1965, 1968; Popplewell and Boocock, 1968; Stover *et al.*, 1968a; Bruenger *et al.*, 1969b, 1971b; Taylor, 1973a,b; Ham, 1974; Luckey and Venugopal, 1977).

The total concentrations of $Ca^{2+}$ and $Mg^{2+}$ in normal human plasma are about 2.5 and 1.0 mM, respectively. Assuming that $Ca^{2+}$ and $Mg^{2+}$ are distributed similarly among the constituents of plasma and that the strengths of their binding to the plasma proteins are similar, the fractions of the metal-binding sites of the plasma proteins normally occupied by the alkaline earth elements can be estimated. In human plasma, about 0.65 mM of $Ca^{2+}$ is bound to albumin and about 0.17 mM is bound to the globulins; 0.26 and 0.07 mM of plasma $Mg^{2+}$ are assumed to be associated with albumin and the globulins, respectively. The maximum $Ca^{2+}$ and $Mg^{2+}$ binding capacities of the plasma albumin and globulins are, on average, 11 and 6 moles of metal per $10^5$ g of protein, respectively (Neuman and Neuman, 1958). The concentrations of albumin and the globulins in plasma are $6.5 \times 10^{-4}$ and $21.0 \times 10^{-4}$ M, respectively (Table 31.8). The mean molecular weights of serum albumin and the globulins are about 67 000 and 160 000, respectively (Hawk *et al.*, 1947). Calculations suggest that about 22% of the potential metal-binding sites of the plasma

proteins are normally occupied. Thus, binding sites are available for occupancy by foreign cations without need to displace their normal loads of $Ca^{2+}$ and $Mg^{2+}$.

Nonspecific binding of the actinides by the plasma proteins is likely to be stronger than that of the alkaline earths, but weaker than specific binding to Tf (see below). The abundances of the plasma proteins and their potential binding sites may favor nonspecific actinide binding strong enough to withstand renal filtration, but too weak to compete with the ligands in liver, bone, and connective tissue.

### (b) Transferrin

#### (*i*) *Structure*

Iron is transported in the plasma of mammals as $Fe^{3+}$ bound to Tf, a specialized glycoprotein of molecular weight 79.6 kDa that migrates electrophoretically with the β-globulins. The amino acid sequence of transferrin has been defined. Each end of the Tf molecule has a globular sialoprotein moiety at which one $Fe^{3+}$ atom may be bound in association with one bicarbonate molecule. The two iron-binding sites of Tf differ slightly. The C-terminal site is larger and binds $Fe^{3+}$ more tightly than the smaller N-terminal site. At pH 7.4, the C-terminal site has an affinity for $Fe^{3+}$ about five times greater than that of the N-terminal site. However, the weaker N-terminal site is preferentially occupied by $Fe^{3+}$, so kinetic and/or access factors may be more important than thermodynamic effects. Iron binding by Tf is pH-dependent, and $Fe^{3+}$ is released at pH $< 7.4$.

#### (*ii*) *Function*

Tf is a true carrier molecule in that it is conserved for many cycles of $Fe^{3+}$ delivery to the erythroblasts and reticulocytes (early and late stages of developing red cells) in the red bone marrow. Iron-bearing Tf, preferentially diferric Tf, binds to cell surface Tf receptors, forming clusters in surface pits, and these are internalized by endocytosis. Inside the developing red cells, the Fe–Tf receptor complex is contained in coated vesicles, which fuse with endosomes. Within the endosomes, the low pH ($\sim$5) releases one $Fe^{3+}$ presumably from the N-terminal site. Release of a second $Fe^{3+}$ may be mediated by other molecules and may involve reduction of $Fe^{3+}$ to $Fe^{2+}$. Neither the Tf nor the Tf-receptor is degraded in the process. The Tf–Tf-receptor complex minus one or two $Fe^{3+}$ atoms is returned to the cell membrane where, at pH 7.4, apotransferrin (iron-free Tf, apoTf) and/or monoferric Tf are released to the interstitial fluid and ultimately reenter the plasma to take up more $Fe^{3+}$. In addition to the developing red blood cells, hepatic cells and to a lesser degree most other cells possess surface Tf receptors and are able to endocytose Tf. When Tf is fully saturated with iron,

the iron absorbed from the GI tract is deposited in the liver (Katz, 1970; Aisen and Listowsky, 1980; Fairbanks and Beutler, 1995).

Tf is synthesized mainly in the parenchymal cells of the liver. At any time about 50% of the exchangeable Tf is located extravascularly in interstitial fluid, and it is returned to the plasma compartment with a half-time of about 17 h. As is the case with the other serum proteins, Tf is destroyed at a first-order rate. Its survival half-time of about 9 days is significantly shorter than that of serum albumin. The sites of Tf destruction are believed to be liver and kidneys (Katz, 1970).

#### (*iii*) *Binding of foreign metal ions*

Tf binds $Fe^{3+}$ ($r = 0.0645$ nm, $e/r = 46.5$ e nm$^{-1}$) in preference to other biologically essential metal ions. Iron binding at both sites involves deprotonation of two tyrosine moieties and the association of one bicarbonate molecule. If a foreign multivalent cation is to occupy either binding site, it must be small enough to fit into the Fe-binding cavity, and have sufficient charge density ($e/r$) to deprotonate both of the two tyrosine phenols required for stable binding (Luk, 1971; Harris *et al.*, 1981).

Metal coordination with apoTf was investigated by spectrophotometric titration of the Tf complexes of metal ions with a broad range of electric charge and ionic radius. Two tyrosines were coordinated at both binding sites by the small transition metal ions and the smaller lanthanides; each Tf molecule bound two metal ions and released four tyrosine protons (Fig. 31.2, Pecoraro *et al.*, 1981). The larger lanthanide ions were able to fit only into one Fe-binding site, presumably the larger C-terminal site, and the number of coordinated tyrosines per Tf molecule decreased from four to two. Because of the size difference in the two sites, the larger $Th^{4+}$ ion is bound stably at one site and weakly at the other, whereas the smaller $Zr^{4+}$ and $Pu^{4+}$ ions are expected to be bound stably at both sites. Europium appears to be an indicator of the maximum size (0.095 nm) of a multivalent cation that can fit into and bind stably at both Tf-binding sites, whereas the larger $La^{3+}$, $Am^{3+}$, and $Cm^{3+}$ ions are expected to bind only at the larger C-terminal site.

### (c) Actinide binding by transferrin

Under appropriate experimental conditions all of the actinides investigated, except $NpO_2^+$ form variably stable complexes with plasma Tf (Popplewell and Boocock, 1968; Stevens *et al.*, 1968; Stover *et al.*, 1968a; Turner and Taylor, 1968a,b; Bruenger *et al.*, 1969b, 1971b; Taylor, 1970, 1998; Stevens and Bruenger, 1972; Durbin *et al.*, 1976; Cooper and Gowing, 1981; Peter and Lehmann, 1981; Guilmette *et al.*, 1982; Wirth *et al.*, 1985; Taylor and Farrow, 1987; Paquet *et al.*, 1996). The apparent stabilities of those actinide Tf

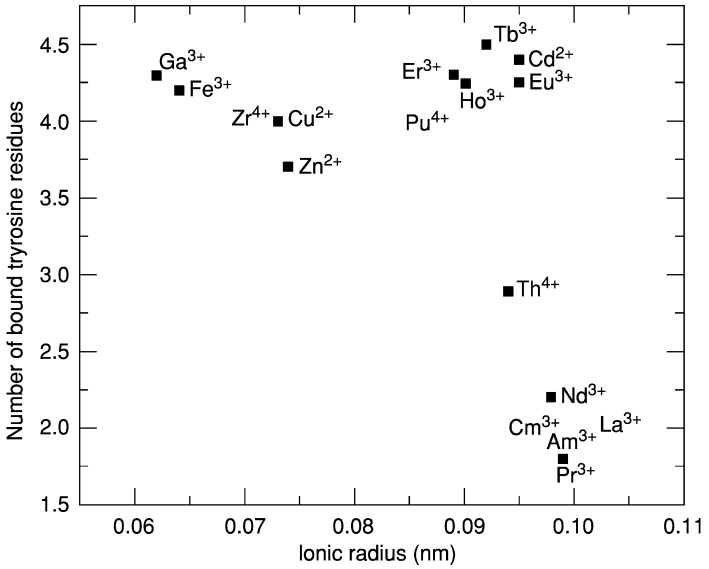


**Fig. 31.2** *Number of tyrosine moieties engaged in binding metal ions as related to their six-coordinate radii* (*Shannon*, 1976). *Data of Harris* et al. (1981) *and Pecoraro* et al. (1981). *Not measured but noted by their elemental abbreviations are* $Zr^{4+}$ *and* $Pu^{4+}$, *which are small enough to fit into both Fe-binding sites and displace four tyrosine protons, and* $La^{3+}$, $Am^{3+}$, *and* $Cm^{3+}$, *which are too large to occupy the smaller N-terminal site and would be expected to displace only two tyrosine protons per transferrin molecule.*

complexes is in the order expected based on their tendencies to form stable complexes:

$$Pa^{5+} > Pu^{4+} > Th^{4+} > Np^{4+} \gg UO_2^{2+} > Cf^{3+} > Am^{3+} > Cm^{3+}$$

Each Tf molecule possesses only two Fe-binding sites, and the concentrations of Tf in mammalian plasma are low (Table 31.10). Thus, the capacity of circulating Tf for transporting actinide ions is limited by both the total number of binding sites and the number of sites not already occupied by $Fe^{3+}$, that is, the degree of Fe saturation of the Tf. Stover *et al.* (1968a,b) showed that Tf binding of $Pu^{4+}$ in plasma varied inversely with Fe–Tf saturation, and that relationship has also been demonstrated for $Th^{4+}$ and $Np^{4+}$ (Peter and Lehmann, 1981; Wirth *et al.*, 1985).

The actinide Tf complexes, with the possible exception of $Pa^{5+}$–Tf, are less stable than Fe–Tf, and the actinides are readily displaced from Tf by adding $Fe^{3+}$ to the reaction medium (Popplewell and Boocock, 1968; Stover *et al.*, 1968a; Peter and Lehmann, 1981; Wirth *et al.*, 1985). Similarly to Fe–Tf, the $Pu^{4+}$, $Th^{4+}$, and $UO_2^{2+}$ Tf complexes are pH-dependent and they begin to dissociate at pH $< 7$ (Bruenger *et al.*, 1971b). Presumably, the stabilities of the

Tf complexes with the other actinides are similarly pH-dependent (Popplewell and Boocock, 1968; Bruenger *et al.*, 1971b; Stevens *et al.*, 1980).

### (d) Association of actinides with erythrocytes

The trivalent and tetravalent actinides form variably stable complexes with the Fe-transport protein, Tf, and the iron storage protein, ferritin, but they are not incorporated into hemoglobin or associated with the stroma of erythrocytes (red blood cells).

The primary function of Tf is delivery of iron to the developing erythroblasts in the red bone marrow for synthesis of hemoglobin. Iron-bearing Tf binds to specific Tf-receptors on the erythroblast surfaces, and the complete complex, Fe–Tf–Tf-receptor, is internalized by endocytosis. Within the erythroblasts, the complex is taken up by lysosomes, where the reduced pH (5 to 5.5) causes dissociation of the complex and release of $Fe^{3+}$. The released Tf is extruded from the cells for reuse (Aisen and Listowsky, 1980).

The simplest explanation for the absence from the interior of the erythroblasts of actinides and other multivalent cations that bind to Tf is that the foreign metal ions bound to Tf induce a conformational change in the protein structure that is not recognized by the erythroblast Tf-receptor. It is possible, but less likely, that foreign metal ions like $Pu^{4+}$, freed from their pH-dependent Tf complexes at the low lysosomal pH, are rapidly shuttled out of the erythroblasts, bound to new Tf molecules, extruded at the cell surface, and recirculated. However, because the latter mechanism probably would be imperfect, small amounts of residual foreign metal ions could be left in the red cells, perhaps bound to the stroma, and that is not observed.

There is evidence that some actinides can bind transiently to the red cell membrane. Actinides in the 3+, 4+, 5+, $MO_2^+$, and $MO_2^{2+}$ oxidation states were equilibrated with aliquots of whole blood *in vitro*. Except for $^{239}Pu^{3+}$ and $UO_2^{2+}$, the actinide concentrations in the washed red cells were $\leq$10% of those in the plasma (Chevari and Likhner, 1968; Bruenger *et al.*, 1971b; Stevens *et al.*, 1980).

Small fractions ($\leq$4%) of iv-injected $UO_2^{2+}$ and $PuO_2^{2+}$ are transiently associated with the red cell membrane (Painter *et al.*, 1946; Lipsztein, 1981; Durbin *et al.*, 1997a). Clearance of $UO_2^{2+}$ from the plasma volume is much faster than the rate of release of $UO_2^{2+}$ from the red cell membrane. Consequently, most of the U in samples of whole human blood from individuals in equilibrium with their normal daily intakes of U in drinking water and foods is associated with the red cells (Hursh and Spoor, 1973; Wrenn *et al.*, 1985).

Evaluation of the clearance of iv-injected $^{228}Th^{4+}$ citrate from the blood of beagles included measurements of the $Th^{4+}$ bound to centrifugally separated red cells (Lloyd *et al.*, 1984a). The association of the $Th^{4+}$ with red cells is

greater and somewhat more persistent than, but otherwise similar to, that of $UO_2^{2+}$. The red cell associated $Th^{4+}$ rose rapidly from zero at the time of the injection to about 8% at 1 min and 30% at 6 h; at that time the blood $Th^{4+}$ was about equally divided between plasma and cells. From 6 to 48 h, red cells accounted for as much as two-thirds of the $Th^{4+}$ in whole blood, and the red cell fraction was being cleared with a half-time of about 14 h, one-half of the plasma clearance rate. By 30 days, the $Th^{4+}$ associated with red cells was nearly 100 times that of the plasma. Between 2 and 30 days, a small fraction of the $Th^{4+}$ was released from the red cells (3.5%) with a half-time of about 15 days. In the special case of $Th^{4+}$, binding to the red cell membrane is competitive with complexation by plasma Tf. Binding to the membrane is the most likely mechanism for the association of actinides with red cells. If, for example, $Th^{4+}$ had entered the red cell interior, a much larger fraction of the 6 h maximum amount of the $Th^{4+}$ associated with red cells would be expected to remain with the circulating red cells for a longer time (the life span of mammalian red cells is about 90 days (Cronkite, 1973)).

## 31.4 CLEARANCE OF ACTINIDES FROM THE CIRCULATION

Data for plasma clearances and early urinary excretion of the actinides in laboratory animals and man can be combined with the information developed for their reactions with the plasma constituents to assess their status in the circulation.

Plasma clearances of nine actinides injected iv in soluble form have been investigated in at least one mammalian species (data are not available for $Ac^{3+}$ or $Bk^{3+}$). Industrially important $UO_2^{2+}$, $Pu^{4+}$, and $Am^{3+}$ have been studied in several species. Plasma clearance data are available for two valence states of U ($U^{4+}$, $UO_2^{2+}$), two of Pu ($Pu^{4+}$, $PuO_2^{2+}$), and three of Np ($Np^{4+}$, $NpO_2^{+}$, $NpO_2^{2+}$). Plasma clearance curves of the actinides are shown in Figs. 31.3–31.7, in rats, mice, beagles, nonhuman primates, and human adults, respectively. The plasma clearances of iv-injected $Pu^{4+}$, $Am^{3+}$, and $UO_2^{2+}$ in the laboratory animals and human adults are compared in Figs. 31.8, 31.9, and 31.10, respectively.

The rates of clearance of the several actinides from mammalian plasma are determined largely by their chemical properties, in particular by their tendencies to form stable complex(es) with plasma Tf. The actinides that form the most stable Tf complexes are cleared slowly, whereas those that form only weak Tf complexes are cleared at much faster rates. The order of disappearance of the actinides introduced into mammalian plasma is independent of the animal used for study (Figs. 31.3–31.7). Combining the data for all of the animals, and based

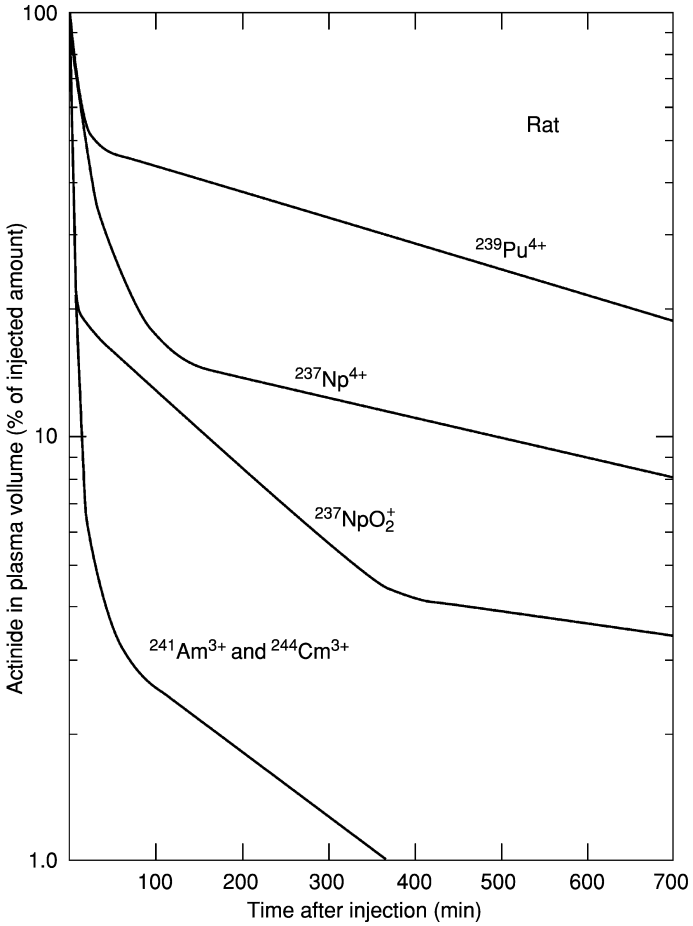


**Fig. 31.3** *Clearance of iv-injected actinides from plasma volume of rats:* $^{239}Pu^{4+}$ (*Durbin* et al., 1972); $^{241}Am^{3+}$ *and* $^{244}Cm^{3+}$ (*Turner and Taylor*, 1968a); $^{237}Np^{4+}$ *and* $^{237}NpO_2^+$ (*Ramounet* et al., 1998).

on the time (min) required to clear 90% of the iv-injected actinide from the plasma volume, plasma clearance rates are in the order:

$$[UO_2^{2+}, Am^{3+}, Cm^{3+}, NpO_2^+] > [Cf^{3+}, Es^{3+}] \gg [Th^{4+}, Np^{4+}, Pa^{5+}, Pu^{4+}].$$

Note that the 90% plasma clearance measure does not differentiate among the rapidly clearing lighter trivalent actinides and the actinide dioxo ions, which are all cleared at about the same rate, but by different mechanisms.

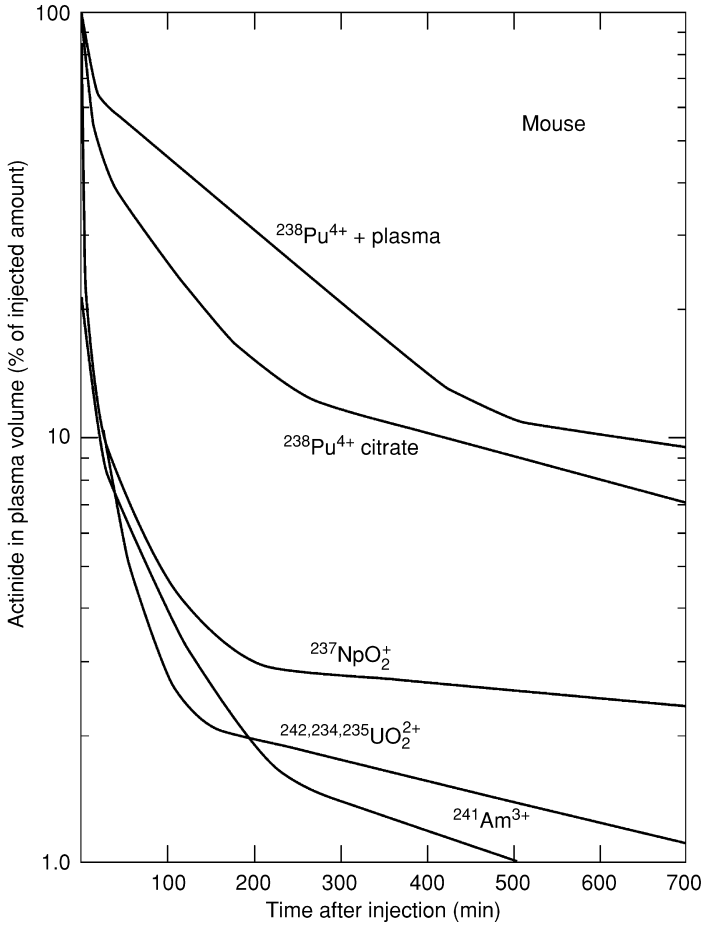


**Fig. 31.4** *Clearance of iv-injected actinides from plasma volume of mice*: $^{238}Pu^{4+}$ *citrate* (*Durbin* et al., 1997b); $^{237}NpO_2^+$ (*Durbin* et al., 1998b); $^{232,234,235}UO_2^{2+}$ (*Durbin* et al., 1997a); $^{241}Am^{3+}$ and $^{238}Pu^{4+}$ + *plasma* (*P. W. Durbin and B. Kullgren, unpublished data*).

Plasma clearance of the actinides is modulated by the physiology of the animals used for study. Plasma retention of $Pu^{4+}$, $Am^{3+}$, and $UO_2^{2+}$ in the different animals, as illustrated in Figs. 31.8–31.10, is in the order:

$$\text{adult man} > \text{dog} > \text{baboon} \geq \text{monkey} > \text{rat} > \text{mouse}.$$

Plasma actinide retention among the different animals is directly related to body size and inversely related to metabolic rate, renal filtration rate, and the degree of Fe saturation of the plasma Tf (Brody, 1945; Durbin *et al.*, 1997b; Table 31.10).

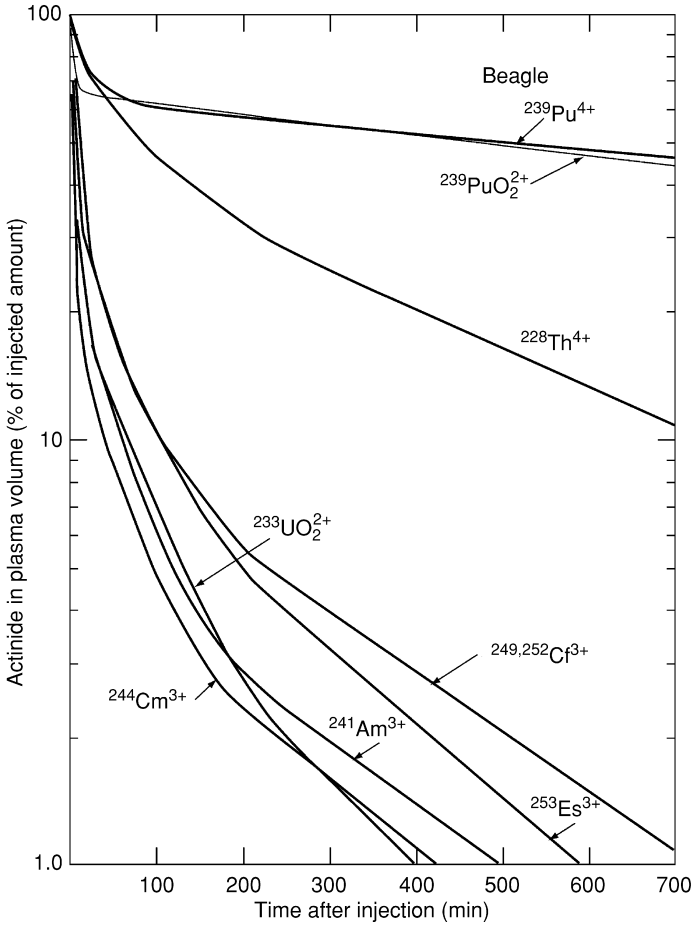


**Fig. 31.5** *Clearance of iv-injected actinides from plasma volume of beagles:* $^{239}Pu^{4+}$, $^{228}Th^{4+}$, $^{241}Am^{3+}$, $^{249}Cf^{3+}$, and $^{252}Cf^{3+}$ (*Stevens and Bruenger,* 1972); $^{244}Cm^{3+}$ (*Atherton* et al., 1973); $^{253}Es^{3+}$ (*Atherton* et al., 1974); $^{233}UO_2^{2+}$ (*Stevens* et al., 1980); $^{239}PuO_2^{2+}$ (*Painter* et al., 1946).

### 31.4.1 Trivalent actinides

#### (a) $Ac^{3+}$

Timed plasma data for $Ac^{3+}$ injected iv in rats are insufficient to define a clearance curve, however, the pattern of disappearance of $^{227}Ac^{3+}$ from the plasma is similar to $Am^{3+}$ and $Cm^{3+}$ in the same animals (Fig. 31.3). Clearance was 90% complete in about 50 min and 99% complete in about 400 min. Also

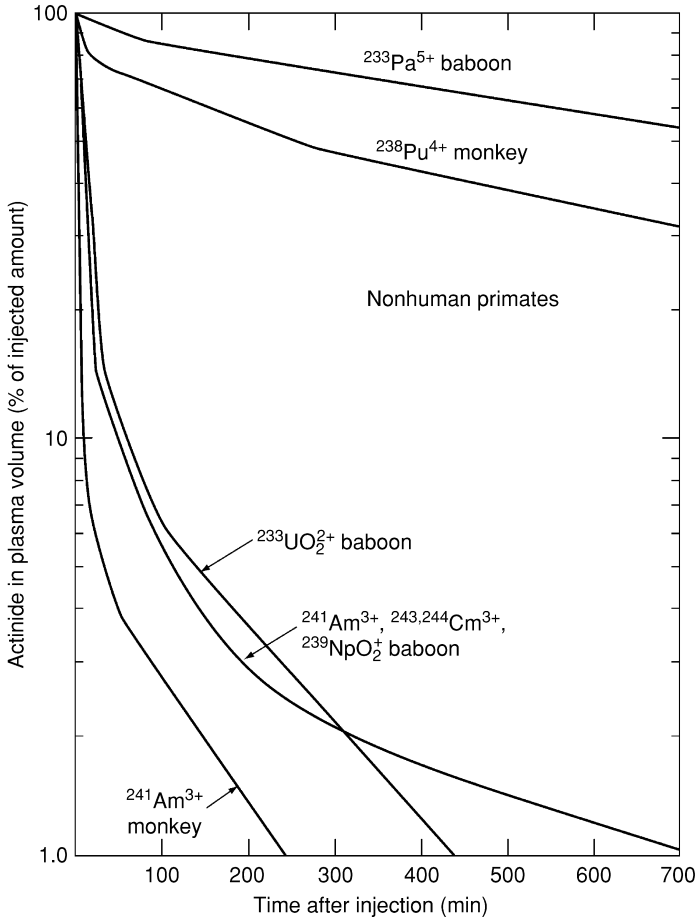


**Fig. 31.6** *Clearance of iv-injected actinides from plasma volume of nonhuman primates: monkey* – $^{238}Pu^{4+}$ (*Durbin* et al., 1985), $^{241}Am^{3+}$ (*Durbin,* 1973); *baboon* – $^{241}Am^{3+}$ (*Guilmette* et al., 1980), $^{243,244}Cm^{3+}$ (*Lo Sasso* et al., 1981), $^{233}UO_2^{2+}$ (*Lipsztein,* 1981), $^{239}NpO_2^{+}$ and $^{233}Pa^{5+}$ (*Ralston* et al., 1986). (*Note: The curves for* $^{241}Am^{3+}$, $^{243,244}Cm^{3+}$, and $^{239}NpO_2^{+}$ *in the baboons coincide, and a single curve is shown for all three nuclides.*)

similarly to $Am^{3+}$ and $Cm^{3+}$, tissue uptake was fast, and early urinary excretion was negligible (Taylor, 1970).

### (b) $Am^{3+}$, $Cm^{3+}$, $Cf^{3+}$, $Es^{3+}$

Plasma clearances of iv-injected $^{241}Am^{3+}$ citrate or nitrate have been studied in five laboratory animals (Figs. 31.3–31.6, 31.9), and $^{243}Cm^{3+}$ or $^{244}Cm^{3+}$ citrate have been studied in three (Figs. 31.3, 31.5, and 31.6). Separate plasma curves

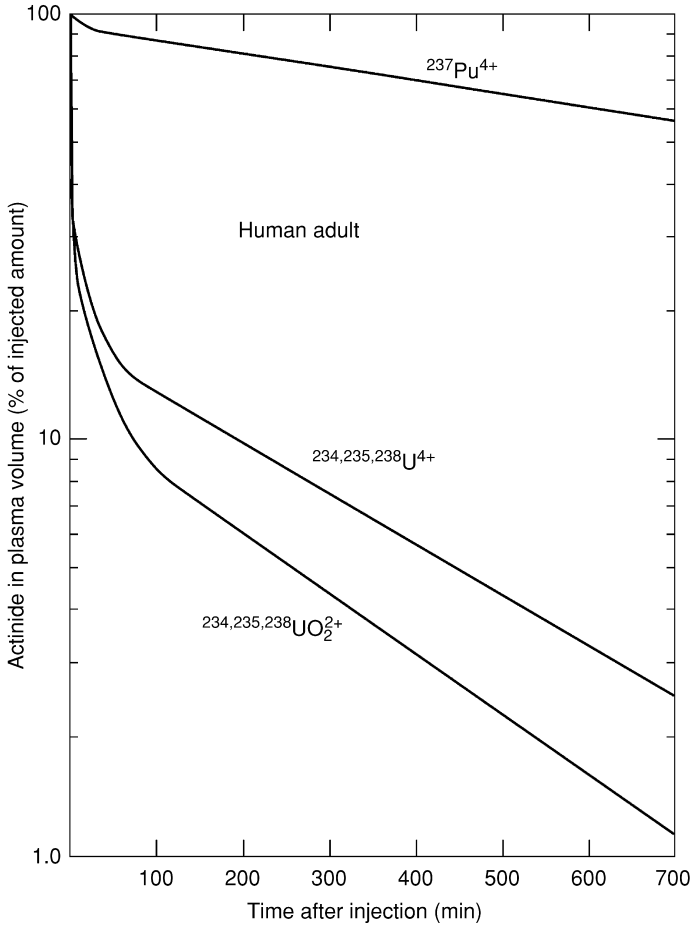


**Fig. 31.7** *Clearance of iv-injected actinides from blood volume of adult human males:* $^{237}Pu^{4+}$ (*Talbot* et al., 1993); $^{234,235,238}U^{4+}$ *and* $^{234,235,238}UO_2^{2+}$ (*Bernard and Struxness*, 1957).

are not shown for $Cm^{3+}$ in the rats (Fig. 31.3) or the baboons (Fig. 31.6), because they are indistinguishable from those for $Am^{3+}$ in those animals. Clearances of $Am^{3+}$ and $Cm^{3+}$ from the plasma are fast: in all of the animals studied, they were 90% complete in 60 min and 99% complete in $\leq$600 min. Tissue uptake of both trivalent actinides is fast, and only small amounts are excreted in urine in the first 24 h (Taylor, 1962; Turner and Taylor, 1968a; Belyayev, 1969; Durbin, 1973).

Clearances of $^{249,252}Cf^{3+}$ and $^{253}Es^{3+}$ from the plasma of beagles was 90% complete in about 100 min, compared with 60 min for the two lighter larger

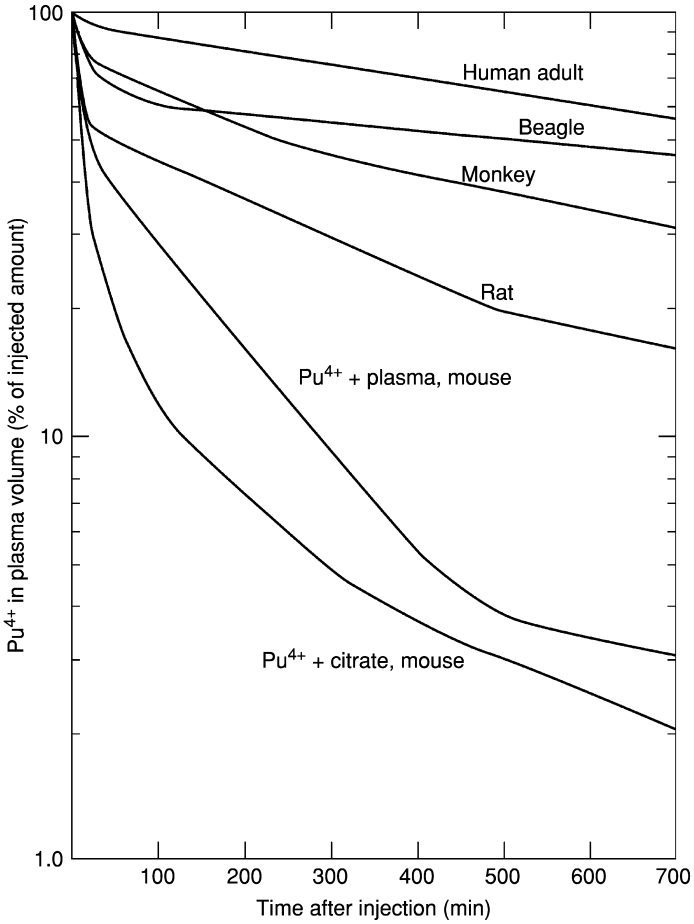


**Fig. 31.8** *Clearance of iv-injected* $Pu^{4+}$ *from plasma volume of animals and man:* $^{239}Pu^{4+}$, *rat* (*Durbin* et al., 1972); $^{238}Pu^{4+}$, *mouse* (*Durbin* et al., 1997b); $^{239}Pu^{4+}$, *beagle* (*Stevens and Bruenger,* 1972); $^{238}Pu^{4+}$, *monkey* (*Durbin* et al., 1985); $^{237}Pu^{4+}$, *adult human male* (*Talbot* et al., 1993); $^{238}Pu^{4+}$ + *plasma, mouse* (*P. W. Durbin and B. Kullgren, unpublished data*).

trivalent actinides, and the time required for 99% clearance of $Cf^{3+}$ and $Es^{3+}$ was about 200 min longer (Fig. 31.5). The slower plasma clearances of $Cf^{3+}$ and $Es^{3+}$, compared with $Am^{3+}$ and $Cm^{3+}$, confirmed the expectation that the two heavier smaller trivalent actinides would form more stable plasma protein complexes (Stevens and Bruenger, 1972; Atherton *et al.*, 1974).

Immediately after iv injection, the plasma contains rapidly declining fractions of the trivalent actinides in the form of the filterable low molecular weight complex injected (Turner and Taylor, 1968a). The major fraction apparently

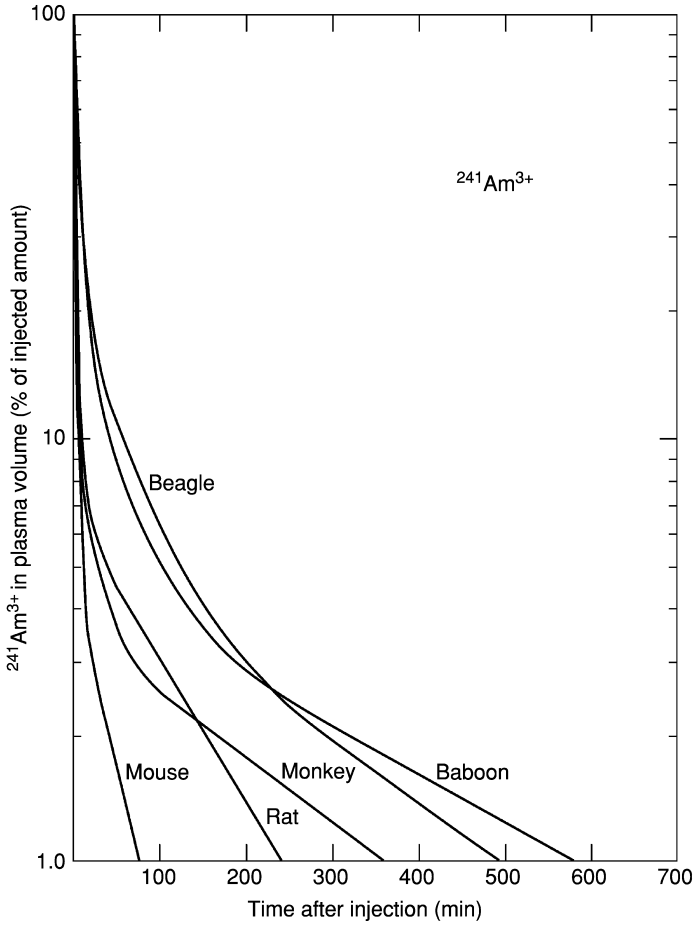


**Fig. 31.9** *Clearance of iv-injected* $^{241}Am^{3+}$ *from the plasma volume of animals: rat* (*Turner and Taylor,* 1968a); *mouse* (*P. W. Durbin and B. Kullgren, unpublished data*); *beagle* (*Stevens and Bruenger,* 1972); *monkey* (*Durbin,* 1973); *baboon* (*Guilmette* et al., 1980).

forms weak nonfilterable complex(es) with Tf and other plasma proteins, which prevent renal filtration into urine, but are much less stable than the complexes that the trivalent actinides can form with ligands on hepatic cell and bone surfaces and in connective tissue.

In rats injected iv with $Am^{3+}$ or $Cm^{3+}$ citrate, about 50% was protein bound at 1 min and 95% was bound at 60 min (Turner and Taylor, 1968a). *In vivo* and *in vitro* studies of the associations of $Ac^{3+}$, $Am^{3+}$, $Cm^{3+}$, and $Cf^{3+}$ with plasma proteins show that Tf is a major carrier of the trivalent actinides in mammalian plasma, however, those complexes are weak, and they do not survive the more

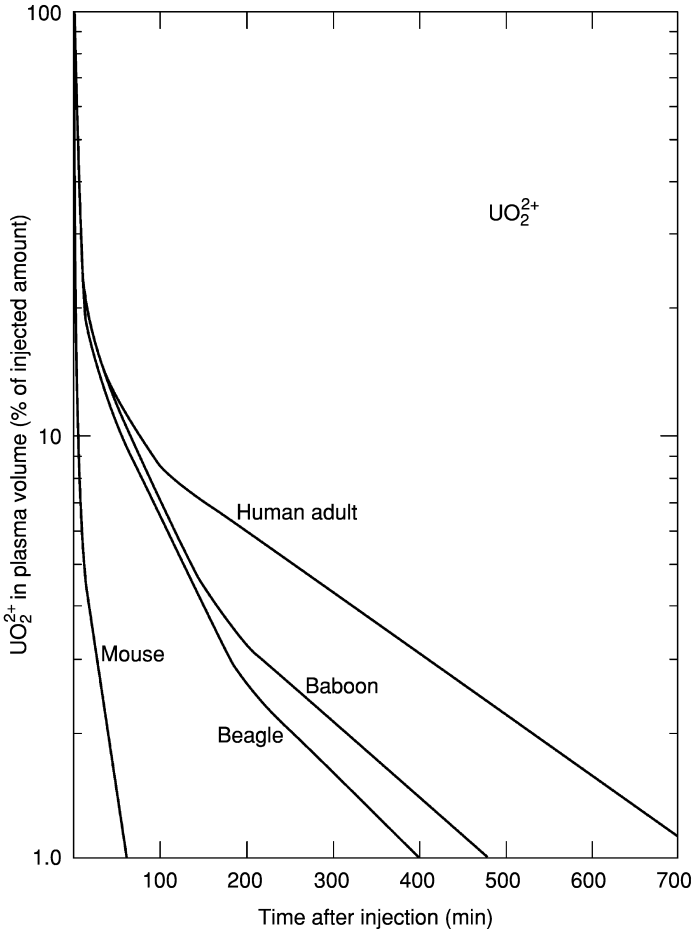


**Fig. 31.10** *Clearance of iv-injected* $UO_2^{2+}$ *from the plasma volume of animals and man:* $^{232}UO_2^{2+}$ *mouse* (*Durbin* et al., 1997a); $^{233}UO_2^{2+}$ *beagle* (*Stevens* et al., 1980); $^{233}UO_2^{2+}$ *baboon* (*Lipsztein,* 1981); $^{234,235,238}UO_2^{2+}$ *adult human male* (*Bernard and Struxness,* 1957).

rigorous analytical procedures (Popplewell and Boocock, 1968; Turner and Taylor, 1968a; Bruenger *et al.*, 1969b, 1971b; Taylor, 1970; Stevens and Bruenger, 1972; Cooper and Gowing, 1981). Provisional formation constants (log $K_1$) have been calculated, 5.3 and 6.5 for $Am^{3+}$ and $Cm^{3+}$, respectively (Taylor, 1998), and these are similar to the value of the apparent stability constant for binding of $Gd^{3+}$ to the C-terminal site of human Tf (Zak and Aisen, 1988).

Binding of $Am^{3+}$ by Tf is reduced when $Fe^{3+}$ saturation of Tf is high and eliminated altogether by addition of $Fe^{3+}$ in excess of the Tf iron-binding

capacity (Popplewell and Boocock, 1968; Bruenger *et al.*, 1969b). The trivalent actinides also bind to plasma proteins other than Tf. Depending on the experimental conditions and the analytical methods, variable fractions of the trivalent actinides in plasma associate with the heaviest proteins and with albumin (Turner and Taylor, 1968a; Bruenger *et al.*, 1969b, 1971b; Stevens and Bruenger, 1972).

### 31.4.2 Tetravalent and pentavalent actinides

#### (a) $Th^{4+}$

Clearance of iv-injected $^{228}Th^{4+}$, studied only in beagles, is somewhat faster than, but comparable to that of $^{239}Pu^{4+}$ in the same animal (Fig. 31.5). Reduction to 10% occurred in 0.5 day, and 99% of the injected $Th^{4+}$ had disappeared from the plasma in 1.5 days. A larger fraction of the $Th^{4+}$ was excreted in 21 days than was found for $Pu^{4+}$ (Table 31.4).

Transferrin is the main protein carrier of $Th^{4+}$ in the plasma. The larger $Th^{+}$ ion forms a Tf complex that appears to be less stable than the $Pu^{4+}$–Tf complex. Similarly to $Pu^{4+}$, the $Th^{4+}$–Tf complex is destabilized by excess $Fe^{3+}$. Binding of $Th^{4+}$ to Tf is suppressed in $Fe^{3+}$-saturated plasma, permitting formation of less stable complexes with the heavier plasma proteins and small filterable ligands (Bruenger *et al.*, 1971a; Peter and Lehmann, 1981; Pecoraro *et al.*, 1981).

#### (b) $U^{4+}$

Clearance from the blood of iv-injected $^{234,235,238}U^{4+}$ was studied in rats (data not shown, Neuman, 1949) and an adult man (Table 31.7, Fig. 31.7; Bernard and Struxness, 1957). Based on their similar properties, the disposition of $U^{4+}$ *in vivo* would be expected to resemble $Th^{4+}$ and $Pu^{4+}$, with stable binding to plasma protein and delayed blood clearance (Tables 31.4, 31.7; Figs. 31.5, 31.7). However, disappearance from the blood of both the rats and man of U injected iv as $U^{4+}$ was fast. In humans, it was 90% complete in 200 min and 99% complete in 24 h. During the first hour after injection, clearance from the blood of U injected as $U^{4+}$ was nearly the same as that of $UO_2^{2+}$ (Fig. 31.7). Thereafter, U in the blood declined at nearly the same rate as $UO_2^{2+}$, but the U concentration in the blood was about 1.7 times greater that of $UO_2^{2+}$. Overall, the clearance of $U^{4+}$ from human blood closely resembled that of $UO_2^{2+}$ and differed markedly from the plasma clearances of $Th^{4+}$ and $Pu^{4+}$ in the dogs and $Pu^{4+}$ in adult men.

By analogy to $Th^{4+}$ and $Pu^{4+}$, binding of $U^{4+}$ by circulating Tf would be expected, but there is little evidence for such stable binding *in vivo*. The absence from the $U^{4+}$ blood curve of a major rapidly forming and slowly clearing component argues against formation of a stable $U^{4+}$–Tf complex *in vivo*.

When $^{233}U^{4+}$ citrate was added to plasma *in vitro* and chromatographed on G-25 Sephadex, <10% of the U eluted with the plasma proteins (Bruenger *et al.*, 1971b).

### (c) $Np^{4+}$

Plasma clearance of $Np^{4+}$ was studied in rats injected iv with about 310 μg $kg^{-1}$ (0.4 μmol per rat) of $^{237}Np^{4+}$ citrate, and plasma was sampled at 1, 2, 6, and 24 h (Fig. 31.3, Ramounet *et al.*, 1998). Paquet *et al.* (1996) injected rats iv with a tracer of $^{239}Np^{4+}$ citrate (17 pg $kg^{-1}$) or 1.2 mg $kg^{-1}$ (1.1 μmol per rat) of $^{237}Np^{4+}$ citrate. Blood was sampled only at 24 h, at which time the plasma volumes of both groups contained 4 to 5% of the injected Np, in good agreement with the data of Fig. 31.3. Because no blood samples were taken sooner than 60 min after injection, the earliest phases of the plasma clearance curve for $Np^{4+}$ are poorly defined. Renal excretion of Np at 24 h was about 20% of the amount injected regardless of the mass of $Np^{4+}$ injected.

Based on their similar chemical properties, plasma clearances of $Np^{4+}$ and $Pu^{4+}$ would be expected to be similar, that is, slow clearance accompanied by slow tissue uptake and little early urinary excretion (Table 31.2). In the rats, plasma clearances of $Np^{4+}$ and $Pu^{4+}$ were 90% complete in 500 and 1150 min, respectively. After 2 h, their clearance rates were similar, and 99% of both actinides disappeared from the blood in 2 days. Extrapolation of the terminal slope of the $Np^{4+}$ plasma curve (Fig. 31.3) to $t = 0$ suggests that about 16% of the injected $Np^{4+}$ circulated bound to nonfilterable protein, compared with stable protein binding of ≥50% of the $Pu^{4+}$.

Sephacryl S-300 and DEAE-cellulose chromatography were used to investigate protein binding of Np in the plasma taken from rats 30 min after iv injection of 10 μCi of $^{239}NpO_2^+$ nitrate. At 30 min after injection, based on the plasma clearances of $NpO_2^+$ in other animals (Figs. 31.3, 31.4, and 31.6), it may be estimated that about 5% of the injected Np would still be in the plasma, most likely bound to protein. Both chromatographic techniques showed that ≥95% of the Np applied to the columns colocated with the Fe–Tf peak. Results were essentially the same when $^{239}NpO_2^+$ was incubated with rat serum *in vitro*, except that the fraction of Np applied to the columns eluting with the Tf peak was reduced to about 70%. Specific Np binding to Tf was confirmed by manipulation of the Fe saturation of the Tf; the association of the Np with the Tf peak decreased as the iron saturation of the Tf was increased. In highly $Fe^{3+}$-saturated preparations, larger fractions of the Np tended to be associated with both the heavier plasma proteins and with the low molecular weight solutes (Wirth *et al.*, 1985). These studies demonstrated binding of Np to Tf, but as Wirth *et al.* (1985) and Taylor (1998) suggest, it is likely to be complexation of $Np^{4+}$ rather than of the weakly complexing $NpO_2^+$. These results also imply that some of the $^{239}NpO_2^+$ injected in the rats or added to rat serum *in vitro* was reduced to $Np^{4+}$.

### (d) $Pu^{4+}$

Plasma clearances of iv-injected $Pu^{4+}$ citrate are shown in Figs. 31.3–31.7 for rats, mice, beagles, monkeys, and human adults, respectively, and Fig. 31.8 compares the clearances of $Pu^{4+}$ in all of these animals. Clearance of $Pu^{4+}$ from the plasma is slow in all of the mammals studied. It was 90% complete in 0.2 to 0.75 day in mice and rats and 1.5 to 5 days in monkeys, beagles, and human adults. Reduction of plasma $Pu^{4+}$ to 1% of its initial value required from 0.7 to 1 day in the rodents and 2.5 to 21 days in the larger animals and man.

Delayed clearance from the plasma of rats and dogs of iv-injected $^{239}Pu^{4+}$ or $^{239}PuO_2^{2+}$ and minimal amounts of urinary Pu excretion in the first 24 h were indications that Pu introduced into mammalian plasma was rapidly and almost quantitatively bound to nonfilterable plasma protein (Finkle *et al.*, 1946; Painter *et al.*, 1946; Muntz and Guzman-Barron, 1947; Stevens *et al.*, 1968). Slow plasma clearance of $Pu^{4+}$ along with minimal renal excretion is evidence for rapid formation of a stable $Pu^{4+}$ complex with plasma protein and for the slow kinetics of the exchanges of $Pu^{4+}$ between Tf and the tissue ligands.

Transferrin is the main, if not the only, protein carrier of $Pu^{4+}$ in normal mammalian plasma (Popplewell and Boocock, 1968; Stevens *et al.*, 1968, 1975; Stover *et al.*, 1968a; Turner and Taylor, 1968a,b; Bruenger *et al.*, 1971a; Durbin *et al.*, 1976; Lehmann *et al.*, 1983; Taylor, 1998). A provisional stability constant derived for $Pu^{4+}$–Tf (log $K_1$=21.8, Taylor, 1998) is close to but less than that derived for $Fe^{3+}$–Tf (log $K_1$=24; Raymond *et al.*, 1980). Pu–Tf is destabilized by reduction of the pH, by addition of excess $Fe^{3+}$, and by increasing the concentration of citrate ion to ten times that of normal plasma. The latter two reactions may contribute to the release of $Pu^{4+}$ from Tf to competing tissue ligands.

A small fraction ($\leq$5%) of circulating $Pu^{4+}$ is associated with low molecular weight plasma ligands, suggesting that an equilibrium exists between those ligands and the Tf-bound fraction of circulating $Pu^{4+}$. In highly $Fe^{3+}$-saturated plasma, $Pu^{4+}$ can bind to the heavier proteins, and a larger than usual fraction associates with the low molecular weight ligands (Popplewell and Boocock, 1968; Stover *et al.*, 1968a).

### (e) $Pa^{5+}$

Baboons were injected iv with $10^{-6}$ μg $kg^{-1}$ of $^{233}Pa^{5+}$ in 0.08 M Na citrate pH 3.2, and blood was sampled frequently for 21 days (Fig. 31.5, Cohen and Ralston, 1983; Ralston *et al.*, 1986). Clearance of the $Pa^{5+}$ from the plasma was slower than that of $^{239}Pu^{4+}$ citrate in beagles (Figs. 31.5 and 31.8), and comparable to that of $^{237}Pu^{4+}$ in adult men (Figs. 31.7 and 31.8). Plasma clearance was 90% complete in 6 days and 99% complete in 21 days. It was as slow as the plasma clearances of $Pu^{4+}$ and $Th^{4+}$ in the beagles, and along with low early urinary excretion, a good indication of the formation of a stable $Pa^{5+}$ plasma protein complex.

$Pa^{5+}$, incubated with normal human plasma *in vitro*, was associated with the Tf peak, indicating that the stable complex was $Pa^{5+}$–Tf (Bruenger *et al.*, 1971b). Taylor and Farrow (1987) prepared a solution for animal injection by diluting a stock solution of $^{233}Pa^{5+}$ in 8 M HCl with normal saline and adjusting to pH 7 with $NaHCO_3$. The distribution of the $Pa^{5+}$ in the serum from rats killed and bled at 5 and 50 min after injection was investigated by gel and ion-exchange chromatography and electrophoresis. In all procedures, the $^{233}Pa^{5+}$ was associated only with the Tf fraction of the serum proteins.

In normal mammalian plasma, Tf binds $Th^{4+}$, $Np^{4+}$, and $Pu^{4+}$ (Peter and Lehmann, 1981; Lehmann *et al.*, 1983; Wirth *et al.*, 1985). Binding of those tetravalent actinides by Tf is reduced in Fe-saturated serum, and they are all released from their Tf complexes by treatment with excess $Fe^{3+}$. These findings are regarded as evidence that $Fe^{3+}$–Tf is more stable than the actinide$^{4+}$–Tf complexes. In contrast, Tf binding of $Pa^{5+}$ was not prevented by presaturation of Tf with $Fe^{3+}$, nor was it reversed by addition *in vitro* of excess iron to rat serum containing $Pa^{5+}$ (Taylor and Farrow, 1987). Those findings suggest that the $Pa^{5+}$–Tf complex is more stable than the Tf complexes of the tetravalent actinides and also more stable than $Fe^{3+}$–Tf.

### (f) Summary

The charge/radius ratios of ferric iron and the tetra- and pentavalent actinides are, in units of e $nm^{-1}$, as follows: $Pa^{5+}$, 54.9; $Fe^{3+}$, 46.2; $Pu^{4+}$, 41.7; $Np^{4+}$, 40.8; $Th^{4+}$, 38.1 (eight-coordination is assumed for the actinides, six-coordination is assumed for $Fe^{3+}$, Table 31.8) (Shannon, 1976). Based on the positive correlation of the stabilities of actinide complexes and their charge/radius ratios, the stabilities of their Tf complexes would be predicted to be in the above order. The apparent stabilities of their Tf complexes in normal mammalian plasma relative to one another and to $Fe^{3+}$ are in that expected order.

## 31.4.3 The dioxo ions

### (a) $UO_2^{2+}$

Plasma clearance of iv-injected $UO_2^{2+}$ has been studied in mice, beagles, baboons, and human adults (Figs. 31.4–31.7, 31.10). It was fast in all of the species studied; clearance was 90% complete in 10 to 80 min, and 99% was cleared in 60 to 700 min. Urinary excretion and uptake of $UO_2^{2+}$ in the tissues are fast, as illustrated by measurements in mice (Durbin *et al.*, 1997a). Both processes begin immediately after the $UO_2^{2+}$ is introduced into the blood and continue until the plasma is cleared (about 100 min). Diffusion of filterable low molecular weight complexes between the plasma and tissue fluid and weak binding to plasma protein briefly delay, but do not otherwise interfere with renal filtration of $UO_2^{2+}$ or its deposition in the skeleton.

During the first few days after intake to blood about 85% of absorbed $UO_2^{2+}$ is filtered through the kidneys, about 85% of the filtered fraction is eliminated in passed urine, but about 12% of the injected $UO_2^{2+}$ is deposited in the kidneys (Tables 31.2–31.7). The $UO_2^{2+}$ retained in the kidneys is bound mainly to the brush border of the luminal surfaces of the cells that line the proximal tubules, the site of the renal injury (Tannenbaum, 1951a,b). Binding of $UO_2^{2+}$ to cell membranes is the presumed cause of the cell damage, but the mechanism – conformational changes, blockage of ion channels that interfere with the cell's absorptive functions, and/or inhibition of membrane enzymes required for cell respiration – is not certain (Dounce, 1949; Kirschbaum and Oken, 1979; Kirschbaum 1982; Leggett, 1989).

The large fraction of circulating $UO_2^{2+}$ that is rapidly excreted in urine is indicative of formation of ultrafilterable $UO_2^{2+}$ complexes with low molecular weight ligands in the plasma. Uranyl ion is rapidly and quantitatively absorbed from an im or sc injection site (Tables 31.2 and 31.5), even though formation of *in situ* poorly transportable hydrolysis products is expected at physiological pH, indicating that sufficient concentrations of ligands for $UO_2^{2+}$ are also present in tissue fluid. Bicarbonate was presumed to be the dominant ligand for $UO_2^{2+}$ in the body fluids; $UO_2^{2+}$ complexes with phosphate and organic acids were considered to be of lesser importance (Dounce and Flagg, 1949; Muntz and Guzman-Barron, 1951).

The evidence for bicarbonate as the principal low molecular weight ligand for $UO_2^{2+}$ in body fluids was indirect. Addition of $HCO_3^-$ greatly increased the ultrafilterability of $UO_2^{2+}$ added to blood serum. Protein precipitated with $UO_2^{2+}$ redissolved, and enzymes inhibited with $UO_2^{2+}$ were reactivated by addition of $HCO_3^-$. The urinary pH of cats and rabbits was lowered or raised by manipulation of their diets: acidification of the urine reduced $UO_2^{2+}$ excretion and increased $UO_2^{2+}$ deposition in the kidneys. Conversely, alkalinization increased urinary $UO_2^{2+}$ excretion and reduced $UO_2^{2+}$ deposition in the kidneys. Infusion of excess $HCO_3^-$ in rabbits injected iv with $UO_2^{2+}$ resulted in more and more rapid urinary $UO_2^{2+}$ excretion and even less $UO_2^{2+}$ retention in the kidneys than increasing urinary pH alone. The stability of the filtered $UO_2^{2+}$ complex was more dependent on the concentration of $HCO_3^-$ in the filtrate than on the pH (Dounce, 1949; Dounce and Flagg, 1949; Wills, 1949; Muntz and Guzman-Barron, 1951).

The abundance of $HCO_3^-$ in both plasma and tissue fluid greatly exceeds those of the other low molecular weight ligands (phosphate, organic acids, Table 31.9). Uranyl carbonate complexes are more stable than those with phosphate and citric acid (Table 31.8; Grenthe *et al.*, 1992). The circulating filterable $UO_2^{2+}$ complex is pH-dependent, whereas $UO_2$ citrate is stable over the physiological pH range (Dounce and Flagg, 1949).

About 40% of circulating $UO_2^{2+}$ is bound to nonfilterable plasma protein. Based on estimated molecular weight and electrophoretic properties, the protein that bound $UO_2^{2+}$ was originally thought to be serum albumin (Dounce, 1949;

Dounce and Flagg, 1949; Muntz and Gurman-Barron, 1951). Stevens *et al.* (1980) demonstrated that the protein that binds $UO_2^{2+}$ in plasma is Tf. The $UO_2^{2+}$–Tf complex is demonstrably weaker than the complexes that $UO_2^{2+}$ forms with carbonate. As the plasma $UO_2^{2+}$ is depleted by glomerular filtration of the low molecular weight complexes, the equilibrium between the filterable and nonfilterable complexes is continuously reestablished by dissociation of the nonfilterable protein complex and shift to the filterable complex until $UO_2^{2+}$ has been cleared from the plasma by renal filtration and binding to bone.

As the plasma ultrafiltrate formed by the renal glomeruli is converted to bladder urine >99% of the water and electrolytes are reabsorbed, mainly in the proximal tubules, and the pH is reduced. Bicarbonate and phosphate are preferentially reabsorbed as the fluid passes through the proximal tubule, and by the time the tubular fluid enters the last third of the proximal tubule (the site of $UO_2^{2+}$ deposition and renal injury), their concentrations are 0.35 and 0.50, respectively, of those in the plasma (Wong *et al.*, 1986). Under these conditions $UO_2^{2+}$ carbonate complexes formed in the plasma will become less stable.

The concentration of $HCO_3^-$ in bladder urine is usually <1% of that in plasma, and the pH is about 6, whereas the concentrations of phosphate and citrate are slightly greater than in the plasma (Table 31.9). The $UO_2^{2+}$ carbonate complexes formed in the plasma cannot survive the transit through the entire renal tubule system to the bladder, and the chemical form of $UO_2^{2+}$ in urine is not likely to be the same as in the circulating fluids.

Speciation calculations can be used to identify and provide estimates of the relative concentrations of the $UO_2^{2+}$ complexes that are likely to form in biological fluids. Concentrations of the important constituents of human plasma and bladder urine are shown in Table 31.9. The concentrations of these constituents in the fluid entering the last third of the proximal renal tubules (site of $UO_2^{2+}$ deposition and renal injury) were estimated from the renal micropuncture data of Wong *et al.* (1986) (Table 31.9). Concensus values are available for the formation constants of the $UO_2^{2+}$ complexes with the ligands in biological fluids at $T = 25°C$ and ionic strength $I = 0.1$ M, the closest match to the conditions in biological fluids. A very stable soluble neutral dicalcium uranyl triscarbonate complex, $Ca_2UO_2(CO_3)_3(aq)$, was shown to influence the speciation of $UO_2^{2+}$ in the region pH 6 to 10 of calcite-rich U mining waters (Bernhard *et al.*, 2001). That complex was included in the present calculations, because the chemical conditions in the mine waters resemble those in blood plasma and renal tubular fluid, both of which are nearly neutral and contain significant concentrations of $Ca^{2+}$ and $HCO_3^-$.

### (*i*) *Complexes in plasma*

The conditions for the plasma calculations were, as follows: Data for the human $UO_2^{2+}$ injection case (Table 31.7) were combined with human data for fluid volumes and Tf concentrations (Table 31.10) to calculate an initial $UO_2^{2+}$

concentration in plasma of $10^{-5}$ M and a concentration of available Tf-binding sites of $3.6 \times 10^{-5}$ M. The partitioning of $UO_2^{2+}$ in the plasma was set at 60% associated with ultrafilterable ligands and 40% bound to nonfilterable Tf (Stevens *et al.*, 1980). No correction was made for the small fraction of newly injected $UO_2^{2+}$ ($\leq$4%) that is transiently associated with red blood cells (Dounce, 1949; Stevens *et al.*, 1980; Lipsztein, 1981; Durbin *et al.*, 1997a).

The set of equations for the competing reactions was solved simultaneously. The predominant filterable $UO_2^{2+}$ complex in the plasma, identified as $Ca_2UO_2(CO_3)_3(aq)$, can account for 86% of the filterable $UO_2^{2+}$, with 13% in the form of the triscarbonate complex, and about 1% as the biscarbonate (Table 31.11). The selected concentration of Tf-binding sites and fraction of $UO_2^{2+}$ bound to Tf yielded a value for the formation constant of $UO_2^{2+}$–Tf, $\log K_f = 14.5$, which agrees reasonably well with a reported value of $\log K_f = 16$ determined in a solution much more dilute than 0.1 M NaCl (Ansoborlo *et al.*, 2003).

### (*ii*) *Complexes in proximal renal tubular fluid*

Only a crude estimate can be made of the speciation of the $UO_2^{2+}$ complexes that exist in the chemical milieu of the fluid flowing through the late proximal renal tubules, because the fluid in the last third of the proximal tubules is not accessible to micropuncture sampling. The composition of the tubular fluid shown in

**Table 31.11** $UO_2^{2+}$ *complexes with the low molecular weight ligands of biological fluids as identified by speciation calculations.*[a,b]

| | *Distribution of* $UO_2^{2+}$ *complex species* (% *of total*) | | | |
|---|---|---|---|---|
| $UO_2^{2+}$ *complex* | $\log K_f$ | *Plasma ultrafiltrate* | *Late proximal tubule fluid*[c] | *Bladder urine* |
| $UO_2(CO_3)_2^{2-}$ | 16.2[c] | 0.6 | 7.0 | 0.2 |
| $UO_2(CO_3)_3^{4-}$ | 21.6[c] | 13 | 6.3 | <0.1 |
| $Ca_2UO_2(CO_3)_3(Aq)$ | 28.1[d] | 86 | 73 | 0.4 |
| $UO_2HPO_4$ | 7.2[c] | <0.1 | 0.3 | 77 |
| $UO_2$ citrate | 7.4[e] | <0.1 | 0.5 | 22 |
| 'Tubule protein'[f] | – | – | 13 | – |

[a] Values for formation constants at $T$=25°C and ionic strength $I$=0.1 used as best match to 0.14 M NaCl in biological fluids.
[b] The ionization constant for $HCO_3^-$ given in Grenthe *et al.* (1992) was recalculated to $\log K_{i=}$–9.9 at ionic strength $I$=0.1 M.
[c] NEA (1992). Calculated from composition of fluid entering last third of proximal tubules.
[d] Bernhard *et al.* (2001).
[e] Martell and Smith (1977).
[f] Membrane of proximal tubule microvilli.

Table 31.9 is the set of measurements made closest to the beginning of the last third of the proximal tubules (Wong *et al.*, 1986). The concentration of $HCO_3^-$ and the tubular fluid pH continue to be reduced during the traverse of the last portion of the proximal tubule, but by how much before the fluid enters the more distal nephron cannot be estimated, because Wong *et al.* (1986) did not report measurements of the concentration of $HCO_3^-$ in the distal tubules.

Specification of chemical conditions for the tubular fluid calculations introduces additional uncertainty. During its transit through the last third of the proximal tubules, about 13% of the injected $UO_2^{2+}$ is lost from the fluid phase and is deposited on the membrane of the brush border microvilli. To take account of that loss to protein binding, it was assumed that the contact between the tubular fluid and the membrane of the microvilli was so intimate that the membrane protein could be considered to be 'virtually' in solution. The concentration of membrane protein-binding sites was set at $10^{-4}$ M, assuming that the binding sites for $UO_2^{2+}$ were three times more abundant than those of Tf. The concentrations of the $UO_2^{2+}$ complexes calculated for the plasma ultrafiltrate were used as starting conditions for the $UO_2^{2+}$ content of the tubular fluid.

The dominant complex is still $Ca_2UO_2(CO_3)_3(aq)$ (Table 31.11), which can account for 73% of the $UO_2^{2+}$ entering the system, 13% is bound to kidney protein (fixed by starting conditions), the biscarbonate (7%) is more important than in the plasma, whereas the triscarbonate (6.3%) is less important than in plasma. In addition, about 1% of the $UO_2^{2+}$ in this system is predicted to be associated with phosphate and citrate. The selected concentration and fractional binding of $UO_2^{2+}$ to tubule membrane protein yielded a value for a 'formation constant' of $UO_2^{2+}$-membrane protein, $\log K_f = 9.6$. The fixed protein 'concentration' and $\log K_f$ are coupled, and both are uncertain.

### (*iii*) *Complexes in bladder urine*

The conditions for the urine calculations were as follows: The human $UO_2^{2+}$ injection case (Table 31.7) excreted 59% of the injected $UO_2^{2+}$ (14 μmol) in 1.4 L of urine in the first 24 h (Hursh and Spoor, 1973), and the concentration of $UO_2^{2+}$ in urine was $10^{-5}$ M. The concentrations of the constituents of urine of humans consuming an ordinary diet are those given in Table 31.9. The speciation calculations indicate that only 1% of the excreted $UO_2^{2+}$ would still be a carbonate complex, and 99% would be present as phosphate and citrate complexes (Table 31.11). Diets that raise the pH and/or increase $HCO_3^-$ in urine and $HCO_3^-$ infusion, which increases both the $HCO_3^-$ concentration and the pH of the urine, would allow survival of greater fractions of the carbonate complexes filtered from plasma and their excretion in the urine.

Two questions that have received little attention are the near absence at low $UO_2^{2+}$ intakes to blood of significant $UO_2^{2+}$ deposition in portions of the renal tubular system distal to the proximal tubules and the spreading out of the renal injury at toxic $UO_2^{2+}$ doses. The degree and extent of renal injury

caused by $UO_2^{2+}$ are dose-dependent. At low to moderately toxic intakes to blood, cell damage is limited to the later portion of the proximal tubules, seen in microscopic sections as occupying the region near the cortico-medullary junction. With increasing doses of $UO_2^{2+}$, the cellular injury becomes progressively more widespread, extending proximally to the earlier portions of the proximal tubules and the distal tubules in the cortical region and distally to the loops of Henle in the medulla (Barnett and Metcalf, 1949). Autoradiographs of the kidneys of rodents given low doses of $^{232}UO_2^{2+}$ or $^{233}UO_2^{2+}$ verified that deposition of the $UO_2^{2+}$ coincided with the zone of low-dose cellular injury. When the shorter-lived U isotopes were given augmented with toxic amounts of $^{238}UO_2^{2+}$, autoradiographs showed more U deeper in the cortex (earlier portions of the proximal tubules and distal tubules) and deeper into the medulla (loops of Henle) than were seen with the lower doses of $UO_2^{2+}$.

In chemical terms, when high concentrations of $UO_2^{2+}$ ($10^{-3}$ M) were circulating, the carbonate complexes filtered from the plasma apparently begin to destabilize at the conditions of the earlier portions of the proximal tubules (Table 31.9), and the concentrations of phosphate and citrate are insufficient to prevent $UO_2^{2+}$ binding to the presumably lower affinity proteins of the membrane of the later segments of the renal tubule system.

The microvilli of the proximal tubule brush border are specialized for absorption, and the brush border presents a surface area many orders of magnitude greater than the luminal surface of the more distal portions of the renal tubule system (Berliner, 1973). Combined, the lower concentrations of potential $UO_2^{2+}$ binding sites and lower affinities for $UO_2^{2+}$ of these sites (less than those of phosphate and citrate) could account for the apparent lack of binding of low doses of $UO_2^{2+}$ in the more distal tubule segments.

### (b) $NpO_2^+$

Plasma clearance of iv-injected $^{237}NpO_2^+$ was studied in rats and mice (Figs. 31.3 and 31.4). Clearance of $NpO_2^+$ from mouse plasma was fast, with 90% clearance in 10 min and 99% clearance in 60 min. At 100 min, skeletal uptake and urinary excretion accounted for 80% of the injected Np (Table 31.3). Plasma clearance of Np was also investigated in baboons injected iv with 1 ng $kg^{-1}$ of $^{239}Np$ or 100 μg $kg^{-1}$ of $^{237}Np$ reported as $NpO_2^+$ or $NpO_2^{2+}$ in solutions of Na citrate, $NaHCO_3$, or $NaNO_3$ (Ralston *et al.*, 1986). No differences were found in the plasma clearances, urinary excretion rates, or whole-body retentions of the differing masses of Np or Np oxidation states or chemical compositions of the injection media. Those findings indicate that either $NpO_2^{2+}$ had not been formed or that it was promptly reduced to $NpO_2^+$ *in vivo*. Plasma clearance of $NpO_2^+$ was fast in the baboons; it was 90% complete in about 45 min and 99% complete in about 300 min (Fig. 31.6).

The plasma clearance of iv-injected $^{237}NpO_2^+$ nitrate in the rats differs somewhat from those of the other animals (Figs. 31.3, 31.4, and 31.6). About 80% of

the injected Np was cleared from the plasma as rapidly as in the mice and baboons (in about 20 min, Figs. 31.4 and 31.6), but clearance of the remaining 20% was slow and resembled that of $Np^{4+}$ in the same animal models. Overall clearance was slow; it was 90% complete in 160 min and 99% complete only after 1.7 days. In the three animals, a small fraction of the iv-injected $NpO_2^+$ was cleared from the plasma as slowly as $Pu^{4+}$ (0.5% in the mice, 2% in the baboons, and 5.5% in the rats). The complexes of $NpO_2^+$ are weak (Table 31.8), and it is reasonable to consider that these small slowly clearing fractions of the injected Np had been reduced to $Np^{4+}$ *in vivo* and were circulating complexed with serum proteins.

Human plasma was incubated with $^{237}Np$ as $Np^{4+}$, $NpO_2^+$, or $NpO_2^{2+}$ in 0.08 M Na citrate buffer pH 3.2. Chromatography on G-25 Sephadex indicated that about 20% of the Np in all these preparations was associated with serum proteins. Chromatography on G-100–200 Sephadex indicated that the $^{237}Np$, applied as $NpO_2^+$, was distributed among the heavy proteins (22%), the albumin-Tf peak (33%), and low molecular weight species (44%). Re-chromatography of the albumin-Tf peak on DEAE-Sephadex showed only a moderate tendency of the Np to be associated with the Tf peak (Bruenger *et al.*, 1971b).

Protein precipitation, dialysis, ultrafiltration, and gel chromatography (150-Sephadex) were used to study protein binding of $^{239}NpO_2^+$ incubated with dog serum. All of those procedures indicated that about 50% of the Np was associated with protein, but no specific protein(s) could be identified. Protein binding was weak, and gel chromatography showed that about 20% of the applied Np was associated with the heaviest proteins and 80% eluted with the low molecular weight species in the same fraction as $NpO_2NO_3$ (Guilmette *et al.*, 1982).

Intravenously injected $NpO_2^+$ is rapidly cleared from the plasma of mice, rats, and baboons, mainly to urinary excretion and uptake in bone (Tables 31.2, 31.3, 31.5, and 31.6; Figs. 31.3, 31.4, and 31.6). There is little evidence for protein binding of $NpO_2^+$ in the plasma. Combined, these observations are good indicators that, in accord with its tendency to form only weak complexes, $NpO_2^+$ does not form stable complexes with plasma protein (Bruenger *et al.*, 1971b; Guilmette *et al.*, 1982). Stable binding of Np to Tf apparently requires that the injected $NpO_2^+$ be reduced *in vivo* to $Np^{4+}$, which forms complexes as stable as those of $Pu^{4+}$. *In vivo* reduction of $NpO_2^+$ to $Np^{4+}$ is likely to be slow, because it involves the breaking of M–O bonds, but as Durbin *et al.* (1998b) and Taylor (1998) point out, at pH 7.4 in the presence of ligands with great affinity for $Pu^{4+}$ and $Np^{4+}$ but little affinity for $NpO_2^+$ and an average eH in mammalian plasma of about 270 mV (Van Rossum and Schamhart, 1991), such reduction is theoretically possible.

The low molecular weight $NpO_2^+$ species transported in the plasma, filtered by the kidneys into the urine, and rapidly deposited in bone (Tables 31.2, 31.3, and 31.5) have not been identified. Hydrolysis of $NpO_2^+$ is not expected at physiological pH. Some of the $NpO_2^+$, which behaves like a large monovalent

cation, may exist as a hydrated ion, and carbonate is known to stabilize $NpO_2^+$ (Ahrland, 1986). Both an aqueous ion and a $NpO_2^+$ carbonate complex should be ultrafilterable and excreted by the kidneys into the urine.

The identities of the $NpO_2^+$ species that may be expected in mammalian plasma can be calculated for the specific set of conditions in the plasma volume of a 6.2 kg monkey immediately after iv injection of 42 μg $kg^{-1}$ of $^{237}NpO_2^+$ (Table 31.5); the concentration of the $NpO_2^+$ would be $4.5 \times 10^{-6}$ M in 0.025 M $HCO_3^-$ at pH 7.4 (Tables 31.8 and 31.9). The stability constants of the $NpO_2^+$ carbonate, phosphate, and citrate complexes are as shown in Table 31.8.

The speciation calculations predict that in mammalian plasma hydrolysis of $NpO_2^+$ is negligible, and about 20% of the injected $NpO_2^+$ circulates as a hydrated ion, $NpO_2^+(aq)$, 50% as $NpO_2CO_3^-$, 20% as $NpO_2HPO_4^-$, and 10% as a $NpO_2^+$ citrate complex. The concentration of $HCO_3^-$ and the pH are too low to allow formation of a biscarbonate.

The $NpO_2CO_3^-$ complex is unstable at the reduced $HCO_3^-$ and pH in the renal tubules (Table 31.9). In the urine, $NpO_2^+$ is likely to be about equally divided between its $HPO_4^{2-}$ and citrate complexes.

The fraction of iv-injected $NpO_2^+$ that deposits in the kidneys is $\leq$3% (Tables 31.2, 31.3, and 31.6), the tendency of $NpO_2^+$ to bind to kidney tissue protein is apparently much less than that of $UO_2^{2+}$. However, if the amount of Np injected (oxidation state not certain) is in the toxic range ($\geq$6 mg $kg^{-1}$), even that small fractional kidney deposit will result in renal tubular injury of the same nature at the same anatomical location that is typically seen with much smaller doses of $UO_2^{2+}$ (Maynard and Hodge, 1949; Ballou *et al.*, 1962; Mahlum and Clarke, 1966).

### (c) $PuO_2^{2+}$

A dog was injected iv with 0.84 μg Pu per kg of $^{239}PuO_2^{2+}$ in a solution containing 0.01 M Na citrate and 0.14 M NaCl, pH 7 (Painter *et al.*, 1946). About 35% of the injected Pu was cleared from the plasma in the first 20 min, but in contrast to its analog, $UO_2^{2+}$, clearance of about 65% of the injected $PuO_2^{2+}$ from the plasma was as slow as that of $Pu^{4+}$ in beagles (Fig. 31.5). Comparisons of the plasma clearance pattern and early urinary excretion in the dog and the tissue distributions in rats of Pu injected as $PuO_2^{2+}$ with those of $Pu^{4+}$ and $UO_2^{2+}$ in the same animals (Tables 31.2 and 31.4) show that the disposition of $PuO_2^{2+}$ does not resemble that of $UO_2^{2+}$, but is similar to that of $Pu^{4+}$. Combined, these observations indicate reduction of $PuO_2^{2+}$ to $Pu^{4+}$ *in vivo*. Where in the body that reduction occurs is not known, but because it is rapid, it is likely to take place in the circulating fluids.

The stabilities of the biscarbonate complexes of $UO_2^{2+}$ and $PuO_2^{2+}$ are similar (Table 31.8). However, after iv injection of $^{239}PuO_2^{2+}$ in rats little Pu was excreted in the urine, and the distribution of the Pu was nearly the same as that of iv-injected $^{239}Pu^{4+}$ citrate (Table 31.2; Carritt *et al.*, 1947). These results

also suggest that $PuO_2^{2+}$ is rapidly reduced to $Pu^{4+}$ in the circulation (Table 31.2). However, when $^{239}PuO_2Cl_2$ was injected im in rats, Pu absorption was greater and faster than when the same mass of Pu was injected im as $^{239}PuCl_4$ or $^{239}PuCl_3$, suggesting that some $PuO_2^{2+}$ was mobilized from the wound site in a transportable form before it could be reduced to $Pu^{4+}$ and hydrolyzed *in situ* (Scott *et al.*, 1948b).

## 31.5 TISSUE DEPOSITION KINETICS

The kinetics of the tissue uptake of some actinides and lanthanides have been studied to relate differences in their biological behavior to their chemical properties, to aid in developing procedures for the therapeutic removal of actinides from the body, to identify the biological processes underlying the several components of the plasma clearance curves, and to determine whether the target tissues take up actinide bound to plasma protein or complexed by low molecular weight plasma ligands or both. The experimental design of the kinetic studies, which as a practical matter have been conducted only in rats and mice, involves killing groups of animals at intervals from 1 min to 24 h after iv injection of an actinide and measuring the nuclide content of the blood, and/or plasma, tissues, and excreta.

### 31.5.1 Tissue deposition kinetics in rats

Tissue uptake data have been reported for iv-injected $^{241}Am^{3+}$ by Belyayev (1969), for $^{239}Pu^{4+}$ by Schubert *et al.* (1950) and Rosenthal and Schubert (1957), and for four representative lanthanides (Durbin *et al.*, 1955). Taylor (1962) reported that the pattern of uptake of iv-injected $^{241}Am(NO_3)_3$ or $^{241}Am^{3+}$ citrate in the bones of growing rats more closely resembled that of $Ca^{2+}$ than $Pu^{4+}$. The data from those studies were recalculated to account for nuclide in the contained plasma of the tissues (Durbin *et al.*, 1972; Durbin, 1973). Within the first 5 min after iv injection of $Ca^{2+}$, $Ce^{3+}$, $Eu^{3+}$, $Am^{3+}$, or $Pu^{4+}$ in rats, as much as 50% of the injected nuclide disappeared from the plasma, but could not be accounted for by excretion or uptake in bones and liver. Material balance studies with $Ca^{2+}$ and four lanthanides demonstrated that at that time 75 to 90% of the missing nuclide was present transiently in the bulk soft tissue, indicating association with interstitial water (ISW) rather than with cellular components. The light lanthanides, $Ce^{3+}$ and $Eu^{3+}$, $Ca^{2+}$, and $Am^{3+}$ bind weakly to plasma proteins, and 50 to 60% of the injected amounts of those nuclides had diffused into ISW (Durbin, 1973). Plasma Tf binds stably to $Pu^{4+}$, and only 20 to 40% of iv-injected $Pu^{4+}$ diffused into ISW, depending on whether the $Pu^{4+}$ was administered as the nitrate or complexed with citrate (Durbin *et al.*, 1972).

The fraction of iv-injected nuclide diffusing into ISW depends on the stability of its protein complex(es). The less stable the protein binding, the more slowly the complex forms, and the larger is the fraction that promptly leaves the plasma by diffusion into ISW or immediate uptake by bone and/or liver or urinary excretion.

These kinetic studies of $Am^{3+}$ and lanthanides demonstrated that the initial fast decline in the plasma clearance curves (first exponential component) was the combined result of rapid early deposition in the target tissues and urinary excretion and diffusion of filterable nuclide from the plasma to ISW, most of which is associated with the bulk soft tissues. Delayed return to the plasma compartment from ISW contributes to the second and third components of the plasma clearance curves and supports continued, but slower, uptake in the tissues. The multiexponential equations that describe the uptake of $Am^{3+}$ in the bone and liver of rats have rate terms in common with each other and with the equations of clearance from the plasma and the soft tissues (ISW). Common terms in the transport equations are expected for two communicating fluid compartments (Durbin *et al.*, 1997b). The common rate terms in the liver and skeleton uptake equations indicated that $Am^{3+}$ was being accumulated in both tissues from common pools – initially, from complexes with low molecular weight plasma ligands, and later from the weak plasma protein complexes (Durbin, 1973).

The recalculated data for $Pu^{4+}$ clearance from the plasma and the uptake kinetics of $Pu^{4+}$ in rat skeleton and liver (Schubert *et al.*, 1950; Rosenthal and Schubert, 1957) were combined with data for protein binding of $Pu^{4+}$ in rat and dog plasma measured at times from a few minutes to 24 h after injection of $Pu^{4+}$ citrate (Stevens *et al.*, 1968; Turner and Taylor, 1968a). These data were used to solve a biokinetic compartment model of circulatory transport and tissue uptake (Durbin *et al.*, 1972). The $Pu^{4+}$ complexed with Tf and the $Pu^{4+}$ complexed with filterable low molecular weight plasma ligands were designated as bound or free, respectively. The model structure consisted of four interconnecting transport compartments – plasma-bound, plasma-free, ISW-bound, and ISW-free. The plasma-bound and plasma-free compartments communicated with four effectively nonreturning sinks – liver, skeleton, soft tissue, and excreta. The numerical solutions of the model implied the following: $Pu^{4+}$-free binds to protein, mainly to Tf, in the ISW as well as in the plasma; little, if any $Pu^{4+}$-bound is excreted or deposited in the liver; which suggests that Tf binding is not a necessary precondition for liver uptake of $Pu^{4+}$; both $Pu^{4+}$-bound and $Pu^{4+}$-free are taken up by bone.

### 31.5.2 Tissue deposition kinetics in mice

Detailed studies of tissue uptake kinetics were conducted in mice injected iv with $^{232,235}UO_2Cl_2$ (Fig. 31.11, Durbin *et al.*, 1997a) , $^{237}NpO_2Cl$ (Fig. 31.12, Durbin *et al.*, 1998b) , $^{241}Am^{3+}$ citrate (Fig. 31.13, P. W. Durbin and B. Kullgren,

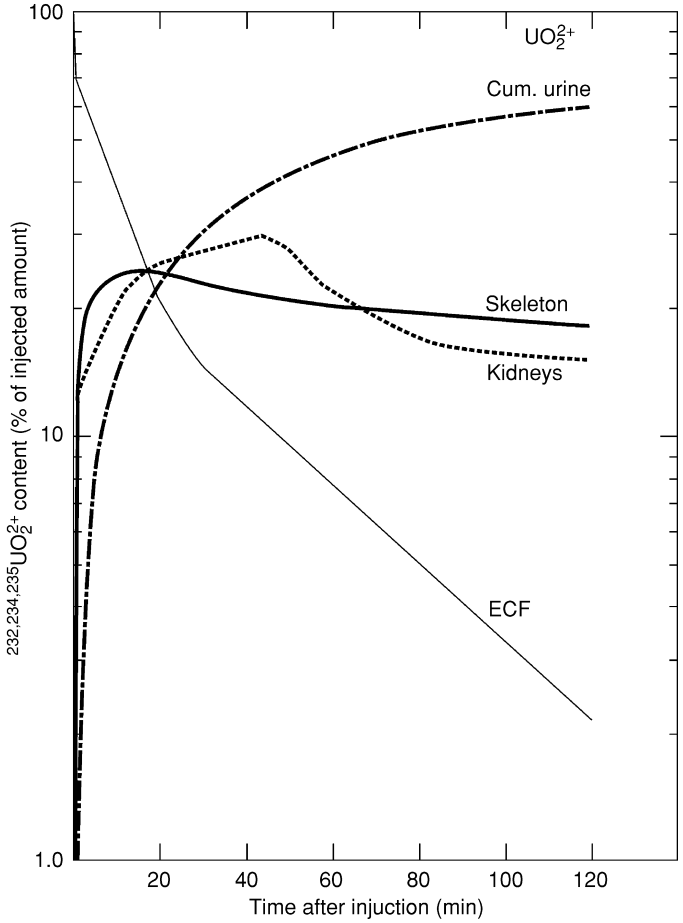


**Fig. 31.11** *Clearance from extracellular fluid* (*ECF*) of mice, uptake in EFC-free skeleton and ECF-free kidneys, and cumulated urinary excretion of iv-injected $^{232,234,235}UO_2Cl_2$ (100 μg $kg^{-1}$ *of U*). *Data of Durbin* et al. (1997a).

unpublished data) , or $^{238}Pu^{4+}$ citrate (Fig. 31.14, Durbin *et al.*, 1997b, P. W. Durbin and B. Kullgren unpublished data) . These studies provide useful comparisons of the deposition kinetics of actinides in their four biologically important oxidation states that form complexes with plasma constituents ranging in stability from very weak to strong. In all of these studies, female mice of the same strain and age were used. Nuclides were injected iv, and data were taken from groups of five mice killed at 16 timed intervals from 1 min to 24 h. Actinide content of plasma and all tissues of each mouse (including its entire skeleton) and pooled excreta of each five-mouse group were determined by

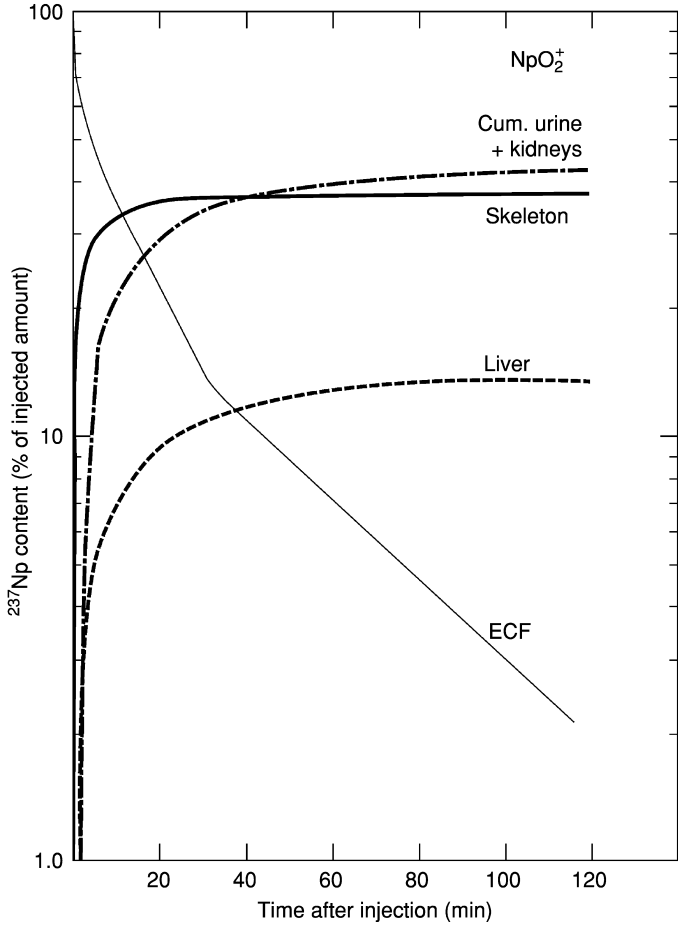


**Fig. 31.12** *Clearance from extracellular fluid (ECF) of mice, uptake in ECF-free skeleton and ECF-free liver, and cumulated urinary excretion plus ECF-free kidneys of iv-injected* $^{237}NpO_2Cl$ (200 μg kg$^{-1}$ *of Np*). *Data of Durbin* et al. (1998b).

scintillation counting. On average, 95% of the injected actinide was recovered in these material balance studies.

The fractional volumes of plasma and ECF in the tissues and whole body had been measured in similar mice (Durbin *et al.*, 1992). Those fluid distributions were used to calculate and apportion among its tissues the actinide removed in the plasma sample of each mouse, approximately recreating the total in-life actinide content of each tissue. The amounts of actinide deposited in the target tissues at each time ($t$), ECF-free tissue ($t$), was estimated by subtracting the amount of actinide calculated to be in their contained plasma [P($t$)] and

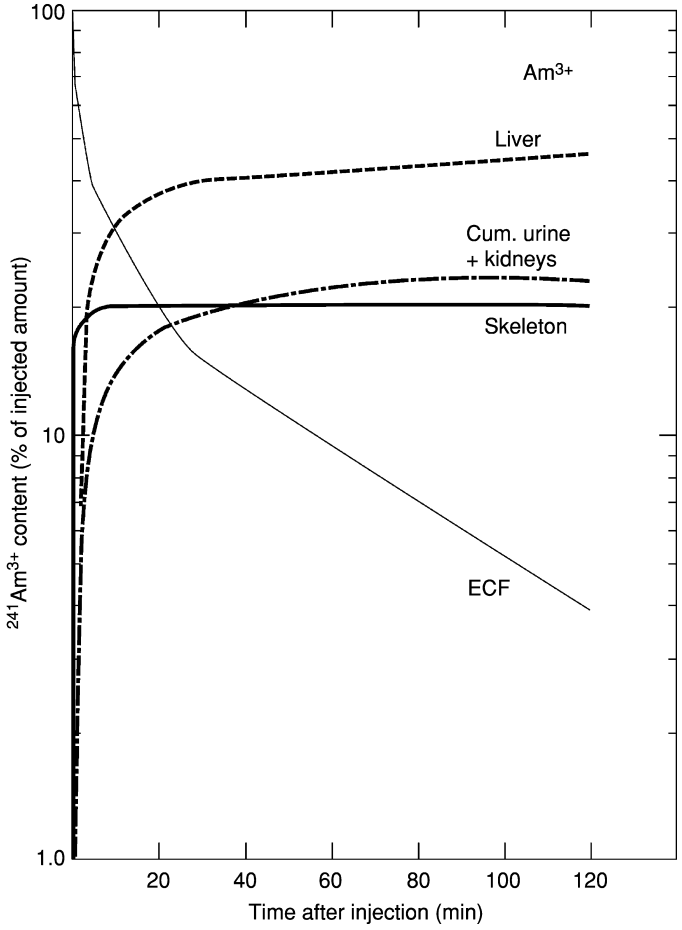


**Fig. 31.13** *Clearance from extracellular fluid (ECF) of mice, uptake in ECF-free skeleton and ECF-free liver, and cumulated urinary excretion plus ECF-free kidneys of iv-injected* $^{241}Am^{3+}$ *citrate* (0.23 μg $kg^{-1}$ *Am*). *Unpublished data of P. W. Durbin and B. Kullgren.*

ISW [I($t$)] from their measured values that had been corrected for blood loss; skeleton [Sk($t$)], liver [L($t$)], and kidneys [K($t$)] (Durbin *et al.*, 1992, 1997a,b, 1998b),

$$\text{ECF-free skeleton} = [\text{Sk}(t) - \text{P}_{\text{Sk}}(t) - \text{I}_{\text{Sk}}(t)]$$
$$\text{ECF-free liver} = [\text{L}(t) - \text{P}_{\text{L}}(t) - \text{I}_{\text{L}}(t)]$$
$$\text{ECF-free kidneys} = [\text{K}(t) - \text{P}_{\text{K}}(t) - \text{I}_{\text{K}}(t)].$$

The tissue uptake data (deposited fractions), expressed as percent of injected actinide in ECF-free tissues, are plotted vs time to 120 min after injection in Figs. 31.11–31.14. Those curves and the parameters of their multiexponential

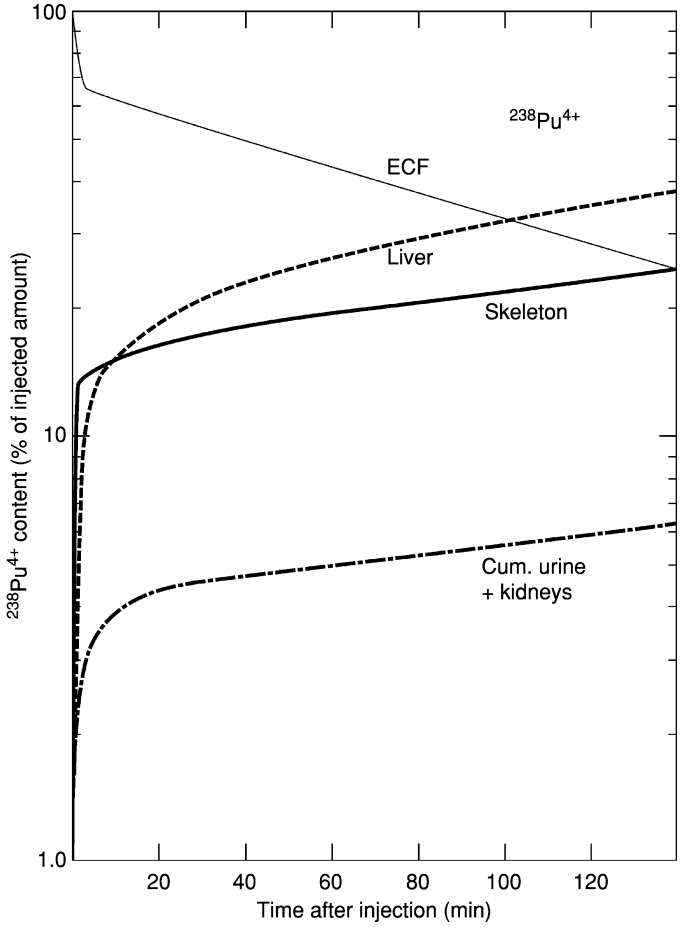


**Fig. 31.14** *Clearance from extracellular fluid (ECF) of mice, uptake in ECF-free skeleton and ECF-free liver, and cumulated urinary excretion plus ECF-free kidneys of iv-injected* $^{238}Pu^{4+}$ *citrate* (0.09 μg $kg^{-1}$ *Pu*). *Data of Durbin* et al. (1997b) *and unpublished data of P. W. Durbin and B. Kullgren.*

equations were obtained by log-linear regression analysis. The curves were plotted for clearance of actinides from the plasma (Fig. 31.4) and ECF (Figs. 31.11–31.14) of mice, and their equations were calculated to 120 min after injection for $UO_2^{2+}$, $NpO_2^{+}$, and $Am^{3+}$ and to 480 min for $Pu^{4+}$. Each has three exponential components,

Plasma ($t$) or ECF($t$) = $\sum A_i e^{-\lambda_i t}$(% of amount injected), $t$ is min after injection.

Maximum actinide accumulations in the ECF-free tissues and urinary excretion were estimated from the tabular data. Equations were derived to describe

the actinide uptake in the target tissues and cumulated urinary excretion using published methods (Comar, 1955; Durbin, 1973). The exponential tissue uptake equations were calculated to 120 min for $UO_2^{2+}$, $NpO_2^{+}$, and $Am^{3+}$ and to 480 min for $Pu^{4+}$. Nearly all of the tissue uptake equations also have three negative exponential terms,

Tissue($t$) or cum. urine($t$) $= \sum A_i(1 - e^{-\lambda_i t})$ (% of injected amount), $t$ is min after injection.

The parameters, coefficients ($A_i$,%), and rate constants ($\lambda_i$, $min^{-1}$) of the plasma and ISW clearance equations and the equations describing actinide uptake in the ECF-free tissues and cumulated urinary excretion are collected in Table 31.12. Table 31.12 also includes the maximum values of the ECF-free tissue deposits and total urinary excretion and the approximate postinjection times of maximum accumulation. This table also includes, for comparison, the parameters of the two-component plasma clearance curves determined in similar mice for the organic tracers, $CaNa_3$–$^{14}$C–DTPA and $^{3}$H-inulin, which are freely diffusible, do not accumulate in any tissue, and are quantitatively filtered into the urine (Durbin *et al.*, 1997b). The deposition kinetics studies of $Am^{3+}$ and $Pu^{4+}$ in the mouse confirmed the findings for those actinides in rats, and deposition kinetic studies were extended to include $UO_2^{2+}$ and $NpO_2^{+}$.

In the mice, the first two exponential terms of the plasma clearance equations of $Am^{3+}$, $UO_2^{2+}$, and $NpO_2^{+}$ are similar to those of the diffusible tracers, $CaNa_3$–$^{14}$C–DTPA and $^{3}$H-inulin (Table 31.12). Within 5 min, about 85% of those injected actinides and the organic molecules have diffused into ISW, been filtered by the kidneys, and, for the actinides, been taken up by the skeleton and liver.

Immediate diffusion of large fractions of these three injected actinides into ISW and some early urinary excretion show that upon introduction into the plasma they exist mainly as 'free' filterable complexes with small ligands (either plasma constituents or, in the case of $Am^{3+}$ with the injected excess citrate). Initially, large fractions of these actinides are taken up in the liver or kidneys and skeleton at very fast rates. The coefficients of the first components of their uptake equations ($A_1$) account for accumulation of 40–80% of the maximum deposits in the skeleton and about 30% of the maximum liver deposits. The rate constants ($\lambda_1$) imply uptake half-times of 0.3 to 0.8 min in bone and 1 to 1.4 min in liver (Table 31.12). Tissue uptake and urinary excretion persist, but more slowly at times longer than 5 min postinjection as is shown by the rate constants of the second and third components of their uptake equations ($\lambda_2$ and $\lambda_3$).

The deposition kinetics of $Pu^{4+}$ differ quantitatively from those of the other three actinides of differing oxidation state, mainly because $Pu^{4+}$ forms a stable complex with plasma Tf, while the complexes that $NpO_2^{+}$, $UO_2^{2+}$, and $Am^{3+}$ form with Tf and other plasma proteins are very weak. In the mice, about 75% of Fe-binding sites of plasma Tf are occupied by $Fe^{3+}$ (Table 31.10). During the first few minutes after iv injection of $Pu^{4+}$ citrate, about one-half of the $Pu^{4+}$ appeared to be 'free' and circulating as a filterable low molecular weight species.

**Table 31.12** *Exponential equations describing clearance from plasma and ISW, accumulation in ECF-free tissues, and urinary excretion of iv-injected actinides in mice.*[a,b]

| | *Compartment maximum* | | *Parameters of clearance and accumulation equations*[c] | | | | | |
|---|---|---|---|---|---|---|---|---|
| *Compartment* | (%)* | min | $A_1$ (%) | $\lambda_1$ ($min^{-1}$) | $A_2$ (%) | $\lambda_2$ ($min^{-1}$) | $A_3$ (%) | $\lambda_3$ ($min^{-1}$) |
| $^{232,234,235}UO_2Cl_2$ | | | | | | | | |
| Plasma | | | 82 | 1.6 | 14 | 0.1 | 3.6 | 0.02 |
| ISW[d] | | | – | – | 25 | 0.1 | 25 | 0.02 |
| Skeleton | 25 | 20 | 10 | 2.1 | 15 | 0.3 | – | – |
| Cum. urine + kidneys[e] | 76 | 120 | 12 | 0.5 | 41 | 0.06 | 23 | 0.02 |
| $^{237}NpO_2Cl$ | | | | | | | | |
| Plasma | | | 84 | 1.5 | 13 | 0.08 | 3.0 | 0.01 |
| ISW[d] | | | – | – | 16 | 0.06 | 25 | 0.03 |
| Skeleton | 36 | 60 | 24 | 0.9 | 10 | 0.1 | 2.3 | 0.02 |
| Liver | 14 | 60 | 4.0 | 0.7 | – | – | 10 | 0.04 |
| Cum. urine + kidneys[e] | 42 | 90 | 3.0 | 1.2 | 26 | 0.07 | 14 | 0.02 |
| $^{241}Am^{3+}$ citrate | | | | | | | | |
| Plasma | | | 86 | 0.8 | 10 | 0.08 | 4 | 0.02 |
| ISW[d] | | | – | – | 12 | 0.07 | 19 | 0.02 |
| Skeleton | 20 | 10 | 17 | 2.3 | 3.2 | 0.4 | – | – |
| Liver | 47 | 150 | 19 | 0.5 | 0.13 | 0.2 | 15 | 0.02 |
| Cum. urine + kidneys[e] | 22 | 60 | 9.5 | 0.6 | 12 | 0.05 | – | – |
| $^{238}Pu^{4+}$citrate | | | | | | | | |
| Plasma | | | 43 | 1.2 | 27 | 0.04 | 30 | 0.006 |
| ISW[d] | | | – | – | – | – | 24 | 0.004 |
| Skeleton | 40 | 720 | 13 | 1.6 | 7.4 | 0.02 | 20 | 0.002 |
| Liver | 42 | 240 | 12 | 0.4 | 31 | 0.01 | – | – |
| Cum. urine + kidneys[e] | 8.8 | 480 | 2.0 | 1.8 | 2.5 | 0.1 | 4.3 | 0.002 |
| $^{14}C$-DTPA | | | | | | | | |
| Plasma[f] | – | – | 86 | 1.3 | 14 | 0.08 | – | – |
| $^{3}H$-inulin | | | | | | | | |
| Plasma[f] | – | – | 82 | 1.0 | 18 | 0.08 | – | – |

* % of injected nuclide and minutes (min) is time after injection.

[a] Data sources are as follows: $^{232,234,235}UO_2Cl_2$, Durbin *et al.* (1997a); $^{237}NpO_2Cl$, Durbin *et al.* (1998b); $^{241}Am^{3+}$ citrate, P. W. Durbin and B. Kullgren (unpublished data); $^{238}Pu^{4+}$ citrate, Durbin *et al.* (1997b) and P. W. Durbin and B. Kullgren (unpublished data).

[b] Equations for plasma and ISW clearance were fitted from $t(0)$ to $t(120$ min), and those for tissue accumulation and urinary excretion were fitted from $t(0)$ to $t$(maximum). Maximum tissue accumulation and cumulated urinary excretion values and the postinjection times at which those maxima were attained were estimated from Figs. 31.11–31.14.

[c] Clearance equations are of the form, plasma($t$) or ISW($t$)$=\sum A_i e^{-\lambda_i t}$, and those for accumulation in the tissues and cumulated urinary excretion are of the form, tissue($t$) or cum. urine($t$)$=\sum A_i(1-e^{-\lambda_i t})$, where plasma ($t$), ISW ($t$), tissue($t$), and cum. urine($t$) are expressed as % of injected actinide and $t$ is min. after injection.

[d] Actinide calculated to have diffused into interstitial water (ISW).

[e] ECF-free kidneys ($t$) are combined with cum. urine ($t$) to account for all actinide filtered by the kidneys.

[f] Durbin *et al.* (1997b).

Only about 25% of the injected $Pu^{4+}$ diffused into ISW, and skeleton and liver uptakes were about 30% of their maximum accumulated amounts (Table 31.12). The initial rates of $Pu^{4+}$ deposition in liver and skeleton were about the same as those for the other study actinides (half-times 0.4 and 1.7 min, respectively, for skeleton and liver).

Subsequently, return of $Pu^{4+}$ from ISW was slower than for the other actinides. Plasma $Pu^{4+}$ retention was prolonged, renal excretion was negligible, and uptake in the target tissues proceeded at rates 1/3 to 1/10 as fast as those observed for the other actinides. Skeletal uptake persisted for about 24 h or until nearly all of the $Pu^{4+}$ had been cleared from the plasma, during which time nearly all of the $Pu^{4+}$ in the plasma was likely to be bound to Tf (components 2 and 3). Renal filtration, although small, also persists, indicating the continuous presence of a small fraction of 'free' $Pu^{4+}$. Net uptake in liver essentially stops when the 'free' $Pu^{4+}$ has been reduced to a low level.

### 31.5.3 Summary

Bone and liver cell surfaces have great affinities for actinides (except that liver does not accumulate $UO_2^{2+}$), and those tissues take up (bind) actinides rapidly during the first few minutes after iv injection, when substantial fractions of the actinides are likely to be circulating as weak complexes with small filterable ligands. The reduced rates of tissue uptake and renal filtration that emerged in the mice at postinjection times longer than 5 min were not likely to be caused by sudden changes in the tissue affinities for actinides or the saturation of metal-binding sites. Alteration of the renal filtration rate is scarcely possible, because that rate is a species-specific constant (Smith, 1951; Durbin and Schmidt, 1989; Durbin *et al.*, 1997b). The reductions in tissue uptake and renal excretion rates and their related plasma clearance rates appear to be due to changes taking place in the transport system. Rapid diffusion of actinides from plasma to ISW and slow return reduce the rate at which the actinides are presented to the tissues. Protein binding, most importantly for $Pu^{4+}$, decreases the differences between the stabilities of the actinide complexes with the tissue ligands and those with the plasma ligands, effectively reducing the competitiveness of the tissue ligands and delaying or preventing the transfer of actinide from plasma ligands to tissue ligands.

## 31.6 ACTINIDES IN THE LIVER

Large fractions of injected soluble trivalent and tetravalent actinides are taken up by the liver, and their retention in liver has been studied because of its importance for tumor induction and radiation dosimetry (Tables 31.1–31.7; Finkle *et al.*, 1946; Painter *et al.*, 1946; Hamilton, 1947b, 1948c; ICRP, 1959,

1972, 1986; Durbin 1960, 1962, 1973; Cochran *et al.*, 1962; Stover *et al.*, 1968b, 1971; Taylor and Bensted, 1969; Mewhinney *et al.*, 1972; McKay *et al.*, 1972; Lloyd *et al.*, 1972b, 1984b; Taylor *et al.*, 1972b; Guilmette *et al.*, 1980; Lo Sasso *et al.*, 1981; Durbin *et al.*, 1985; NCRP, 2001).

Autoradiographic studies show that the actinides initially are distributed nearly uniformly in liver cells. With the passage of time after injection, actinide retained in the liver of rats, dogs, and monkeys tends to be located mainly in the Kupffer cells as aggregates associated with hemosiderin (Cochran *et al.*, 1962; Durbin, 1973, 1975; Durbin *et al.*, 1985).

### 31.6.1 Liver microanatomy

The initial binding sites in the liver for soluble blood-borne metal ions including the tri- and tetravalent actinides are the two sinusoidal membrane surfaces of the one-cell thick sheets of hepatocytes. The membranes facing the sinusoidal blood spaces possess numerous microvilli that project into the fluid-filled space. The microvilli are rich in receptors, enzymes, and transport proteins, and they provide an enormous surface area for absorption of blood-borne substances. Bile is secreted at the canalicular hepatic surfaces between the cells into minute ducts that ultimately coalesce and empty into the common bile duct (Ham, 1974; Ballatori, 1991).

### 31.6.2 Liver blood supply

The liver has an abundant blood supply; it receives about 20% of the cardiac output (Detweiler, 1973). Two-thirds of liver blood is delivered by the portal vein, which transports blood from the GI tract. The hepatic artery supplies the remainder. The two sets of blood vessels branch into capillaries that end in blood-filled spaces (sinusoids), where the venous and arterial blood mix. The thin flat lining cells that separate the sinusoidal hepatic cell surfaces from the sinusoidal blood are porous (pore size about 0.1 μm in diameter), thereby excluding red blood cells and larger particles while allowing access of the whole plasma to the hepatocyte microvilli. The sinusoidal lining contains fixed phagocytes (Kupffer cells) that recognize and ingest colloidal particles (Ham, 1974; Ballatori, 1991).

### 31.6.3 Transport of metals into liver cells

Entry of metal ions into hepatic cells may be via facilitated diffusion and/or by liquid phase, adsorptive, and receptor-mediated endocytosis, followed by temporary residence in the cytosol as complexes formed with binding proteins or in the lysosomes. In endocytosis, a vesicle of membrane envaginates into a sac, which sinks into the cytoplasm matrix. These vesicles fuse with each other or with other vesicles or with lysosomes. It has recently been shown that the liver

cell internalizes more than 20% of its volume and between 5 and 50% of its surface area each hour by a process termed membrane recycling. Rapid membrane recycling is likely to be a major contributor to the hepatic intake of metals that have high affinities for membrane-binding sites (Ballatori, 1991).

Iron is transported into hepatocytes by at least two independent pathways. The dominant mechanism is receptor-mediated endocytosis in which Fe–Tf binds to specialized Tf-receptors on the hepatocyte surface. Membrane binding is followed similarly to the delivery of Fe–Tf to developing erythrocytes, by endocytosis, and internalization of the Fe–Tf–Tf-receptor complex, fusion of the endocytotic vesicle with other vesicles, release of the Fe within the acidic vesicles, and extrusion of the iron-depleted Tf (Ballatori, 1991). Hepatic uptake of the normally very small fraction of $Fe^{3+}$ circulating as a low molecular weight complex has been shown to occur by direct binding to integral membrane protein. Membrane binding is probably followed by internalization in the energy-dependent membrane recycling process (Planas-Bohne *et al.*, 1985, 1989; Planas-Bohne and Duffield, 1988; Planas-Bohne and Rau, 1990).

### 31.6.4 Iron storage

#### (a) Ferritin

Ferritin serves as a source of stored iron that can be mobilized for red cell production. It is a large water-soluble complex of protein (apoferritin, molecular weight about 450 kDa) and ferric oxyhydroxide. At the usual level of iron saturation (18%), the weight of the complex is about 620 kDa. The protein forms a shell within which crystals of iron hydroxide and phosphate are dispersed in a lattice-like relationship. Apoferritin is synthesized in response to intracellular iron by the ribosomes of nearly all mammalian cells, but liver, spleen, and bone marrow are especially rich in stored ferritin. At low iron levels, new iron is incorporated into existing apoferritin molecules, particularly those with a partially iron-filled core. Elevated iron stimulates production of apoferritin, which rapidly takes up excess iron. The residence time of ferritin in the cell cytosol is brief, and it tends to accumulate within lysosomes.

Iron is incorporated into and stored in ferritin as $Fe^{3+}$, but to break the coordination bonds and be released from the ferritin complex, the iron must be reduced to $Fe^{2+}$. It is then reoxidized in the cytosol and bound by intracellular Tf (Aisen and Listowsky, 1980; Fairbanks and Beutler, 1995).

#### (b) Hemosiderin

The other iron storage compound, hemosiderin, is found mainly in the macrophages of the bone marrow, the Kupffer cells of the liver, and phagocytic cells in the spleen. It is not water-soluble. It is composed of ferritin partially stripped of the protein component and contains 25 to 35% iron by weight. Much

hemosiderin appears to consist of ferric hydroxide core crystals (Fairbanks and Beutler, 1995).

### 31.6.5 Actinide association with stored iron

Investigations of actinide retention in the whole liver were extended to include identification of the constituents of hepatic cells that bind and store them (Taylor, 1972; Duffield and Taylor, 1986). Preliminary analysis of clear, particle-free homogenates of the livers of dogs injected iv with $^{239}Pu^{4+}$ citrate indicated that the $Pu^{4+}$ was associated with ferritin (Bruenger *et al.*, 1969a). Competitive binding studies showed that the ferritin complexes of $Pu^{4+}$ and $Am^{3+}$ are more stable than their Tf complexes (Bruenger *et al.*, 1969a; Stover *et al.*, 1970).

The subcellular distributions of soluble iv-injected actinides in the livers of several animal species have been investigated using a variety of techniques. The actinides ($^{227}Ac^{3+}$,$^{233}Pa^{5+}$,$^{238}Pu^{4+}$,$^{239}Pu^{4+}$,$^{241}Am^{3+}$,$^{244}Cm^{3+}$,$^{249}Cf^{3+}$, $^{237}NpO_2^+$, and $^{239}NpO_2^+$) were studied in rats, mice, dogs, rabbits, baboons, and/or hamsters. Homogenates were prepared from the livers, and the subcellular organelles were separated from each other and from the filterable cytosol by means of differential centrifugation and centrifugation through sucrose or salt density gradients into nuclei plus cell debris, mitochondria, lysosomes, microsomes, and cytosol. Marker enzymes were used to identify mitochondria and lysosomes, and $^{59}Fe$ was used to identify ferritin. The nature of the actinide-binding protein(s) in the cytosol was investigated using gel chromatography and electrophoresis (Taylor, 1969, 1970, 1972; Taylor *et al.*, 1969a,b; Boocock *et al.*, 1970; Stover *et al.*, 1970; Bruenger *et al.*, 1971a, 1972, 1976; Grube *et al.*, 1978; Schuppler *et al.*, 1988; Paquet *et al.*, 1995, 1996, 1998). These methods did not provide clear separation of 'iron-rich' heavy lysosomes from the mitochondria.

In more recent studies, actinide-injected animals were pretreated with Triton WR 1339, which causes liver lysosomes to imbibe water and swell, thus reducing their density enough to allow clean separation from the mitochondria (Gruner *et al.*, 1981; Winter and Seidel, 1982; Sutterlin *et al.*, 1984). Carrier-free electrophoresis has also been used to obtain a clear separation of lysosomes from all other organelles (Seidel *et al.*, 1986). Most of those studies were conducted using liver material from rats injected with ultrafilterable $^{239}Pu^{4+}$ citrate, and the results agree with supporting studies of liver material from rats and other animals injected iv or im with other soluble actinides and $^{141}Ce^{3+}$.

Combined, all of the studies of subcellular distribution of actinides in the liver show that ferritin is the predominant actinide-binding protein within the hepatocytes, and the lysosomes are the main subcellular storage organelles. Actinides that have entered the hepatocytes are initially mainly associated with the soluble lighter 'apoferritin-rich' ferritin in the cytosol, and to a lesser degree, they are sequestered in lysosomes. With time, the actinide associated with the soluble ferritin in the cytosol declines and the lysosomal actinide fraction, which includes the heavier 'iron-rich' ferritin, increases (Boocock *et al.*, 1970; Bruenger

*et al.*, 1971a; Grube *et al.*, 1978; Seidel *et al.*, 1986). That is the same time-dependent pattern followed by newly acquired hepatic iron – initial incorporation into freshly synthesized apoferritin in the cytosol followed by gradual accumulation in lysosomes of ferritin that has acquired more iron (Aisen and Listowsky, 1980; Fairbanks and Beutler, 1995). At times longer than 70 days in dogs injected iv with $^{239}Pu^{4+}$ citrate, the concentration of the $Pu^{4+}$ in the nuclei-cell debris fraction increased, and it was shown autoradiographically that the $Pu^{4+}$ was contained in the Kupffer cells in association with hemosiderin (Cochran *et al.*, 1962; Taylor *et al.*, 1969a,b; Bruenger *et al.*, 1971a).

In addition to their presence in the cytosol and lysosomes in association with ferritin, and depending on the mass injected or used to incubate cultured hepatocytes, lower specific activity $^{237}NpO_2^+$, and $^{239}Pu^{4+}$ localized in the hepatic cell nuclei in association with an as yet unidentified nuclear matrix protein (Schuler and Taylor, 1987; Paquet *et al.*, 1995, 1996).

### 31.6.6 Actinide uptake by liver cells

The multivalent lanthanides and actinides, particularly $Pu^{4+}$, share some metabolic properties of iron. They form variably stable complexes with Tf in the plasma and are stored in the liver associated with ferritin. It was reasonable to postulate that, like iron, these metals would be bound to and be taken into hepatic cells by a Tf-mediated receptor mechanism. However, in a series of elegant experiments using cultured liver cells (primary rat hepatocytes and human hepatoma Hep-G2 cells) and isolated rat hepatocyte membrane, Planas-Bohne and coworkers demonstrated that the mechanism by which $Pu^{4+}$ (and presumably other trivalent and tetravalent metals) are bound to and taken into liver cells is not only independent of, but is actually hampered by, Tf binding (Planas-Bohne *et al.*, 1985, 1989; Schuler and Taylor, 1987; Schuler *et al.*, 1987; Planas-Bohne and Duffield, 1988; Planas-Bohne and Rau, 1990).

Uptake of $Pu^{4+}$ from a medium containing $Pu^{4+}$ citrate into liver cells was not influenced substantially by the $Pu^{4+}$ concentration or the molar ratio, citrate: $Pu^{4+}$, suggesting a nonspecific nonsaturatable mechanism. Cell uptake of $Pu^{4+}$ was much reduced at 4°C, compared with 37°C, suggesting that transport into the cells was energy dependent. Cells incubated with $^{239}Pu^{4+}$–$^{14}C$-citrate did not bind or take in the $^{14}C$-citrate suggesting ligand exchange between the $Pu^{4+}$ citrate and the $Pu^{4+}$ receptor complex(es). If the $Pu^{4+}$ was prebound to Tf, uptake of $Pu^{4+}$ into the cells and by isolated perfused rat liver was very low, only about 10% of the uptakes from $Pu^{4+}$ citrate.

Liver cell intake of $Pu^{4+}$ from its citrate complex requires a high activation energy and can be prevented by inhibition of oxidative phosphorylation; other processes seem not to be important. Uptake of $Pu^{4+}$ by liver cells from the $Pu^{4+}$ citrate complex can be prevented by chelators (EDTA, DFO) and by unsaturated Tf suggesting that the $Pu^{4+}$ reacts directly with constituents of the liver cell

membrane. The stabilities of the $Pu^{4+}$ receptor complex(es) appear to be greater than that of $Pu^{4+}$ citrate but less than that of $Pu^{4+}$–Tf or $Pu^{4+}$–EDTA.

Fragments of purified rat hepatocyte membrane were incubated with $Pu^{4+}$ citrate. Binding of $Pu^{4+}$ to the membrane was pH-dependent (optimal at pH 7.4), saturatable, and independent of temperature, suggesting direct binding of $Pu^{4+}$ at a limited number of sites. Binding of $Pu^{4+}$ was prevented by the presence of unsaturated Tf, EDTA, or DFO, indicating that membrane binding of $Pu^{4+}$ involved $Pu^{4+}$ complexation with a spatially suitable arrangement of amino acid residues at the binding sites. The two kinds of binding sites found for $Pu^{4+}$ were shown not to be phospholipids or glycoproteins, but large integral membrane proteins (molecular weight between 150 and 400 kDa), and they are different from the two kinds of binding sites identified with direct uptake of iron. When membrane was incubated with $Pu^{4+}$–$^{125}$I–Tf and then solubilized and subjected to gel filtration, the $Pu^{4+}$ eluted in fractions different from those containing $^{125}$I–Tf bound to membrane protein receptors or unbound $^{125}$I–Tf, indicating dissociation of the $Pu^{4+}$–Tf complex.

### 31.6.7 Summary

From the standpoint of actinide biology, the most important results are that $Pu^{4+}$ can bind directly to a limited number of sites on the hepatic cell membrane and be internalized, that transport of the $Pu^{4+}$ into hepatic cells is not mediated by Tf, and that complexation of $Pu^{4+}$ by Tf suppresses $Pu^{4+}$ binding to hepatic cell membrane. It is reasonable to assume that the elements of group III and subgroup IV and the lanthanides and other actinides can also bind directly, possibly at the same or similar hepatocyte-binding sites as $Pu^{4+}$. Direct metal binding in the liver and its suppression by competition with Tf suggest an explanation for the observed direct correlation between the fractional deposition of the lanthanides and actinides in the liver and the instabilities of their Tf complexes (for which increasing ionic radius and plasma clearance rates are crude proxies) (Tables 31.1–31.7; Figs. 31.3–31.7; Durbin, 1962, 1973). The hepatic cell metal-binding sites compete successfully with bone surfaces for multivalent cations like $Ce^{3+}$ and $Am^{3+}$ that circulate complexed with small plasma ligands like citrate or as weak complexes with Tf or other plasma proteins. However, competition for metals that form more stable Tf complexes, like $Th^{4+}$ and $Pu^{4+}$, favors bone, and the source of the uptake in liver may be mainly the small fraction that circulates as low molecular weight complexes (Durbin *et al.*, 1972; Planas-Bohne *et al.*, 1989).

## 31.7 ACTINIDES IN BONE

The defining characteristic of the biological behavior of the actinides in mammals, and the chemically similar elements of group III, subgroup IV, and the lanthanides, is their intraskeletal distribution. As soon as suitable radioisotopes

became available, autoradiographs were prepared from undecalcified sections of the femora of rats injected with fission products ($^{91}Y^{3+}$, $^{95}Nb^{3+}$, $^{95}Zr^{4+}$, $^{144}Ce^{3+}$, $^{147}Pm^{3+}$, $^{152,154}Eu^{3+}$) and five actinides ($^{227}Ac^{3+}$, $^{234}Th^{4+}$, $^{239}Pu^{4+}$, $^{241}Am^{3+}$, $^{242}Cm^{3+}$) (Axelrod, 1947; Hamilton, 1947b). Autoradiographs of five representative radioelements were included in the original reports; the remainder was published later as a complete set (Durbin, 1962).

The deposition patterns of $^{45}Ca^{2+}$ and $^{89}Sr^{2+}$ in rat bones had already been studied autoradiographically, and it was shown that the alkaline earth elements penetrated into and were nearly uniformly distributed throughout the bone mineral volume (Hamilton, 1941; Pecher, 1942). The internal distribution of the multivalent cations was markedly different. None was initially incorporated into the bone volume. The tetravalent elements ($Zr^{4+}$, $Th^{4+}$, and $Pu^{4+}$) were deposited at endosteal surfaces, particularly on the trabeculae of the spongy bone and beneath the periosteum. The distribution patterns of the trivalent cations generally resembled the tetravalent elements, but there was also substantial spotty deposition in the compact bone, which was later shown to be on the mineralized walls of vascular channels.

The radioisotopes of all of the trivalent and tetravalent elements have been classified for the purposes of radiation dosimetry as 'bone surface seekers'. The methods used for calculating radiation doses to the bone cells and marrow surrounding the deposits of these nuclides in the skeleton have taken into account their nonuniform intraskeletal distribution (ICRP, 1959, 1967, 1979).

Actinide binding to the calcified bone surfaces is the net result of several biological and chemical processes: the nature of the bone mineral crystals and the organic bone matrix, the relative affinities of the individual actinides for the mineralized surface and the plasma ligands, the ability of the circulating actinide complexes to pass through or between the cells on resting surfaces and penetrate the osteoid and active osteoblasts on growing surfaces, and the richness of the blood supply and its proximity to the bone surfaces.

### 31.7.1 Bone surfaces

Detailed descriptions of the microanatomy of the skeleton and of bone growth and maintenance remodeling are available in specialized works (Bourne, 1956; Frost, 1963; Ham, 1974). The periosteal surface is beneath the outer tissue layer that envelops the whole bones. The endosteal surface is the inner aspect of whole bones plus the much larger surface of the three-dimensional interconnected network of the fine bony bars, rods, and plates of the spongy (trabecular) bone. The vascular (Haversian) surface is the cylindrical lining of the numerous vascular channels that penetrate and nourish the compact (cortical) bone. The large anatomical surface of the mammalian skeleton – about 12 $m^2$ in an adult human male – is about equally divided between the endosteal and Haversian surfaces (Spiers, 1968; Lloyd and Marshall, 1972; ICRP, 1979).

Three general bone surface types are recognizable histologically: actively growing, resting, and resorbing. Depending on age and stage of skeletal maturity, the abundances of the three surface types vary in individual bones and in the whole skeleton. New bone is laid down at the active surfaces, which are recognized by the presence of regular rows of tall columnar cells (active osteoblasts) located just above a variably thick layer of uncalcified or poorly calcified bone matrix (osteoid). A thin strongly PAS-positive margin marks the line of calcification. The cell and osteoid layers covering sites of active bone formation make these sites the least accessible to circulating metal ions. Resting surfaces are covered with a layer of thin flattened cells, which line the adjacent calcified surface. The bone beneath the resting cells is usually more calcified than that beneath the cells on the growing surfaces. The mineral–organic interface stains PAS-positive. Resting bone surface sites, which are predominant in human adults, are well mineralized, but their accessibility is somewhat hindered by the overlying cell layer. Resorbing surfaces are recognized by their irregular outline, their high degree of mineralization, the intense PAS-positive stain at the calcified margin, the absence of covering cells, and the presence of the large multinuclear osteoclasts that dissolve and digest bone. The resorbing sites are exposed directly to the circulating blood and/or tissue fluid, making them the most accessible.

The vascular channels of cortical bone (horizontal Volkmann's canals and longitudinal Haversian systems) are short cylindrical tunnels in the well-mineralized compact bone. They are lined with a layer of flattened endosteal cells, so their inner aspect resembles resting bone surface. The central space is filled with loose connective tissue and one large capillary or two small arterial and venous capillaries.

### 31.7.2 Bone blood supply

The blood supplies to the periosteum, the internal skeletal sites containing fatty marrow, and the vascular channels of cortical bone are closed capillary beds that effectively retain the red cells and nearly all of the plasma protein and allow only filterable low molecular weight plasma constituents and filterable metal complexes access to the bone surfaces. Erythropoietic marrow contains large vascular sinusoids with a discontinuous lining that permits whole plasma to pass into the extravascular space. The bony trabeculae embedded in the red marrow are exposed not only to metal ions complexed with the low molecular weight constituents of tissue fluid but also their nonfilterable complexes with plasma proteins (Ham, 1974; Wronski *et al.*, 1980; Miller *et al.*, 1982).

### 31.7.3 Intraskeletal distribution of actinides

More refined and definitive autoradiographic techniques confirmed the early observations of the surface-limited deposition of actinides in bone. Sectioning and autoradiography of undecalcified bone are difficult, and later studies

focused on $^{233}UO_2^{2+}$,$^{239}Pu^{4+}$,$^{241}Am^{3+}$, and most recently $^{237}Np$. In addition to revealing important details of the initial distribution of these actinides in bone, they have helped to define the mechanisms of release of actinides bound to bone and the kinds and extent of local radiation damage.

### (a) $^{241}Am^{3+}$

The initial intraskeletal distribution of $^{241}Am^{3+}$ was investigated autoradiographically in rats (Taylor *et al.*, 1961; Durbin *et al.*, 1969; Durbin, 1973; Priest *et al.*, 1983), dogs (Herring *et al.*, 1962; Lloyd *et al.*, 1972b; Polig *et al.*, 1984), and monkeys (Durbin, 1973, 1975). $^{241}Am^{3+}$ is initially deposited nearly uniformly on all types of bone surfaces – endosteal, periosteal, and Haversian canals. Deposition is somewhat more intense on resorbing and resting surfaces than on actively growing surfaces. No $^{241}Am^{3+}$ was found initially as a diffuse distribution in the bone volume (Herring *et al.*, 1962; Priest *et al.*, 1983). Results for $^{249,252}Cf^{3+}$ in rats were essentially the same as for $^{241}Am^{3+}$ (Durbin, 1973).

### (b) $Pu^{4+}$

Initial intraskeletal distribution of $Pu^{4+}$ ($^{238}Pu^{4+}$ or $^{239}Pu^{4+}$) was studied autoradiographically in rats (Arnold and Jee, 1957; Taylor *et al.*, 1961; Priest and Giannola, 1980), dogs (Arnold and Jee, 1959, 1962; Herring *et al.*, 1962; Wronski *et al.*, 1980), and monkeys (Durbin, 1975). Soluble $Pu^{4+}$ is initially deposited almost entirely on endosteal surfaces, in particular, the surfaces of the trabeculae of spongy bone closest to the sinusoidal circulation of the erythropoietic marrow that surrounds them. In the beagles, the initial surface concentrations of $^{239}Pu^{4+}$ on the fine trabeculae in vertebral bodies, pelvis, and proximal humerus (sites in spongy bone containing red marrow) were four to eight times greater than on the coarser trabeculae in the proximal ulna and distal humerus (sites containing fatty marrow) (Wronski *et al.*, 1980). Endosteal deposition is not uniform, and $Pu^{4+}$ concentrations on endosteal surfaces decrease generally in the order: resorbing > resting > actively growing. Deposits of $Pu^{4+}$ on periosteal surfaces are less intense, and those on Haversian canal surfaces are very low. There is no initial diffuse distribution of $Pu^{4+}$ in the bone volume.

### (c) $UO_2^{2+}$

The initial intraskeletal distribution of $UO_2^{2+}$ ($^{232}UO_2^{2+}$ or $^{233}UO_2^{2+}$) was studied autoradiographically in rats (Priest *et al.*, 1982) and dogs (Rowland and Farnham, 1969; Stevens *et al.*, 1980). Uranyl ion is initially deposited on all bone surface types, but it is found preferentially on actively growing surfaces that are laying down new bone. Similarly to $Ra^{2+}$, $UO_2^{2+}$ is deposited in the calcifying zones of skeletal cartilage. In the dogs, a detectable fraction diffused into the bone volume.

### (d) $^{237}NpO_2^+$

The intraskeletal distribution of $^{237}Np$, injected iv as $^{237}NpO_2NO_3$, was investigated autoradiographically in rats (Wirth and Volf, 1984; Sontag, 1993). The initial distribution appears to be nearly uniform on all endosteal and periosteal surfaces and the vascular canal surfaces of compact bone. There is no evidence for early diffusion of Np into the bone volume.

### (e) $^{91}Y^{3+}$, $^{144}Ce^{3+}$, $^{170}Tm^{3+}$

The initial intraskeletal distribution of these three trivalent metal ions was studied autoradiographically in growing dogs (Jowsey *et al.*, 1958), and $^{91}Y^{3+}$ was also investigated in rachitic young dogs and weanling rabbits (Herring *et al.*, 1962). The distributions of these trivalent elements in bone were similar to $^{241}Am^{3+}$. They were located on all bone surfaces, with the greatest concentrations associated with highly mineralized surfaces of resorbing or resting bone. There was little or no deposition in areas of active bone formation, and no deposition in osteoid tissue. All three radioisotopes were deposited on the mineralized surfaces of the resting and resorbing Haversian systems in cortical bone, but at intensities less than on the endosteal surfaces.

### (f) Summary

Within the skeleton, deposition of multivalent cations is initially limited to the anatomical surfaces in the order: endosteal > periosteal >cortical vascular channels, and among the bone surfaces in the order: resorbing >resting > actively growing.

The intensities of the local surface deposits are positively correlated with accessibility to the blood supply, the nature of the local blood supply, the degree of mineralization of the surface, and the instability of the complexes formed with Tf and other plasma proteins.

## 31.7.4 Retention – remodeling and redistribution

Prolonged skeletal retention is a distinguishing feature of the actinides (ICRP, 1959, 1972, 1979, 1993, 1995; Leggett, 1985, 1989, 1992a,b). The actinides (except $UO_2^{2+}$), once deposited on bone surfaces, appear to be released only when the bone containing them is physically destroyed (Arnold and Jee, 1957, 1959). There are long-term skeletal retention data for several actinides in beagles. The terminal slope of the skeletal retention function for $UO_2^{2+}$ in the beagles has a half-time of about 3 years: $UO_2^{2+}$ is lost from bone by chemical processes as well as by structural remodeling, and because it is efficiently excreted in the urine, little is redeposited in bone (Rowland and Farnham, 1969; Stevens *et al.*, 1980; Leggett, 1989). Retention of the trivalent and tetravalent actinides in the

beagle skeleton is much more prolonged. The half-times of the terminal slopes of the skeletal retention equations for $^{241}Am^{3+}$, $^{249}Cf^{3+}$, and $^{228}Th^{4+}$ are 15 to 18 years (Stover *et al.*, 1960; Lloyd *et al.*, 1972b, 1976, 1984a,b). About 56% of the initial skeletal deposit of $^{239}Pu^{4+}$ is cleared with a half-time of about 1.6 years; later measurements of $^{239}Pu^{4+}$ in the skeletons of individual dogs at postinjection times as long as 4400 days yielded a curve with a slope that could not be distinguished from zero (Stover *et al.*, 1962, 1972; Stover and Atherton, 1974).

The mature mammalian skeleton is not static, and it undergoes much internal structural change throughout the life span. During growth, structural remodeling (both resorption and accretion) is vigorous and extensive, and there is a net increase in bone mass. After skeletal growth is complete, remodeling and bone turnover involve only small fractions of the skeleton at any time, and there is little change in skeletal mass. During the last years of life of some mammals, resorption exceeds replacement leading to a slow decrease in skeletal mass (Bourne, 1956; Frost, 1963).

Bone resorption and accretion are surface-limited processes (Bourne, 1956; Ham, 1974). In the mature skeleton, turnover of bone (resorption and accretion) at the surfaces of the fine trabeculae of spongy bone is faster than at the surfaces of the larger trabeculae in the flat and membranous bones and in the distal ends of the long bones and the surfaces of the cortical bone vascular channels (about eight times faster in young adult beagles and four times faster in human adults) (Arnold and Jee, 1962; Arnold and Wei, 1972; ICRP, 1973; Wronski *et al.*, 1980).

Actinide-labeled bone surfaces may be resorbed by osteoclasts or be buried beneath new bone in the course of structural remodeling, or they may remain unaltered (Copp *et al.*, 1946; Arnold and Jee, 1962; Durbin *et al.*, 1969; Durbin, 1973; Wronski *et al.*, 1980; Sontag, 1993). The actinide content of the resorbed bone is eventually dissolved by the osteoclasts and/or marrow macrophages, released into the circulation, and redistributed among the target tissues (Arnold and Jee, 1962; Priest and Giannola, 1980; Priest *et al.*, 1983; Durbin and Schmidt, 1985; Durbin *et al.*, 1985). There is evidence indicating that solubilized actinide released from bone (or any other body site) is complexed and transported by the same plasma ligands (mainly Tf) and distributed among the same target tissues in the same proportions as the soluble form originally injected (Arnold and Jee, 1962; Durbin *et al.*, 1969; Jee, 1972a,b; Durbin, 1973; Priest and Giannola, 1980; Leggett, 1985, 1989, 1992a,b).

Redeposition in the skeleton can occur on both old (preinjection) surfaces augmenting their existing actinide concentrations and on new (postinjection) surfaces, which will acquire a lighter more diffuse label than those labeled immediately after the injection. With the passage of time, resorption of actinide-labeled bone surfaces (mainly trabeculae at red marrow sites) and redeposition of substantial fractions of the released and solubilized actinide will reduce the concentrations at the bone surfaces and increase the concentration in the

bone volume, tending to equalize the concentration in bones containing red marrow sites (vertebral bodies, ribs, sternum, pelvis, proximal ends of humerus and femur) and those that are mainly cortical bone (Durbin, 1973; Durbin *et al.*, 1985; Durbin and Schmidt, 1985; Sontag, 1993).

### 31.7.5 Summary

Prolonged retention of actinides deposited in the skeleton is the combined result of redeposition in bone of actinide released from soft tissues, removal from bone only by the relatively slow process of bone resorption, recirculation after release bound mainly to plasma proteins (which severely impedes excretion), and redeposition at new bone sites of large fractions of the actinide released from initially labeled bone sites.

## 31.8 ACTINIDE BINDING IN BONE

The specific nature of the initial chemical reactions underlying the fixation of actinides in living bone is incompletely understood.

### 31.8.1 Composition of bone

The compositions of mature mammalian cortical and trabecular bone are, on average, about 61, 26, and 13% by weight and 40, 35, and 27% by volume, mineral, organic matrix, and water, respectively (Gong *et al.*, 1964). The mineral phase [hydroxyapatite, $Ca_{10}(PO_4)_6(OH)_2$] exists as minute tablet-shaped crystals 2 to 2.5 μm wide, 3.5 μm long, and 0.25 to 0.5 μm thick, and these are aligned parallel to the longitudinal direction of the collagen fibers of the matrix (Neuman and Neuman, 1958). At the microscopic level, bone is not homogeneous, but it is reasonable to assume that the proportions of mineral and matrix on fully mineralized bone surfaces are about the same as the bulk volume composition, that is, that the exposed surface area is about equally divided between mineral crystals and organic matrix along with some bound water. By the same reasoning, bone that is not fully developed would be expected to have a smaller proportion of mineral exposed on the surface.

### 31.8.2 Actinide binding to bone *in vivo*

There is good, if inferential, evidence for *in vivo* actinide binding to bone mineral. In living mammals, the initial skeletal binding site of the actinides and their trivalent and tetravalent chemical analogs is at the mineral–organic interface. Actinide deposition is greatest on bare, fully mineralized resorbing surfaces and least on growing surfaces covered by a layer of bone matrix

(osteoid) (Jowsey *et al.*, 1958; Herring *et al.*, 1962). In rachitic animals, bone continues to grow but is very poorly mineralized: In such animals, $Pu^{4+}$ passed through the nonmineralized osteoid and deposited on the first available mineralized structures (Jee and Arnold, 1962). Actinides also accumulate on calcified nonskeletal structures such as renal calculi, calcified scar tissue, and calcified tracheal and bronchial cartilage (Painter *et al.*, 1946; Jee and Arnold, 1962; Durbin, 1973; Durbin *et al.*, 1985).

### 31.8.3 Actinide binding to bone mineral *in vitro*

Neuman (1953) demonstrated that binding of $UO_2^{2+}$ by bone mineral *in vitro* was a reversible ion-exchange process: One $UO_2^{2+}$ displaced two $Ca^{2+}$ ions and immobilized two $PO_4^{3-}$ moieties. *In vivo*, $UO_2^{2+}$ deposits at growth sites in the skeleton, and it accompanies hydroxyapatite crystal growth *in vitro*. However, the evidence indicates that $UO_2^{2+}$ is limited to the crystal surfaces, presumably because it is too large and too polar to 'fit' into the crystal lattice (Neuman and Neuman, 1958).

Jowsey *et al.* (1958) prepared solutions of $^{91}Y^{3+}$, $^{144}Ce^{3+}$, and $^{170}Tm^{3+}$ in human plasma reconstituted with water or with 0.0034 M sodium citrate. Bovine cortical bone was used to prepare the following dry powders (particle size not specified): fat-free whole bone, ED-bone (bone powder heated in ethylenediamine to digest the organic matrix); bone ash (heated at 600°C to destroy the organic matrix); EDTA-bone (bone powder treated with EDTA to remove the mineral fraction). Calcium phosphate [$Ca_3(PO_4)_2$] was included as a bone mineral surrogate, and charcoal and glass wool were included as nonspecific particulate controls. The dry powders (250 mg each) were placed in small paper thimbles, a solution of lanthanide in plasma or in citrated plasma was percolated through the solids, and two rinses of isotope-free media were applied. On average, uptake of the lanthanides by ED-bone, whole bone, $Ca_3(PO_4)_2$, and bone ash was 42, 40, 33, and 19% respectively, of the amounts present in the plasma media. Uptakes were about 30% greater from citrated plasma. The powdered organic matrix, charcoal, and glass wool did not take up the lanthanides from plasma, with or without added citrate. Thin sections of bone embedded in methylmethacrylate were incubated in a solution containing $^{91}Y^{3+}$, and autoradiographs showed that all of the calcified surfaces took up the lanthanide.

Foreman (1962) prepared a solution of $^{239}Pu^{4+}$ in 0.05 M lactate buffer pH 7. Bovine cortical bone was used to prepare the following dry powders (particle size not specified in most cases): fat-free whole bone, bone ash (700°C, 100–200 mesh), coarse bone ash (>100 mesh); KOH-bone (bone powder heated in KOH and ethylene glycol to digest the organic matrix); EDTA-bone (decalcified organic matrix). Carborundum, alundum, and pumice were included as particulate controls. Samples of each powder were shaken for 24 h with 100 to 200 mL of the $Pu^{4+}$-lactate buffer solution, and the clear supernatant was sampled periodically after allowing the solids to settle. After 24 h, the four particulates

containing bone mineral had taken up $\geq$95% of the $Pu^{4+}$ in the medium. The initial uptake rates of the bone mineral samples were in the order: bone ash (fine) > bone ash (coarse) $\gg$ KOH-bone $\gg$ whole bone. At equilibrium, the EDTA-decalcified organic fraction took up $\leq$10% of the available $Pu^{4+}$. The $Pu^{4+}$ did not adhere to the three inert mineral powders. Addition of 0.2 M $Ca^{2+}$ or 0.2 M $Na^{+}$ to the buffer medium did not change either the rates or 24 h uptakes of $Pu^{4+}$ by the whole bone or bone ash powders.

Foreman (1962) also prepared whole rat femora, as follows: fresh bone cleaned of adhering soft tissue; bone ash (700°C furnace); KOH-bone; and EDTA-bone. Four replications of each femur preparation were sealed in cellophane bags and surgically implanted in the peritoneal cavities of 'host' rats. The 'host' rats were injected iv with $^{239}Pu^{4+}$ citrate 24 h later and killed 48 h after the $Pu^{4+}$ injection. Uptake of the $Pu^{4+}$ in the living femora of the 'host' rats was reproducible, on average, 164 400 $\pm$ 66 000 cpm per whole bone. Uptakes of $Pu^{4+}$ in the implanted femora that had been heat or chemically ashed were nearly the same, about 40% of that in the living bone of their 'hosts', while $Pu^{4+}$ uptakes in the implanted fresh bone and EDTA-decalcified bone were 15 and 6%, respectively. The chemically or heat ashed bone preparations that were essentially free of organic tissue barriers had the greatest affinities for the $Pu^{4+}$, while the affinity of the decalcified bone matrix was the least. An important outcome of this experiment was the demonstration of the passage of $Pu^{4+}$ through the semipermeable cellophane membrane, implying the presence of a filterable $Pu^{4+}$ complex in the interstitial fluid of the peritoneal cavity.

Chipperfield and Taylor (1972) prepared dilute solutions of $^{239}Pu^{4+}$, $^{241}Am^{3+}$, and $^{244}Cm^{3+}$ nitrates, each of these was mixed with 3 mL of solutions of tris buffer pH 7.2 containing chelators, including: $3.4 \times 10^{-4}$ M sodium citrate, $3.2 \times 10^{-4}$ M EDTA, $2.4 \times 10^{-4}$ M DTPA, $3.4 \times 10^{-6}$ M Tf, or $4 \times 10^{-6}$ M bone sialoprotein or bone chondroitin sulfate–protein complex. Fine cortical bone ash powder (200–300 mesh) was added (10 mg) to each actinide-chelator solution and stirred vigorously for 1 h. Supernatant containing unbound actinide and solids containing bound actinide were separated by centrifugation. In the absence of a chelator, all three actinides were quantitatively associated with the bone mineral fraction. The fractions bound to the bone mineral (100% – reported solution content) for $Pu^{4+}$, $Am^{3+}$, and $Cm^{3+}$, respectively, were as follows: Tf (98, 99, 84); citrate (73, 100, 100); bone glycoproteins, on average (79, 92, 92); EDTA (91, 70, 61); DTPA (14, 0, 0). Effectiveness for preventing actinide binding to bone mineral, which can be viewed as the stabilities of their complexes with the chelators relative to those formed with the bone ash is in the order: Tf $\leq$ citrate < bone glycoproteins < EDTA < DTPA. Binding of $Am^{3+}$ and $Cm^{3+}$ to bone mineral was the same in this test system and nearly quantitative in the presence of Tf, citrate, or the bone glycoproteins; it was partially prevented by EDTA and completely prevented

by DTPA. Binding of $Pu^{4+}$ to bone mineral was nearly quantitative in the presence of Tf, partially prevented by EDTA, the bone glycoproteins, or citrate, and incompletely prevented by DTPA.

Guilmette *et al.* (1998, 2003) prepared solutions of $^{238}Pu^{4+}$, $^{239}Pu^{4+}$, and $^{241}Am^{3+}$ in 0.0034 to 0.005 M sodium citrate. Finely ground bovine bone ash and synthetic bone mineral (hydroxyapatite, HAP) were characterized by X-ray diffraction, and their measured specific surface areas were 10.7 and 65 $m^2\ g^{-1}$, respectively. Each actinide was stirred for 24 h with 10 mg of a mineral powder in 0.1 M HEPES buffer pH 7.2. The solid and supernatant were separated by ultrafiltration. Under these conditions $\geq$99% of the actinide was bound to the minerals. Varying masses of $^{238}Pu^{4+}$ and $^{239}Pu^{4+}$ (0.001–100 μg) and $^{241}Am^{3+}$ (0.001–1.0 μg) were added to 10 mg of bone ash or HAP to characterize the relationships between actinide binding and mineral surface area, that is, the binding capacity. For $Pu^{4+}$, masses $\leq$10 μg, and for all $^{241}Am^{3+}$ masses studied, binding to both minerals was $\geq$99% in 24 h. However, when the mass of $^{239}Pu^{4+}$ was 100 μg, more than 50% incubated with bone ash and 20% incubated with HAP remained unbound at 24 h. The data are consistent with the larger specific surface area of HAP presenting more binding sites, and they may also be interpreted as signifying that the mineral surfaces contain a saturatable number of potential metal-binding sites per unit area. The DTPA chelates of $^{238}Pu^{4+}$ and $^{241}Am^{3+}$ were incubated with 10 mg of HAP. There was no indication that the $^{241}Am^{3+}$–DTPA complex dissociated in favor of mineral binding. In contrast, 50% of the $^{238}Pu^{4+}$–DTPA complex dissociated in 24 h in favor of binding to the bone mineral. The stability of $^{241}Am^{3+}$–DTPA is evidently greater, while that of $^{238}Pu^{4+}$–DTPA is somewhat less, than the stabilities of their respective bone mineral complexes.

Guilmette *et al.* (2003) investigated removal of $^{238}Pu^{4+}$ and $^{241}Am^{3+}$ from bone mineral by 24 h incubation of those actinides prebound to HAP by chelators in solutions of 0.1 M HEPES buffer pH 7.2. Binding of $^{238}Pu^{4+}$ and $^{241}Am^{3+}$ by HAP is sufficiently stable that $ZnNa_3$–DTPA removed only 1.4% of the $Am^{3+}$ and $\leq$0.1% of the $Pu^{4+}$ sorbed to the mineral. Actinide removal from HAP was tested with a set of tetra-, hexa-, and octadentate ligands with linear or branched backbones containing bidentate catecholate (CAM) or hydroxypyridinonate (HOPO) metal-binding groups. Removal of $Pu^{4+}$ (4–54%) was achieved only by the linear octadentate CAM and HOPO ligands. Removal of $Am^{3+}$ (5–21%) was achieved with several linear or branched tetra-, hexa-, or octadentate ligands.

Bostick *et al.* (2000), Moore *et al.* (2003), and Thomson *et al.* (2003) conducted investigations in support of the management and remediation of actinide-contaminated groundwaters, sediments, and wastewaters. Batch sorption and column tests demonstrated the great affinities of $UO_2^{2+}$, $NpO_2^{+}$, $Pu^{4+}$, $Am^{3+}$, and stable $Ce^{3+}$ for natural and synthetic apatites, including hydroxyapatite, $Ca_3(PO_4)_2$, and bone ash.

### 31.8.4 Actinide binding by bone glycoproteins

A case can be made for the participation of some low abundance organic matrix constituents in the binding of actinides in living bone (reviewed by Duffield and Taylor, 1986). *In vitro* complexation of $Th^{4+}$ and $Pu^{4+}$, and to a lesser degree, $Am^{3+}$ and $Cm^{3+}$ by isolated mucoprotein substituents of bone matrix has been demonstrated.

All of the multivalent lanthanides and actinides studied autoradiographically deposit most intensely on fully mineralized bone surfaces, anatomical sites that also stain positively with PAS for the presence of mucosubstances (Jowsey, 1956; Herring *et al.*, 1962; Williamson and Vaughan, 1964; Vaughan *et al.*, 1973). Paraphrasing Jowsey (1956) in response to a conference participant's question: In areas of bone resorption, the PAS staining is the result of the depolymerized state of the mucopolysaccharides in the ground substance (matrix). In such state there are presumably free side chains of the mucopolysaccharide molecules (containing potentially chelating 1,2-hydroxy groups), which are oxidized by the periodic acid to aldehydes and take up the Schiff stain.

Nearly 90% of the organic bone matrix is collagen, which contributes about 20% of the weight of native bone. Five distinct glycoprotein fractions were extracted from bovine cortical bone. Their designations and weight fractions of native bone (% by weight) are, as follows: bone sialoprotein, 0.25%; bone chondroitin sulfate–protein complex, 0.18%; three less well-characterized glycoprotein fractions – glycoprotein I and II, 1.57% combined; cetylpyridonium chloride (cpc) soluble glycoprotein, 0.1%. While not regarded as conclusive, supporting experiments indicate that the sialoprotein content (and perhaps also the other mucosubstances) of bone are formed and laid down in the matrix during bone formation. The functions of the mucosubstances of mature bone are not known (Herring, 1964). Bone sialoprotein contains large proportions of sialic, glutamic, and aspartic acids; 15, 20, and 15 moles of acids per mole of protein, respectively.

Chipperfield and Taylor (1968, 1970, 1972) used gel filtration (Sephadex G-25 and G-50) to investigate the bonding of ultrafiltered dilute solutions of $^{228}Th^{4+}$, $^{239}Pu^{4+}$, $^{241}Am^{3+}$, and $^{244}Cm^{3+}$ nitrates incubated with the isolated bone glycoproteins noted above. The proteins were dissolved in tris buffer pH 7.2, and the protein:metal molar ratios were 1:1 for $Pu^{4+}$ and 10:1 for the higher specific activity radionuclides. The results of those studies are collected in Table 31.13. Those results, although variable and regarded by the authors as semiquantitative, indicate that at physiological pH the isolated glycoprotein fractions of bone matrix can form complexes with $Th^{4+}$ and $Pu^{4+}$, and to a lesser degree, with $Am^{3+}$ and $Cm^{3+}$. Under these experimental conditions, the affinities of the bone glycoprotein fractions for $Th^{4+}$ and $Pu^{4+}$ apparently exceed the affinities for these actinides of reconstituted human Tf or apo-Tf. Two of the bone glycoproteins, bone sialoprotein and bone chondroitin sulfate–protein

**Table 31.13** *Collected data for association of selected actinides with isolated bone glycoproteins, human transferrin, and poly-L-glutamic acid.*[a]

| *Protein* | *Percent of applied actinide eluted with protein* | | | |
|---|---|---|---|---|
| | $^{228}Th^{4+}$ | $^{239}Pu^{4+}$ | $^{241}Am^{3+}$ | $^{244}Cm^{3+}$ |
| Bone sialoprotein | 96[d] | 71[b], 52[c], 55[d] | 30[b], 10[d] | 12[d] |
| Bone chondroitin sulfate–protein complex | 78[d], 22[e] | 72[b], 49[d], 13[e] | 5.0[b], 15[d], 0.3[e] | 10[d], 0.3[e] |
| Glycoprotein I | 13[d] | 30[d] | 2.8[d] | 38[d] |
| Glycoprotein II | 72[d] | 50[d] | 5.1[d] | 8.2[d] |
| Cpc-soluble glycoprotein | 83[d] | 37[d] | 4.6[d] | 8.7[d] |
| Human transferrin | 61[c,e] | 24[b,c], 19[e] | 0.17[b], 0.2[e] | 0[e] |
| Apotransferrin | 30[c] | 43[c] | – | – |
| Soluble collagen | – | 2.8[b], 23[d] | 0.6[d], 0[e] | 0.9[d] |
| Poly-L-glutamic acid | 80[e] | 69[e] | 8.0[e] | 27[e] |

[a] Reported values of protein binding rounded to two significant figures. Ultrafiltered actinide nitrates incubated with proteins dissolved in tris buffer at pH 7.2. Mixtures eluted with buffer from G-25 or G-50 Sephadex gel columns to determine amount bound to protein.
[b] Chipperfield and Taylor (1968).
[c] Chipperfield and Taylor (1970).
[d] Table I of Chipperfield and Taylor (1972).
[e] Table II of Chipperfield and Taylor (1972).

complex, were about as effective as EDTA in competing with bone ash for $Pu^{4+}$, $Am^{3+}$, and $Cm^{3+}$.

Supporting studies demonstrated that actinide binding by the bone glycoproteins was pH dependent; maximum binding of $Pu^{4+}$ by bone sialoprotein is at pH 6, and of $Am^{3+}$ and $Cm^{3+}$ at pH 8. These results were interpreted by the authors to mean that $Pu^{4+}$ was bound by the abundant carboxyl groups of the protein's amino acid side chains, but that those carboxyl groups were less important for binding the trivalent actinides. Binding of $Pu^{4+}$ by bone sialoprotein was reduced, but not abolished, by mild acid hydrolysis (removal) of the terminal sialic acid moieties, which suggests that the sialic acid groups may also participate in metal binding.

### 31.8.5 Summary

Actinide binding in bone is a surface phenomenon. However, except for $UO_2^{2+}$, binding of the trivalent and tetravalent actinides and $NpO_2^+$ to bone surfaces is so stable that those metals neither migrate into the bone volume via the canaliculi nor are released back into the circulation by ion exchange or complexation with the ligands of the constantly flowing plasma and tissue fluid.

At physiological pH, trivalent and tetravalent lanthanides and actinides, $UO_2^{2+}$ and $NpO_2^+$, bind stably to native and synthetic bone mineral *in vitro*. Actinide uptake by various bone mineral preparations was nearly quantitative

from buffered solutions (lactate, tris, HEPES, pH 7–7.4) even from those solutions that also contained 0.3 to 0.5 mM citrate, whole plasma, or human Tf. In general, actinide uptake by the crystalline bone mineral preparations (synthetic HAP, chemically ashed KOH-glycol bone, or ED-bone) was faster than for bone ash, $Ca_3(PO_4)_2$, or powdered defatted whole bone, in which about one-half of the exposed particle surface is organic matrix. Actinide uptake by bone mineral is positively correlated with the surface area of the particles and appears to be saturable, indicating a fixed number of binding sites per unit surface area.

Hydroxyapatite [$Ca_{10}(PO_4)_6(OH)_2$] presents an organized $Ca^{2+}$-poor negatively charged surface with unsatisfied negative charges on adjacent phosphates. If $Ca^{2+}$ is replaced, as is the case for $UO_2^{2+}$, there is access to the oxygens of two and perhaps three phosphates. The complexes of $Th^{4+}$ and $Pu^{4+}$ with bone mineral are more stable than the complexes that these metal ions form with $ZnNa_3$-DTPA, indicating that the crystals themselves provide spatially suitable multidentate binding sites.

The PAS-positive staining at the organic–mineral interface of bone surfaces, which are the actinide deposition sites in the skeleton, suggested that bone glycoproteins may participate in actinide binding, even though powdered decalcified bone matrix does not bind actinides. Five isolated low abundance bone glycoproteins form variably stable actinide complexes. The binding units of these proteins are considered to be mainly free sialic acid, the monodentate carboxyl groups of glutamic acid, and the bidentate alpha-hydroxy-carboxyl groups of aspartic acid.

The mineral crystals of native bone are sandwiched between layers of matrix collagen fibers, and the exposed bone surfaces do not present as many metal-binding sites as isolated bone mineral crystals. The most stable complexes of the trivalent lanthanides and actinides are six-coordinate (six M–O bonds), and those of the tetravalent actinides are eight-coordinate (eight M–O bonds). It would seem that *in situ* the number and configuration of the exposed potential binding groups of the glycoproteins alone would be insufficient to provide enough suitably arranged binding groups for stable actinide complexation. However, in living bone, both the mineral crystals and the neighboring matrix constituents (glycoproteins) combined may furnish sufficient numbers of binding groups suitably arranged in three-dimensional space for rapid stable actinide complexation *in situ*.

## 31.9 *IN VIVO* CHELATION OF THE ACTINIDES

The potential hazards to human health of the radioactive fission products and new heavy elements created by nuclear fission were recognized early, stimulating the search for effective ways to remove internally deposited radioelements

from the body (Schubert, 1955; Voegtlin and Hodge, 1949, 1953; Stone, 1951). Chemical agents that form stable excretable actinide complexes were soon recognized as the only practical therapy for internal contamination (decorporation) (Voegtlin and Hodge, 1949, 1953; Schubert, 1955; Rosenthal, 1956; Catsch, 1964). Such agents should have greater affinity for actinides at physiological pH than the biological ligands, low affinities for essential divalent metals, and low toxicity at effective dose. Reviews and proceedings of conferences on the development of chelators suitable for removal of internally deposited actinides have dealt with the chemistry of metal chelates, animal studies to determine ligand effectiveness for reducing actinide burdens in the tissues and amelioration of actinide-induced chemical and radiation damage, ligand toxicity, and clinical applications (Rosenthal, 1956; Seven and Johnson, 1960; Kornberg and Norwood, 1968; Volf, 1978; NCRP, 1980; Raymond and Smith, 1981; Taylor, 1991; Bhattacharyya *et al.*, 1992; Durbin *et al.*, 1997a, 1998a,b; Stradling *et al.*, 2000a,b; Wood *et al.*, 2000; Gorden *et al.*, 2003).

### 31.9.1 Polyaminopolycarboxylic acids

The first chelating agent investigated was ethylenediaminetetraacetic acid ($H_4$-EDTA). Its $Ca^{2+}$ salt, $CaNa_2$–EDTA, was introduced to avoid toxic depletion of serum $Ca^{2+}$. It enhanced excretion of $^{91}Y^{3+}$, $^{144}Ce^{3+}$, and $^{239}Pu^{4+}$ in rats (Foreman and Hamilton, 1951; Hamilton and Scott, 1953). But $CaNa_2$–EDTA is a poor actinide decorporation agent: it is renally toxic at effective dose; it depletes essential $Zn^{2+}$ and other divalent metals; its efficacy cannot be improved except by increasing the administered dose.

Pentacarboxyl diethylenetriaminepentaacetic acid ($H_5$-DTPA) and its $Ca^{2+}$ and $Zn^{2+}$ salts ($CaNa_3$–DTPA introduced in 1957 and $ZnNa_3$–DTPA introduced in 1965) improved lanthanide and actinide decorporation compared with $CaNa_2$–EDTA (Catsch and Lê, 1957; Kroll *et al.*, 1957; Smith, 1958; Catsch and von Wedelstaedt, 1965). Those clinically approved DTPA salts are effective decorporation agents for the trivalent lanthanides and actinides, less effective for $Pu^{4+}$ and $Th^{4+}$, and nearly ineffective for reducing the body content of $UO_2^{2+}$ or $NpO_2^+$. [See references cited in Volf, 1978; Durbin *et al.*, 1997a, 1998a,b; Gorden *et al.*, 2003]. Although nominally octadentate, $CaNa_3$–DTPA appears not to coordinate fully with $Pu^{4+}$, and it does not remove $Pu^{4+}$ bound to bone mineral *in vitro* (Raymond and Smith, 1981; Guilmette *et al.*, 2003).

Several variants and derivatives of DTPA have been prepared and tested in animals, including polyaminopolycarboxylic acids with longer central bridges or additional carboxyl groups (Catsch, 1964); a dihydroxamic acid derivative, ZnNa–DTPA–DX (Durbin *et al.*, 1989b; Stradling *et al.*, 1991; Volf *et al.*, 1993); lipophilic derivatives containing long alkane side chains (Volf, 1978; Raymond and Smith, 1981; Miller *et al.*, 1993). None of those DTPA-based

ligands was substantially more effective for *in vivo* chelation of lanthanides or $Pu^{4+}$ or less toxic than native $CaNa_3$–DTPA, and most have been abandoned.

### 31.9.2 Desferrioxamine

Desferrioxamine (DFO), a linear tris-hydroxamate ligand, is a member of a class of compounds (siderophores) elaborated by microorganisms to obtain iron from the environment (Raymond and Smith, 1981). *In vivo* $Pu^{4+}$ chelation is hampered by the weak acidity of the hydroxamic groups, which are not ionized at pH $< 8$; they are deprotonated only slowly at pH 7.4 by $Fe^{3+}$ and $Pu^{4+}$ but not by trivalent actinides (Taylor, 1967; Durbin *et al.*, 1980, 1989b; Rodgers and Raymond, 1983).

### 31.9.3 Siderophores as model chelators

Investigations of the siderophores and their structures and coordination chemistry identified the powerful hexadentate iron-sequestering agent, enterobactin (EB). EB is produced by enteric bacteria (*E. coli*) to obtain $Fe^{3+}$ from the nearly neutral contents of the mammalian intestine (see references in Raymond and Smith, 1981 and Gorden *et al.*, 2003). It contains three bidentate catecholate binding groups attached through amide linkages to a cyclic 1-serine backbone and is preorganized for binding. The properties and structure of EB and similarities in the coordination properties of $Pu^{4+}$ and $Fe^{3+}$ provided the basis for rational design of highly selective multidentate actinide chelators that would be effective at physiological pH.

#### (a) Catecholate ligands

Multidentate catecholate ligands based on the EB model (denticity 4–8) were prepared containing catechol (CAM), sulfocatechol [CAM(S)], carboxycatechol [CAM(C)], or catecholamide (TAM) metal-binding groups (Fig. 31.15) attached through amide linkage to linear (LI-), cyclic (CY-), aromatic (ME-), or branched (TREN-, H(2,2)-) backbones. Syntheses and structures of the CAM ligands are collected in Gorden *et al.* (2003). All of those ligands were evaluated for promotion of excretion of $^{238}Pu^{4+}$ from mice (30 μmol $kg^{-1}$ ligand ip 1 h after iv injection of $^{238}Pu^{4+}$ citrate, kill at 24 h). Catecholate ligands of denticity $<8$ and those containing only CAM groups were marginally effective for *in vivo* $Pu^{4+}$ chelation. The water-soluble octadentate ligands with flexible linear backbones based on spermine were more effective than octadentate ligands with attached lipophilic side chains or those with cyclic backbones. Reduction of skeleton $Pu^{4+}$ by 3,4,3-LICAM(S) and of liver $Pu^{4+}$ by 3,4,3-LICAM(C) were greater than obtained with an equimolar amount of $CaNa_3$–DTPA (Durbin *et al.*, 1980, 1984, 1989a,b, 1996; Lloyd *et al.*, 1984c). Those

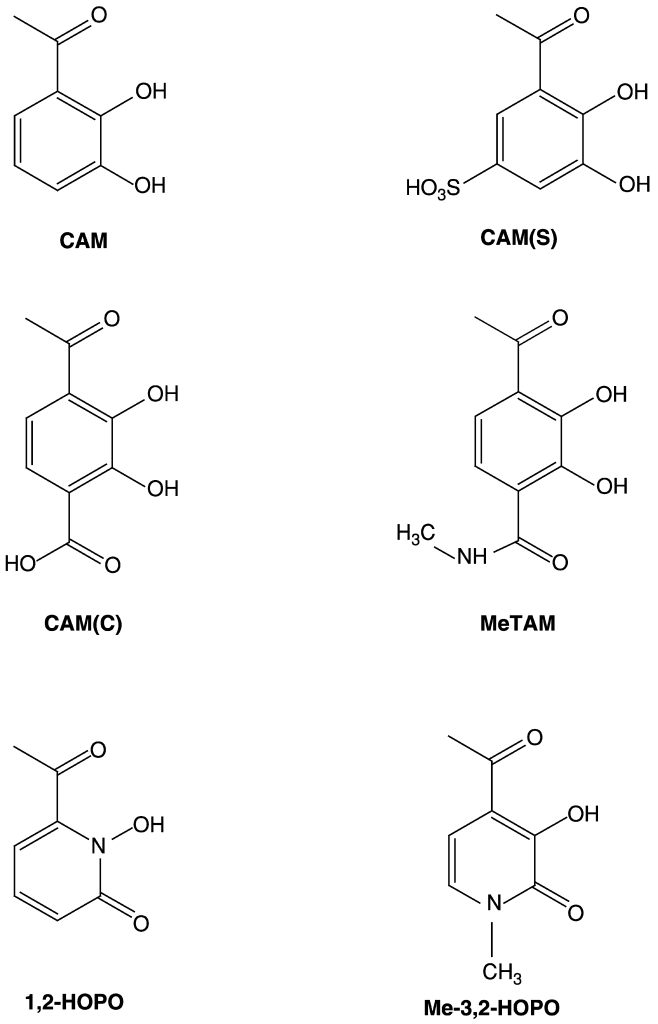


**Fig. 31.15** *Catecholate and hydroxypyridonate metal-binding units incorporated into multidentate ligands for* in vivo *chelation of actinides. Catechol* (*CAM*), 5-*sulfocatechol* (*CAM*(*S*)), 4-*carboxycatechol* (*CAM*(*C*)), *methylterephthalamide* (*METAM*), 1,2 *hydroxypyridinone* (1,2-*HOPO*), *Me*-3,2-*hydroxypyridinone* (*Me*-3,2-*HOPO*).

ligands were much more effective than $CaNa_3$–DTPA at doses $\leq$30 μmol $kg^{-1}$, and they were orally active.

Although some of the *in vivo* properties of the two octadentate catecholate ligands are favorable, both are defective. *In vivo* chelation of $Am^{3+}$ (and presumably other trivalent actinides and lanthanides) was significantly less than with $CaNa_3$–DTPA (Lloyd *et al.*, 1984c; Stradling *et al.*, 1986, 1989;

Volf, 1986; Volf *et al.*, 1986). The specific electric charge ($e/r$) of $Am^{3+}$ is not great enough to deprotonate more than three of the eight OH groups of the tetracatecholate ligands at pH 7.4 (Kappel *et al.*, 1985). Furthermore, both of these nominally octadentate ligands are only functionally hexadentate at pH < 12. As the pH is reduced below 7.4, binding of $Pu^{4+}$ by the more lipophilic 3,4,3-LICAM(C) becomes progressively less stable, and at pH 6 to 6.5 (the ambient pH of the lungs and renal tubules), the tetradentate species of the $Pu^{4+}$–3,4,3-LICAM(C) complex dominates (Kappel *et al.*, 1985; Durbin *et al.*, 1989a). Chelation of inhaled $Pu^{4+}$ deposited in the lungs is weak and less effective than with $CaNa_3$–DTPA. The $Pu^{4+}$ complex with 3,4,3-LICAM(C) that formed in the blood at pH 7.4 partially dissociates at the reduced pH of the kidneys depositing $Pu^{4+}$ residues (Stradling *et al.*, 1986, 1989; Volf, 1986; Volf *et al.*, 1986; Durbin *et al.*, 1989a). 3,4,3-LICAM(S) was found to be renally toxic in dogs at the effective dose (Lloyd *et al.*, 1984c).

At pH 7.4, methylterephthalamide (MeTAM) forms a more stable ferric complex than any other catecholate-binding group (Durbin *et al.*, 1996). MeTAM was introduced into three octadentate ligands with differing backbones; the MeTAM group was attached to the N-terminal of DFO, and four MeTAM groups were incorporated into linear spermine (3,4,3-LIMeTAM) and branched PENTEN [H(2,2)-MeTAM]. Reductions of body $Pu^{4+}$ by these octadentate ligands were similar to each other, somewhat greater than for 3,4,3-LICAM(C), and significantly greater than for $CaNa_3$–DTPA. Their $Pu^{4+}$ complexes are stable over the physiological pH range, and no $Pu^{4+}$ residues were left in the kidneys. These lipophilic ligands are sparingly soluble at pH < 8, their solutions are rapidly air oxidized, and their reductions of body $Pu^{4+}$ in mice, similar to that obtained with 3,4,3-LICAM(C), suggested that they were also functionally hexadentate at pH 7.4.

### (b) Hydroxypyridinonate ligands

Bidentate metal-binding groups more acidic than derivatized catechol and were required to achieve full eight-coordination with $Pu^{4+}$ and to stably bind trivalent actinides in dilute aqueous solution at physiological pH. Highly selective HOPO metal-binding units occur in a few siderophores. The 1,2-HOPO and Me–3,2-HOPO isomers (Fig. 31.15) are structural and electronic analogs of hydroxamic acid and catechol, respectively. Their $Fe^{3+}$ complexes are exceptionally stable, and both isomers are deprotonated and ready for metal binding at physiological pH (Scarrow *et al.*, 1985).

The 1,2-HOPO and Me–3,2-HOPO binding units were derivatized by attaching a carboxyl group adjacent to the OH group on the pyridinone ring; the COOH group can then be attached to amines on the selected molecular backbones through amide linkages. An important feature of the 1,2-HOPO and Me–3,2-HOPO complexes is that, as is observed in the catecholamide complexes, strong hydrogen bonds between the amide proton and the adjacent oxygen

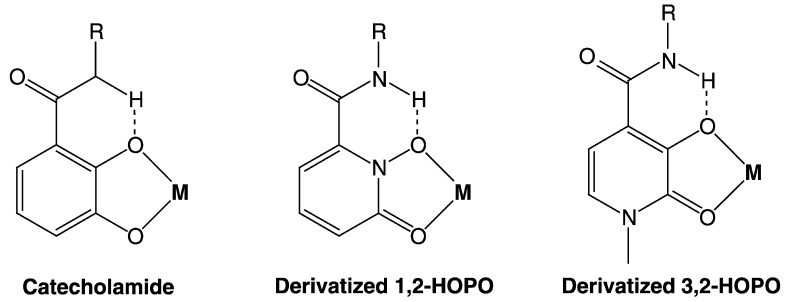


**Fig. 31.16** *Strong hydrogen bonds between the amide proton and the adjacent oxygen donor enhance the stabilities of the metal complexes of the catecholate and hydroxypyridinonate ligands* (*Xu* et al., 2001).

donor increase the stabilities of their metal complexes (Fig. 31.16) (Xu *et al.*, 1995, 2001). Sets of multidentate 1,2-HOPO and Me–3,2-HOPO ligands were prepared, as follows: tetradentate with linear backbones (α-ω-alkanediamines – 3-LI-, 4-LI-, 5-LI- 6-LI- and 2-aminoethylether, 5-LIO-); hexadentate with a linear spermidine backbone (3,4-LI-) or with a tripodal branched backbone triethyleneamine (TREN-); octadentate with a linear spermine backbone (3,4,3-LI-), or through attachment of one HOPO group to the N-terminal of DFO (DFO-), (Fig. 31.17) (White *et al.*, 1988; Xu *et al.*, 1995; Xu and Raymond, 1999; Durbin *et al.*, 2000b).

Ligand efficacies were assessed for *in vivo* $Pu^{4+}$ chelation by administering them to mice that had been injected iv with $^{238}Pu^{4+}$ citrate, as follows: ligand injected ip (30 μmol $kg^{-1}$) at 1 h (prompt injection), variable ligand dose at 1 h (dose effectiveness), ligand ip at 24 h (delayed effectiveness), ligand given orally at 5 min (oral activity). The ferric complexes of some ligands were administered promptly by ip injection or orally to assess competition between the ferric and $Pu^{4+}$ complexes. Mice were killed 24 h after the ligand administration, and all tissues and excreta were radioanalyzed for $Pu^{4+}$ (White *et al.*, 1988; Xu *et al.*, 1995; Durbin *et al.*, 2000b; Gorden *et al.*, 2003). Selected ligands were also assessed for *in vivo* chelation of $^{241}Am^{3+}$,$^{232}UO_2^{2+}$ or $^{233}UO_2^{2+}$, and $^{237}NpO_2^{+}$ (Durbin *et al.*, 1994, 1997a, 1998b, 2000a).

### (c) Ligands for $Pu^{4+}$

1,2-HOPO and Me–3,2-HOPO ligands (tetradentate with 4-LI-, 5-LI-, 5-LIO-backbones, hexadentate with a TREN- backbone, and octadentate with a 3,4,3-LI- or H(2,2)- backbone) given ip or orally after the $Pu^{4+}$ iv injection at doses ranging from 0.1 to 100 μmol $kg^{-1}$ were significantly and markedly superior to equimolar amounts of $CaNa_3$–DTPA for promoting $Pu^{4+}$ excretion. Promotion of $Pu^{4+}$ excretion by ip injection of 30 μmol $kg^{-1}$ of the linear 1,2-HOPO ligands (injected ip 1 h after the $Pu^{4+}$ injection) was positively correlated with

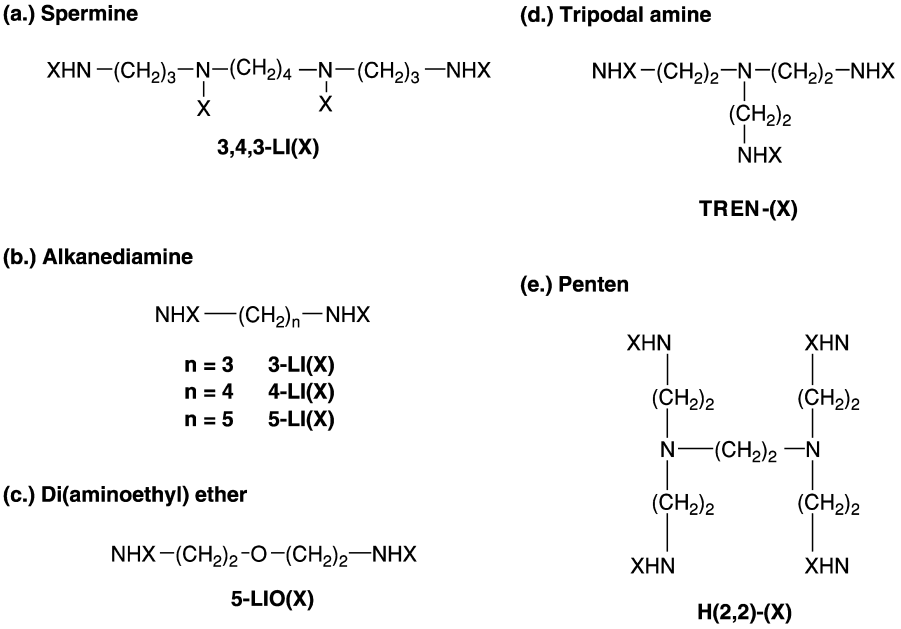


**Fig. 31.17** *Linear and branched molecular backbones used for multidentate actinide chelating agents: tetradentate* (*b, alkanediamines; c, di*(*aminoethyl*)*ether*); *hexadentate* (*d, tripodal amine*); *octadentate* (*a, spermine; e, penten*).

ligand denticity, indicating formation of a complete eight-coordinate complex with octadentate 3,4,3-LI(1,2-HOPO) (White *et al.*, 1988; Gorden *et al.*, 2003).

At the standard 30 μmol $kg^{-1}$ dose given to mice ip at 1 h after the $Pu^{4+}$ injection, the tetra-, hexa-, and octadentate Me–3,2-HOPO ligands all promoted nearly the same amount of $Pu^{4+}$ excretion. Apparently, the stabilities of the $Pu^{4+}$ complexes with the tetradentate and hexadentate Me–3,2-HOPO ligands and the ligand concentrations established in the blood at this dose level are large enough to allow those ligands to compete for $Pu^{4+}$ with the bioligands. However, when the Me–3,2-HOPO ligands were given orally, at lower doses, or as ferric complexes, the octadentate ligands, which have 1:1 stoichiometry for binding $Pu^{4+}$, were clearly more effective for *in vivo* $Pu^{4+}$ chelation than the ligands of lesser denticity (Durbin *et al.*, 1989b, 2000b; Xu *et al.*, 1995; Gorden *et al.*, 2003).

The efficacies of the structurally analogous pairs of 1,2-HOPO and Me–3,2-HOPO ligands were compared in several $Pu^{4+}$ removal protocols in mice. Overall, the Me–3,2-HOPO ligands were more effective for *in vivo* $Pu^{4+}$ chelation than their structural 1,2-HOPO analogs (Durbin *et al.*, 2000b). The greater affinity of Me–3,2-HOPO for $Pu^{4+}$ *in vivo* agrees with the greater stabilities of

the Me–3,2-HOPO complexes with other 'hard' metal ions like $Fe^{3+}$ and $Th^{4+}$ (Scarrow *et al.*, 1985; Veeck *et al.*, 2004).

Both octadentate HOPO ligands with the branched H(2,2)-backbone were highly effective for *in vivo* $Pu^{4+}$ chelation, but they were considered to be too toxic to warrant further investigation (Durbin *et al.*, 1997a, 2000b). Low-toxicity DFO-(1,2-HOPO) given by ip injection is about as effective as 3,4,3-LI(1,2,-HOPO) for *in vivo* $Pu^{4+}$ chelation, and it is moderately effective when given orally or at low dose (White *et al.*, 1988; Durbin *et al.*, 1989b). However, the weak acidity of the three hydroxamate groups prevents that ligand from competing effectively for inhaled $Pu^{4+}$ deposited in the lungs and from stably binding $Am^{3+}$ (Stradling *et al.*, 1991; Volf *et al.*, 1993, 1996a). *In vivo* $Pu^{4+}$ chelation by DFO-(Me-3,2-HOPO) was significantly poorer than was obtained with its analog, DFO-(1,2-HOPO), but better than with native DFO. The lower than expected efficacy of DFO-(Me-3,2-HOPO) may be attributed to its lower aqueous solubility and the instability of its $Pu^{4+}$ complex at the lower end of the physiological pH range (Xu *et al.*, 1995).

Among the ligand sets, the most effective for *in vivo* $Pu^{4+}$ chelation is linear octadentate 3,4,3-LI(1,2-HOPO). Although it contains the less stably binding 1,2-HOPO unit, it has good aqueous solubility, and the flexible linear spermine backbone apparently confers advantages for $Pu^{4+}$ binding by allowing a more favorable spatial arrangement of the four binding groups around the $Pu^{4+}$ center. The 3,4,3-LI(1,2-HOPO) ligand is markedly superior to $CaNa_3$–DTPA for reducing $Pu^{4+}$ in all tissues when given by injection, oral administration, or subcutaneous infusion after an iv or im injection or inhalation of $Pu^{4+}$ nitrate or citrate in rats and mice (White *et al.*, 1988; Durbin *et al.*, 1989b, 2000b; Stradling *et al.*, 1992, 1993; Volf *et al.*, 1993, 1996a,b; Gray *et al.*, 1994). It is effective at doses as low as 0.03 μmol $kg^{-1}$ in mice. When injected or infiltrated into an im wound site, it is more effective than $CaNa_3$–DTPA for reducing the body and wound site content of $Th^{4+}$ (Stradling *et al.*, 1995a).

It was considered that the effectiveness of the octadentate 3,4,3-LI(1,2-HOPO) ligand might be improved, if the thermodynamically more potent Me-3,2-HOPO were introduced. Concerns about toxicity, lipophilicity, and aqueous solubility of a tetra-Me-3,2-HOPO ligand led to the synthesis of the mixed ligand, 3,4,3-LI(1,2-Me-3,2-HOPO). Two 1,2-HOPO units occupy the central secondary amines and two Me-3,2-HOPO units are attached to the terminal primary amines of spermine. Substitution of the two Me-3,2-HOPO groups for 1,2-HOPO slightly increased the stability of the $Pu^{4+}$ complex at pH 7.4 and the lipophilicity and oral activity of the ligand, while somewhat reducing acute toxicity at high dose (Xu *et al.*, 2002). However, the modest thermodynamic gain was offset by the reduction in hydrophilicity, which appears to be an important property of 3,4,3-LI(1,2-HOPO), most likely facilitating its access to $Pu^{4+}$ in the skeleton (Durbin *et al.*, 2000b, 2003).

Crystals have been prepared from water of structurally analogous $Ce^{4+}$[5-LI-(Me–3,2-HOPO)$_2$] and $Pu^{4+}$[5-LIO-(Me–3,2-HOPO)$_2$] complexes (Fig. 31.18).

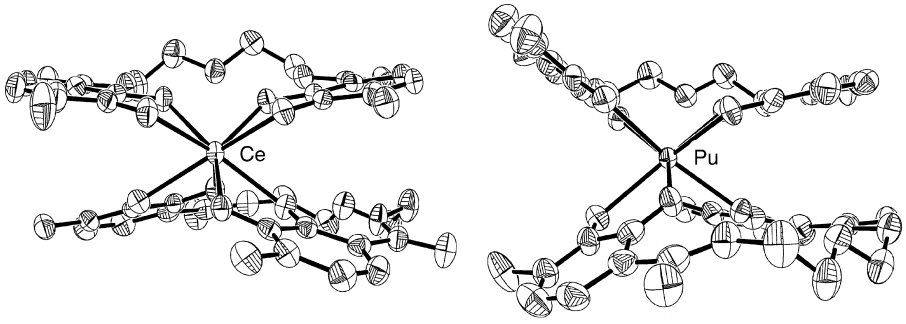


**Fig. 31.18** *Molecular structures* (*viewed from the side*) *of Ce*(IV)[5-*LIO*(*Me*-3,2-*HOPO*)]$_2$ (*left side, Xu* et al., 2000) *and Pu*(IV)[5-*LIO*(*Me*-3,2-*HOPO*)]$_2$ (*right side, Gorden* et al., 2005).

In both cases the 2:1 structure is demonstrated. The overall ligand geometries resemble sandwich structures that are defined by the oxygen atoms coordinating to the $Ce^{4+}$ and $Pu^{4+}$ centers (Xu *et al.*, 2000; Gorden *et al.*, 2005). Solution thermodynamic studies of the $Ce^{4+}$ complex system gave an overall formation constant of the complex (log $\beta_2$) of 41.6, and the formation constant of the analogous $Pu^{4+}$ complex is expected to be essentially the same.

### (d) Ligands for $Am^{3+}$

The efficacies of ligands containing HOPO groups for *in vivo* chelation of $Am^{3+}$ and for removing $Am^{3+}$ from bone mineral are generally in the order: octadentate > hexadentate > tetradentate (Guilmette *et al.*, 2003). The octadentate ligands more than satisfy the requirement for six-coordination preferred by $Am^{3+}$, and if three of their bidentate metal-binding units can bind to $Am^{3+}$ without steric hindrance, the extra binding group appears to enhance the stabilities of their $Am^{3+}$ complexes. As noted above, *in vivo* chelation of $Am^{3+}$ by the octadentate ligands containing carboxy- or sulfocatechol [CAM (C), CAM(S)] or by hydroxamate (as in the octadentate ligands with the DFO-backbone) is weak because too few of the hydroxyl groups of those ligands can be deprotonated by $Am^{3+}$ (and presumably other trivalent actinides) to form stable complexes at physiological pH (Lloyd *et al.*, 1984c; Kappel *et al.*, 1985; Stradling *et al.*, 1986, 1989; Volf, 1986; Volf *et al.*, 1986; Zhu *et al.*, 1988).

Four HOPO ligands have been investigated in rats and mice for *in vivo* chelation of $Am^{3+}$: octadentate 3,4,3-LI(1,2-HOPO), hexadentate TREN-(Me–3,2-HOPO), tetradentate 5-LI(Me–3,2-HOPO), and 5-LIO(Me–3,2-HOPO). When given by injection or orally (30 μmol $kg^{-1}$) to rats or mice contaminated with $^{241}Am^{3+}$ by injection or infiltration into a wound, all four of those ligands were more effective than an equimolar amount of

$CaNa_3$–DTPA. Octadentate 3,4,3-LI(1,2-HOPO) was about as effective as $CaNa_3$–DTPA, while the other HOPO ligands of lesser denticity were less effective than $CaNa_3$–DTPA for reducing body and lung $Am^{3+}$ when the $Am^{3+}$ had been inhaled (Stradling *et al.*, 1992; 1993, 1995b; Volf *et al.*, 1993, 1996; Durbin *et al.*, 1994; Gray *et al.*, 1994; Volf, 1996; Gorden *et al.*, 2003).

### (e) Ligands for $UO_2^{2+}$

Soluble uranyl ion, $UO_2^{2+}$, is nephrotoxic, and because bone is the major storage organ for $UO_2^{2+}$, the high specific activity uranium isotopes also induce bone cancer (Voegtlin and Hodge, 1949, 1953; Finkel and Biskis, 1968; Hodge, 1973). Although sought since the 1940s, no multidentate ligand was identified that would efficiently bind $UO_2^{2+}$ *in vivo*, promote its excretion, and reduce deposits in kidneys and bone (reviewed by Durbin *et al.*, 1997a). The modest reductions of acute $UO_2^{2+}$ poisoning obtained with tiron, a bidentate sulfocatecholate, suggested that multidentate ligands containing similar binding groups would be effective *in vivo* $UO_2^{2+}$ chelators.

Representative tetra-, hexa-, and octadentate ligands with linear or branched backbones containing CAM(S), CAM(C), MeTAM, 1,2-HOPO, or Me-3,2-HOPO groups (20 in all) were evaluated in mice for *in vivo* chelation of $UO_2^{2+}$. Experimental conditions were: $^{232\,+\,235}UO_2Cl_2$ or $^{233}UO_2Cl_2$ pH 4 injected iv, 30 μmol $kg^{-1}$ of ligand injected ip at 5 min (see Fig. 31.11), ligand: U molar ratio 75 to 91, kill at 24 h. All of the test chelators were screened for acute toxicity. Except for the two tetradentate 1,2-HOPO ligands and $CaNa_3$–DTPA, all of the injected test chelators significantly reduced $UO_2^{2+}$ in the kidneys compared with controls, and ligands containing CAM(S), CAM(C), or MeTAM groups also significantly reduced $UO_2^{2+}$ in the skeleton. Administered orally at molar ratios from 90 to 300, the linear tetradentate ligands containing Me-3,2-HOPO, CAM (S), or CAM(C) and 3,4,3-LI(1,2-HOPO) significantly reduced $UO_2^{2+}$ binding in the kidneys, but not in the skeleton. The combined assessments of ligand efficacy and acute toxicity identified tetradentate 5-LIO(Me-3,2-HOPO) and 5-LICAM(S) as the most effective low toxicity agents for $UO_2^{2+}$. They efficiently removed circulating $UO_2^{2+}$ at molar ratios as low as 20, removed useful amounts of newly deposited $UO_2^{2+}$ from kidneys and/or bone at molar ratios $\geq$100, and reduced kidney $UO_2^{2+}$ significantly when given orally at molar ratios $\geq$100. 5-LIO(Me-3,2-HOPO) has greater affinity for $UO_2^{2+}$ in the kidneys, 5-LICAM(S) has greater affinity for $UO_2^{2+}$ in bone, and a 1:1 mixture of the two ligands (total ligand: U molar ratio 91) reduced kidney and bone $UO_2^{2+}$ to 15 and 58% of control, respectively – more than an equimolar amounts of either ligand alone (Durbin *et al.*, 1989b; 1997a, 2000a; Gorden *et al.*, 2003).

Crystals of uranyl chelates with the set of linear tetradentate Me–3,2-HOPO ligands demonstrate a 1:1 structure and show that those ligands bind in a nearly planar ring perpendicular to the plane of the dioxo oxygens (Fig. 31.19) (Xu and Raymond, 1999).

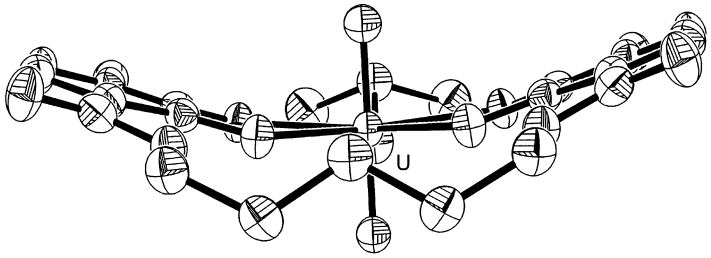


**Fig. 31.19** *Molecular structure of* $UO_2$[5-*LI*(*Me*-3,2,-*HOPO*)] (*Xu and Raymond*, 1999).

### (f) Ligands for $NpO_2^+$

As noted above in the sections dealing with tissue distribution, circulatory transport, and tissue uptake kinetics, the oxidation state of Np *in vivo* is uncertain and probably variable. Rapid plasma clearance and substantial urinary excretion of $NpO_2^+$ resemble the behavior of $UO_2^{2+}$, while the deposition in the skeleton of nearly one-half of Np taken into blood and its prolonged retention resemble $Pu^{4+}$. Redox conditions *in vivo* range from an oxidizing environment in the lungs to more reducing environments in the tissues. Depending on the oxidation state of the Np introduced into the blood ($Np^{4+}$, $NpO_2^+$, $NpO_2^{2+}$), the local conditions in the blood and tissues, and the availability of stabilizing bioligands, both reduction of $NpO_2^+$ and oxidation of $Np^{4+}$ may be expected (Duffield and Taylor, 1986; NCRP, 1988; Taylor, 1998). The complexes formed by $NpO_2^+$ are weak, while those of $Np^{4+}$ are about as stable as those of $Pu^{4+}$ with the same ligands (Table 31.8).

$CaNa_3$–DTPA was injected ip at ligand:Np molar ratios $\geq$50 in rats that had been injected iv with $^{237}Np$ or $^{239}Np$ citrate solutions (oxidation states uncertain). Excretion of both Np isotopes was increased, the Np content of liver and kidneys was reduced, but there was little reduction in skeleton Np (Smith, 1972b). Effective reduction of $^{239}Np$ in the body of rats was achieved by ip injection of octadentate 3,4,3-LICAM(C), given at very large ligand:Np molar ratios 1 h after iv injection of $^{239}NpO_2NO_3$. But similarly to the experience with *in vivo* chelation of $Pu^{4+}$ by that ligand, the Np complex formed in the blood partially dissociated leaving a residue of Np in the kidneys (Volf and Wirth, 1986). These observations were taken as an indication of the presence *in vivo* of chelatable $Np^{4+}$.

Based on that encouraging result, a systematic investigation was undertaken of the *in vivo* chelation of Np by a set of representative multidentate ligands. The ligands assessed for Np chelation were tetra-, hexa-, and octadentate with linear or branched backbones containing CAM(C), CAM(S), 1,2-HOPO, or Me-3,2-HOPO binding groups. Mice were injected ip with a ligand (30 μmol $kg^{-1}$,

ligand:Np molar ratio 22) 5 min after the iv injection of $^{237}NpO_2Cl$ (see Fig. 31.12) and killed at 24 h. All 10 test ligands, but not $CaNa_3$–DTPA, significantly reduced body Np, regardless of denticity or the identity of the binding group. Most ligands significantly reduced Np in the liver, and except for 3,4,3-LICAM (C), also in the kidneys. Significant reduction of Np in the skeleton was also achieved with tetradentate 5-LIO(Me-3,2-HOPO) and 5-LI(Me-3,2-HOPO), and octadentate H(2,2)-(1,2-HOPO), H(2,2)-(Me-3,2-HOPO), and 3,4,3-LICAM(C). Except for tetradentate 5-LI(Me-3,2-HOPO), which was orally active at lower dose, ligand:Np molar ratios $\geq$22 were required to obtain significant reductions in body Np, when the test ligands were given orally at 5 min (Durbin *et al.*, 1994, 1998a,b).

Experiments were undertaken to examine the efficacy of 3,4,3-LI(1,2-HOPO) for *in vivo* chelation of $^{237}Np$ in contaminated wounds in rats. Ligand:Np molar ratios ranged from 4.3 to 285. Early infiltration of the wound site with the ligand was effective, but delayed treatments were progressively less effective. 3,4,3-LI (1,2-HOPO) was able to complex the Np at the wound site before it was translocated to blood, but Np deposited in the tissues became progressively less accessible to the ligand (Paquet *et al.*, 1997, 2000).

Based on the combined considerations of ligand efficacy and acute ligand toxicity, the most promising ligands for *in vivo* chelation of Np are in order: tetradentate 5-LIO(Me-3,2-HOPO) and 5-LI(Me-3,2-HOPO), octadentate 3,4,3-LI(1,2-HOPO), and hexadentate TREN-(Me-3,2-HOPO).

## ACKNOWLEDGMENTS

The author wishes to thank the following members of the Lawrence Berkeley National Laboratory, Chemical Sciences Division, for their essential contributions to the preparation of this manuscript: Dr. Wayne W. Lukens, Jr. for the speciation calculations for $UO_2^{2+}$ and $NpO_2^+$ in blood plasma; Lindarae M. Aubert and Lynne A. Dory for manuscript preparation; and Dr. Norman M. Edelstein for his patience and assistance. Flavio Robles of the Creative Services Group and Dr. Jide Xu of the U. C. Department of Chemistry provided the illustrations.

## APPENDIX: SOURCES OF MATERIALS ON ACTINIDE BIOLOGY

The pioneering biological studies with actinides conducted during World War II (1942–1946) encompassed the following: pharmacology and toxicology of injected, ingested, and inhaled uranium compounds (Tannenbaum, 1951a,b; Voegtlin and Hodge, 1949, 1953); biokinetics of injected and ingested fission products, plutonium, and actinide fission by-products (Lanz *et al.*, 1946; 1947a,b, 1948a,b, 1949b; Carritt *et al.*, 1947; Finkle *et al.*, 1946; Hamilton,

1947b, 1948c); acute toxicity of injected fission products and plutonium (Painter *et al.*, 1946; Bloom, 1948; Fink, 1950); biokinetics and acute toxicity of inhaled or intratracheally intubated fission products and plutonium (Abrams *et al.*, 1946a,b, 1947; Scott *et al.*, 1947b, 1949a). Stannard (1988) summarized the designs and major findings of those studies and provided the tables of contents for the otherwise unpublished Plutonium Project documents and reports.

Actinide biology summaries and reviews include: General reviews – (Durbin, 1960, 1962), Finkel and Biskis (1968), Stover and Jee (1972), Nenot and Stather (1979), ICRP (1972, 1986), Duffield and Taylor (1986), Stannard (1988), Thompson (1989); Element-specific reviews, uranium – Hursh and Spoor (1973), Yuile (1973), Durbin and Wrenn (1975); neptunium – Thompson (1982), NCRP (1988); plutonium – Bair *et al.* (1973), Vaughan *et al.* (1973), Bair (1974), Durbin (1975); transplutonium elements – Durbin (1973); conference proceedings – Rosenthal (1956), Dougherty *et al.*, 1962), Thompson (1962), Mays *et al.* (1969), Thompson and Bair (1972), Healy (1975), Wrenn (1975), Jee (1976), Wrenn (1981), Gerber *et al.* (1989), Stather and Karaoglou (1994), Métivier *et al.* (1998), Stather *et al.* (2003); databases compiled for radiation protection guidance – ICRP (1959, 1972, 1979, 1980, 1986).

The bibliographies of three reports dealing with the deposition and biological effects of plutonium and other selected radionuclides provide an introduction to the large research program on internally deposited radionuclides undertaken in the USSR (Buldakov *et al.*, 1969; Moskalev *et al.*, 1969; Moskalev, 1972).

## LIST OF ABBREVIATIONS

| | |
|---|---|
| CN | coordination number |
| d | days |
| DFO | desferrioxamine |
| DTPA | diethylenetriaminepentaacetic acid |
| EB | enterobactin |
| ECF | extracellular fluid |
| EDTA | ethylenediaminetetraacetic acid |
| GI | gastrointestinal |
| h | hours |
| HAP | synthetic hydroxyapatite |
| HEPES | 4-(2-hydroxyethyl)1-piperazine ethanesulfonic acid |
| ICRP | International Commission on Radiological Protection |
| im | intramuscular |
| ip | intraperitoneal |
| ISW | interstitial water |
| iv | intravenous |
| min | minutes |
| NCRP | National Council on Radiation Protection |

| | |
|---|---|
| PAS | periodic-acid Schiff |
| *r* | ionic radius |
| s | seconds |
| sc | subcutaneous |
| Tf | transferrin |
| tris | tris-(hydroxy methyl) aminomethane hydrochloride |
| y | years |

## REFERENCES


Abrams, R., Seibert, H. C., Forker, L., Greenberg, D., Lisco, H., Jacobson, L. O., and Simmons, E. L. (1946a) *Acute Toxicity of Intubated Plutonium*, USAEC, CH-3875.

Abrams, R., Seibert, H. C., Potts, A. M., Lohr, W., and Postel, S. (1946b) *Metabolism of Inhaled Fission Products*, CH-3485 MDDC-248.

Abrams, R., Seibert, H. C., Potts, A. M., Forker, L. L., Greenberg, D., Postel, S., and Lohr, W. (1947) *Metabolism and Distribution of Inhaled Plutonium in Rats CH-3655 MDDC-677*.

Ahrland, S. (1986) Solution chemistry and kinetics of ionic reactions, in *The Chemistry of the Actinide Elements* (eds. J. J. Katz, G. T. Seaborg, and L. R. Morss), Chapman and Hall, London, pp. 1480–546.

Aisen, P. and Listowsky, I. (1980) *Ann. Rev. Biochem.*, **49**, 357–93.

Altman, P. L. and Dittmer, D. S. (1971) *Blood and Other Body Fluids*, Federation of American Societies for Experimental Biology, Bethesda, MD.

Ansoborlo, E., Chiappini, R., and Moulin, V. (2003) *Clefs CEA*, **48**, 14–18.

Arnold, J. S. and Jee, W. S. S. (1957) *Am. J. Anat.*, **101**, 367–418.

Arnold, J. S. and Jee, W. S. S. (1959) *Lab. Invest.* **8**, 194–204.

Arnold, J. S. and Jee, W. S. S. (1962) *Health Phys.*, **8**, 705–8.

Arnold, J. S. and Wei, C.-T. (1972) Quantitative morphology of vertebral trabecular bone, in *Radiobiology of Plutonium* (eds. B. J. Stover and W. S. S. Jee), The J. W. Press, University of Utah, pp. 333–54.

Atherton, D. R. and LLoyd, R. D. (1972) *Health Phys.*, **22**, 675–8.

Atherton, D. A., Bruenger, F. W., and Stevens, W. (1974) On the early retention and distribution of 253Es by the beagle, in *Research in Radiobiology*, University of Utah School of Medicine Annual Report COO-119-249, pp. 247–54.

Atherton, D. A., Stevens, W., and Bruenger, F. W. (1973) Early retention and distribution of curium in soft tissues and blood of the beagle, in *Research in Radiobiology*, University of Utah School of Medicine Annual Report COO-119-248, pp. 178–85.

Axelrod, D. (1947) *Anat. Rec.*, **98**, 19–24.

Bair, W. J. (1974) Toxicology of plutonium, in *Advances in Radiation Biology*, vol. 4, Academic press, New York, pp. 255–315.

Bair, W. J., Ballou, J. E., Park, J. F., and Sanders, C. L. (1973) Plutonium in soft tissue with emphasis on the respiratory tract, in *Uranium, Plutonium, Transplutonic Elements* (eds. H. C. Hodge, J. N. Stannard, and J. B. Hursh), Springer-Verlag, New York, pp. 503–68.

Ballatori, N. (1991) *Drug Metabol. Rev.*, **23**, 83–132.

Ballou, J. E., Bair, W. J., Case, A. C., and Thompson, R. C. (1962) *Health Phys.*, **8**, 685–8.

Ballou, J. E., Park, J. F., and Morrow, W. G. (1972) *Health Phys.*, **22**, 857–62.

Barnett, T. B. and Metcalf, R. G. (1949) Pathological anatomy following uranium poisoning, in *Pharmacology and Toxicology of Uranium Compounds*, vol. 1 (eds. C. Voegtlin and H. C. Hodge), McGraw-Hill, New York, pp. 207–36.

Belyayev, Y. A. (1969) *Americium-241 Distribution in Rats and the Effect of Complexing Substances on Its Elimination*, AEC-tr-7195, pp. 168-74.

Berliner, R. W. (1973) The excretion of urine, in *Best and Taylor's Physiological Basis of Medical Practice* (ed. J. R. Brobeck), Williams and Williams, Baltimore, 5-1–5-37.

Bernard, S. R. and Struxness, E. G. (1957) *A Study of the Distribution and Excretion of Uranium in Man*, ORNL-2304.

Bernhard, G., Geipel, G., Reich, T., Brendler, V., Amayri, S., and Nitsche, H. (2001) *Radiochim. Acta*, **89**, 511–18.

Bhattacharyya, M. H., Breitenstein, B. D., Metivier, H., Muggenburg, B. A., Stradling, G. N., and Volf, V. (1992) *Radiat. Protect. Dosim.*, **41**, 1–49.

Bloom, W. (ed.) (1948) *Histopathology of Irradiation from External and Internal Sources*, McGraw-Hill, New York.

Boocock, G., Danpure, C. J., Popplewell, D. S., and Taylor, D. M. (1970) *Radiat. Res.*, **42**, 381–96.

Bostick, W. D., Stevenson, R. J., Jarabek, R. J., and Conca, J. L. (2000) *Adv. Environ. Res.*, **3**, 488–98.

Bourne, G. H. (ed.) (1956) *The Biochemistry and Physiology of Bone*, Academic Press, New York.

Brody, S. (1945) *Bioenergetics and Growth*. Reinhard Publications, New York.

Bronner, F. (1964) Dynamics and function of calcium, in *Mineral Metabolism*, vol. II, Part A (eds. C. L. Comar and F. Bronner), Academic Press, New York, pp. 342–5.

Bruenger, F. W., Stover, B. J., Stevens, W., and Atherton, D. R. (1969a) *Health Phys.*, **16**, 339–40.

Bruenger, F. W., Stevens, W., and Stover, B. J. (1969b) *Radiat. Res.*, **37**, 349–60.

Bruenger, F. W., Stover, B. J., and Stevens, W. (1971a) *Health Phys.*, **21**, 679–87.

Bruenger, F. W., Atherton, D. R., Stevens, W., and Stover, B. J. (1971b) Interaction between blood constituents and some actinides, in *Research in Radiobiology, Annual Report*, COO-119-244, University of Utah College of Medicine, pp. 212–27.

Bruenger, F. W., Atherton, D. R., and Stevens, W. (1972) *Health Phys.*, **22**, 685–9.

Bruenger, F. W., Grube, B. J., Atherton, D. R., Taylor, G. N., and Stevens, W. (1976) *Radiat Res.*, **66**, 443–52.

Bruenger, F. W., Smith, J. M., Atherton, D. R., Jee, W. S. S., Lloyd, R. D., and Stevens, W. (1983) *Health Phys.*, **44**(Suppl. 1), 513–27.

Buldakov, L. A., Lyubchanskii, Moskalev, Y. I., and Nifatov, A. P. (1969) *Problems of Plutonium Toxicology*. Atom Publications, Moscow (English translation).

Bulman, R. A. (1978) *Struct. Bonding*, **34**, 39–77.

Bulman, R. A. (1980) *Coord. Chem. Rev.*, **31**, 221–50.

Carritt, J., Fryxell, R., Kleinschmidt, J., Kleinschmidt, R., Langham, W., San Pietro, A., Schaffer, R., and Schnap, B. (1947) *J. Biol. Chem.*, **171**, 273–83.

Catsch, A. (1964) *Radioactive Metal Mobilization in Medicine*, Charles C. Thomas, Springfield, IL.

Catsch, A. and Lê, D. K. (1957) *Strahlentherapie*, **104**, 494–506.
Catsch, A. and von Wedelstaedt, E. (1965) *Experientia*, **21**, 210.
Chalk River (1949) *Permissible Doses Conference*, September 29–30, 1949, pp. 17.1–17.38.
Chevari, S. and Likhner, D. (1968) *Med. Radiol. ANL-trans-898*, **13**, 53–7.
Chipperfield, A. R. and Taylor, D. M. (1968) *Nature*, **219**, 609–10.
Chipperfield, A. R. and Taylor, D. M. (1970) *Radiat. Res.*, **43**, 393–402.
Chipperfield, A. R. and Taylor, D. M. (1972) *Radiat. Res.*, **51**, 15–30.
Clarkson, T. W. (1961) Discussion: the interaction of metals with epithelia, in *University of Rochester*, *Atomic Energy Project*, *UR-549*, pp. 37–47.
Cochran, T. H., Jee, W. S. S., Stover, B. J., and Taylor, G. N. (1962) *Health Phys.*, **8**, 699–704.
Cohen, N. and Ralston, L. (1983) Actinide biokinetics in man and the baboon: a comparison, in *Proceedings of the Seventh International Congress of Radiation Research*, Amsterdam, E5-02.
Comar, C. L. (1955) *Radioisotopes in Biology and Agriculture*, McGraw-Hill, New York.
Cooper, J. R. and Gowing, H. S. (1981) *Int. J. Radiat. Biol. Relat. Study Phys. Chem. Med.*, **40**, 569–72.
Copp, D. H., Greenberg, D. M., Hamilton, J. G., Chace, M. J., Middlesworth, L. V., Cuthbertson, E. M., and Axelrod, D. J. (1946) *The Deposition of Plutonium and Certain Fission Products in Bone as a Decontamination Problem*, *CH-3591*, AECD-2483.
Cotton, F. A. and Wilkinson, G. (1980) The actinide elements, chap. 24, in *Advanced Inorganic Chemistry*, Wiley, New York, pp. 1005–84.
Cronkite, E. P. (1973) Blood and lymph, in *Best and Taylor's Physiological Basis of Medical Practice*, 9th edn (ed. J. R. Brobeck), Williams and Wilkins, Baltimore, pp. 4-1–4-113.
Detweiler, D. K. (1973) Circulation, in *Best and Taylor's Physiological Basis of Medical Practice*, 9th edn (ed. J. R. Brobeck), Williams and Wilkins, Baltimore, pp. 3-1–3-24.
Dougherty, T. F., Jee, W. S. S., Mays, C. W., and Stover, B. J. (eds.) (1962) *Some Aspects of Internal Irradiation*, Pergamon Press, Oxford.
Dounce, A. L. (1949) The mechanism of action of uranium compounds in the animal body, in *Pharmacology and Toxicology of Uranium Compounds*, vol. 2 (eds. C. Voegtlin and H. C. Hodge), McGraw-Hill, New York, pp. 951–92.
Dounce, A. L. and Flagg, J. F. (1949) The chemistry of uranium compounds, in *Pharmacology and Toxicology of Uranium Compounds*, vol. 1 (eds. C. Voegtlin and H. C. Hodge), McGraw-Hill, New York, pp. 55–146.
Dounce, A. L. and Lan, T. H. (1949) The action of uranium on enzymes and proteins, in *Pharmacology and Toxicology of Uranium Compounds*, vol. 2 (eds. C. Voegtlin and H. C. Hodge), McGraw-Hill, New York, pp. 759–888.
Duffield, J. R. and Taylor, D. M. (1986) The biochemistry of the actinides, in *Handbook on the Physics and Chemistry of the Actinides*, (eds. A. J. Freeman and C. Keller), vol. 4 North-Holland, Amsterdam, pp. 129–57.
Durbin, P. W. (1960) *Health Phys.*, **2**, 225–38.
Durbin, P. W. (1962) *Health Phys.*, **8**, 665–71.
Durbin, P. W. (1973) Metabolism and biological effects of the transplutonium elements, in *Uranium, Plutonium, Transplutonic Elements* (eds. H. C. Hodge, J. N. Stannard, and J. B. Hursh), Springer-Verlag. Berlin, pp. 739–896.
Durbin, P. W. (1975) *Health Phys.*, **29**, 495–510.

Durbin, P. W. and Schmidt, C. T. (1985) *Health Phys.*, **49**, 623–61.
Durbin, P. W. and Schmidt, C. T. (1989) *Health Phys.*, **57**(Suppl. 1), 165–74.
Durbin, P. W. and Wrenn, M. E. (1975) Metabolism and effects of uranium in animals, in *Conference on Occupational Health Experience with Uranium* (ed. M. E. Wrenn), ERDA Report 93, pp. 67–129.
Durbin, P. W., Asling, G. W., Johnston, M. E., Hamilton, J. G., and Williams, M. H. (1955) The metabolism of the lanthanons in the rat, in *Rare Earths in Biochemical and Biomedical Research*, October 1955, Oak Ridge, TN, ORINS-12, pp. 171–92.
Durbin, P. W., Jeung, N., and Williams, M. H. (1969) Dynamics of $^{241}$Am in the skeleton of the rat, in *Delayed Effects of Bone-seeking Radionuclides* (ed. C. W. Mays), University of Utah Press, Salt Lake City, pp. 137–56.
Durbin, P. W., Horovitz, M. W., and Close, E. R. (1972) *Health Phys.*, **22**, 731–41.
Durbin, P. W., Heavy, L. R., and Garcia, J. F. (1976) *Radiat. Res.*, **67**, 578[Abstract].
Durbin, P. W., Jones, E. S., Raymond, K. N., and Weitl, F. L. (1980) *Radiat. Res.*, **81**, 170–87.
Durbin, P. W., Jeung, N., Jones, E. S., Weitl, F. L., and Raymond, K. N. (1984) *Radiat. Res.*, **99**, 85–105.
Durbin, P. W., Jeung, N., and Schmidt, C. T. (1985) $^{238}$*Pu(IV) in Monkeys; Overview of Metabolism*, U.S. Nuclear Regulatory Commission Report NUREG/CR-4355.
Durbin, P. W., Jeung, N., and Bucher, J. J. (1987) Initial distribution of neptunium-237 in a monkey, in *Division of Biology and Medicine Annual Report*, Lawrence Berkeley Laboratory, LBL-22300, pp. 78–86.
Durbin, P. W., White, D. L., Jeung, N. L., Weitl, F. L., Uhlir, L. C., Jones, E. S., Bruenger, F. W., and Raymond, K. N. (1989a) *Health Phys.*, **56**, 839–55.
Durbin, P. W., Jeung, N., Rodgers, S. J., Turowski, P. N., Weitl, F. L., White, D. L., and Raymond, K. N. (1989b) *Radiat. Protect. Dosim.*, **26**, 351–8.
Durbin, P. W., Jeung, N., Kullgren, B., and Clemons, G. K. (1992) *Health Phys.*, **63**, 427–41.
Durbin, P. W., Kullgren, B., Xu, J., and Raymond, K. N. (1994) *Radiat. Protect. Dosim.*, **53**, 305–9.
Durbin, P. W., Kullgren, B., Jeung, N., Xu, J., Rodgers, S. J., and Raymond, K. N. (1996) *Human Experiment. Toxicol.*, **15**, 352–60.
Durbin, P. W., Kullgren, B., Xu, J., and Raymond, K. N. (1997a) *Health Phys.*, **72**, 865–79.
Durbin, P. W., Kullgren, B., and Schmidt, C. T. (1997b) *Health Phys.*, **72**, 222–35.
Durbin, P. W., Kullgren, B., Xu, J., and Raymond, K. N. (1998a) *Radiat. Protect. Dosim.*, **79**, 433–43.
Durbin, P. W., Kullgren, B., Xu, J., Raymond, K. N., Allen, P. G., Bucher, J. J., Edelstein, N. M., and Shuh, D. K. (1998b) *Health Phys.*, **75**, 34–50.
Durbin, P. W., Kullgren, B., Ebbe, S. N., Xu, J., and Raymond, K. N. (2000a) *Health Phys.*, **78**, 511–21.
Durbin, P. W., Kullgren, B., Xu, J., and Raymond, K. N. (2000b) *Int. J. Radiat. Biol.*, **76**, 199–214.
Durbin, P. W., Kullgren, B., Xu, J., Raymond, K. N., Henge- Napoli, M. H., Bailly, T., and Burgada, R. (2003) *Radiat. Protect. Dosim.*, **105**, 503–8.
Erleksova, E. V. (1960) *Distribution of Radioactive Elements in the Animal Organism*, Megziz English Translation, AEC-tr-6982 (1969), Moscow.

Everett, N. B., Simmons, B., and Lasher, E. P. (1956) *Circ. Res.*, **4**, 419–24.
Fairbanks, V. F. and Beutler, E. (1995) Iron metabolism, in *Williams Hematology*, 5th edn (eds. E. Beutler, M. A. Lichtman, B. S. Coller, and T. J. Kipps), McGraw-Hill, New York pp. 369–80.
Fink, R. M. (ed.) (1950) *Biological Studies with Polonium, Radium, and Plutonium*, McGraw-Hill, New York.
Finkel, M. P. and Biskis, B. O. (1968) *Prog. Exp. Tumor Res.*, **10**, 72–111.
Finkle, R. D., Snyder, R. H., Jacobson, L. O., Kisieleski, W., Lawrence, B., and Simmons, E. L. (1946) *The Toxicity and Metabolism of Plutonium in Laboratory Animals*, CH-3783 MDDC-1140.
Flagg, J. F. (1949) Analytical methods for determining uranium and fluorine, in *Pharmacology and Toxicology of Uranium Compounds*, vol. 1 (eds. C. Voegtlin and H. C. Hodge), McGraw-Hill, New York, pp. 147–94.
Foreman, H. (1962) *Health Phys.*, **8**, 713–16.
Foreman, H. and Hamilton, J. G. (1951) *The Use of Chelating Agents for Accelerating Excretion of Radionuclides*, UCRL–1351. University of California Radiation Laboratory, Berkeley, CA.
Frost, H. M. (ed.) (1963) *Bone Biodynamics*, Little, Brown, Boston, MA.
Gamble, J. L. (1954) *Chemical Anatomy, Physiology, and Pathology of Extracellular Fluid*, Harvard University Press, Cambridge, MA.
Gerber, G. B., Metivier, H., and Stather, J. W. (eds.) (1989) Biological assessment of occupational exposure to actinides, *Radiat. Protect. Dosim.*, **26**, 1–4.
Gindler, J. E. (1973) Physical and chemical properties of uranium. in *Uranium, Plutonium, Transplutonic Elements* (eds. H. C. Hodge, J. N. Stannard, and J. B. Hursh), Springer-Verlag, New York, pp. 69–164.
Gong, J. K., Arnold, J. S., and Cohn, S. H. (1964) *Anat. Rec.*, **149**, 325–31.
Gorden, A. E. V., Xu, J. D., Raymond, K. N., and Durbin, P. (2003) *Chem. Rev.*, **103**, 4207–82.
Gorden, A. E. V., Shuh, D. K., Tiedemann, B. E. F., Wilson, R. E., Xu, J. D., and Raymond, K. N. (2005) *Chem. Eur. J.*, **11**, 2842–8.
Gray, S. A., Stradling, G. N., Pearce, M. J., Wilson, I., Moody, J. C., Burgada, R., Durbin, P. W., and Raymond, K. N. (1994) *Radiat. Protect. Dosim.*, **53**, 319–22.
Green, D., Howells, G., Vennart, J., and Watts, R. (1977) *Int. J. Appl. Radiat. Isot.*, **28**, 497–501.
Gregersen, M. I., Sear, H., Rawson, R. A., Chien, S., and Saiger, G. L. (1959) *Am. J. Physiol.*, **196**, 184–7.
Grenthe, I., Fuger, J., Konings, R. J. M., Lemire, R. J., Muller, A. B., Nguyen- Trung, C., and Wanner, H. (1992) *Chemical Thermodynamics of Uranium*, North-Holland, Amsterdam.
Grube, B. J., Stevens, W., and Atherton, D. R. (1978) *Radiat. Res.*, **73**, 168–79.
Gruner, R., Seidel, A., and Winter, R. (1981) *Radiat. Res.*, **85**, 367–79.
Guilmette, R. A., Cohen, N., and Wrenn, M. E. (1980) *Radiat. Res.*, **81**, 100–19.
Guilmette, R. A., Medinsky, M. A., and Petersen, D. A. (1982) *Binding of Neptunium to Serum Proteins* In vitro, Annual Report of the Inhalation Toxicology Research Institute, Lovelace Biomedical and Environmental Research Institute, LMF-102, pp. 209–11.
Guilmette, R. A., Lindhorst, P. S., and Hanlon, L. L. (1998) *Radiat. Protect. Dosim.*, **79**, 453–8.

Guilmette, R. A., Hakimi, R., Durbin, P. W., Xu, J., and Raymond, K. N. (2003) *Radiat. Protect. Dosim.*, **105**, 527–34.
Gurd, F. R. N. and Wilcox, P. E. (1956) *Adv. Protein Chem.*, **11**, 311–427.
Hahn, F. F., Guilmette, R. A., and Hoover, M. D. (2002) *Environ. Health Perspect.*, **110**, 51–9.
Ham, A. W. (1974) *Histology*, 7th edn. J. B. Lippincott, Philadelphia.
Hamilton, J. G. (1941) *J. Appl. Phys.*, **12**, 440–60.
Hamilton, J. G. (1947a) Medical and Health Physics Quarterly Report UCRL-41, University of California Radiation Laboratory, p. 15.
Hamilton, J. G. (1947b) *Radiology*, **49**, 325–43.
Hamilton, J. G. (1948a) Medical and Health Physics Quarterly Report UCRL-157, University of California Radiation Laboratory, pp. 6–11.
Hamilton, J. G. (1948b) Medical and Health Physics Quarterly Report UCRL-193, University of California Radiation Laboratory, p. 13.
Hamilton, J. G. (1948c) *Rev. Mod. Phys.*, **20**, 718–28.
Hamilton, J. G. (1953) Medical and Health Physics Quarterly Report UCRL-2553, University of California Radiation Laboratory, pp. 28–30.
Hamilton, J. G. (1956) Medical and Health Physics Quarterly Report UCRL-3268, University of California Radiation Laboratory, pp. 5–10.
Hamilton, J. G. and Scott, K. G. (1953) *Proc. Soc. Exp. Biol. (N.Y.)* **83**, 301–5.
Harris, W. R., Carrano, C. J., Pecoraro, V. L., and Raymond, K. N. (1981) *J. Am. Chem. Soc.* **103**, 2231–7.
Haven, F. and Hodge, H. C. (1949) Toxicity following parenteral administration of certain soluble uranium salts, in *Pharmacology and Toxicology of Uranium Compounds*, (eds. C. Voegtlin and H. C. Hodge), vol. 1 , McGraw-Hill, New York, pp. 281–308.
Hawk, P. B., Oser, B. L., and Summerson, W. H. (1947) *Practical Physiological Chemistry*, 12th edn, The Blakiston Co., Philadelphia.
Healy, J. W. (ed.) (1975) Plutonium — health implications for man. *Health Phys.*, **29**, 441–632.
Herring, G. M. (1964) Mucosubstances of cortical bone, in *Bone and Tooth* (ed. H. J. J. Blackwood), Pergamon, London, pp. 263–8.
Herring, G. M., Vaughan, J., and Williamson, M. (1962) *Health Phys.*, **8**, 717–24.
Hodge, H. C. (1949) Introduction to part I. The pharmacology and toxicology of uranium compounds, in *Pharmacology and Toxicology of Uranium Compounds*, (eds. C. Voegtlin and H. C. Hodge), vol. 1 , McGraw-Hill, New York, pp. 15–54.
Hodge, H. C. (1973) A history of uranium poisoning (1824–1942), in *Uranium, Plutonium, Transplutonic Elements* (eds. H. C. Hodge, J. N. Stannard, and J. B. Hursh), Springer-Verlag, New York, pp. 5–68.
Hodge, H. C., Stannard, J. N., and Hursh, J. B. (eds.) (1973) *Uranium, Plutonium, Transplutonic Elements*, Springer-Verlag, New York.
Hulet, E. K. (1986) Einsteinium, in *The Chemistry of the Actinide Elements* (eds. J. J. Katz, G. T. Seaborg, and L. R. Morss), Chapman and Hall, London, pp. 1071–84.
Hungate, F. P. and Baxter, D. W. (1972) 253-Es and 249-Bk Distribution in rat tissues following intragastric and intravenous administration, in *Pacific Northwest Laboratory Annual Report for 1971*, BNWL-1650 PT1, pp. 88–92.

Hursh, J. B. and Spoor, N. L. (1973) Data on man, in *Uranium, Plutonium, Transplutonic Elements* (eds. H. C. Hodge, J. N. Stannard, and J. B. Hursh), Springer-Verlag. New York, pp. 197–240.

ICRP. (1959) *Health Phys.*, **3**, 1–380.

ICRP. (1967) *A Review of the Radiosensitivity of Tissues in Bone, ICRP Pub. 11*, International Commission on Radiological Protection.

ICRP. (1972) *The Metabolism of Compounds of Plutonium and Other Actinides, ICRP Pub. 19*, Pergamon Press, Oxford.

ICRP. (1973) *Alkaline Earth Metabolism in Adult Man. ICRP Pub. 20*, *Health Phys.*, **24**, 125–221.

ICRP (1974) *Report of the Task Group on Reference Man*, ICRP Pub. 23, Pergamon Press, Oxford.

ICRP. (1979) *Limits for intakes of radionuclides by workers*, ICRP Pub. 30, Part 1. Ann. ICRP 2: (3–4).

ICRP. (1980) *Limits for intakes of radionuclides by workers*, ICRP Pub. 30, Part 2. Ann. ICRP 4: (3–4).

ICRP. (1986) *The metabolism of plutonium and related elements*. ICRP Pub. 48. Ann. ICRP 16: (2–3).

ICRP. (1993) Age-dependent doses to members of the public from intake of radionuclides: part 2 ingestion dose coefficients. ICRP Pub. 67, part 2. Ann. ICRP 23: (3–4).

ICRP. (1995) Age-dependent doses to members of the public from intake of radionuclides: Part 3. Ingestion dose coefficients. Ann. ICRP 25. (1).

Jee, W. S. S. (1972a) *Health Phys.*, **22**, 583–96.

Jee, W. S. S. (1972b) $^{239}$Pu in bones as visualized by photographic and neutron-induced autoradiography, in *Radiobiology of Plutonium* (eds. B. J. Stover and W. S. S. Jee), The J. W. Press, University of Utah, Salt Lake City, pp. 171–94.

Jee, W. S. S. (ed.) (1976) *The Health Effects of Plutonium and Radium*, The J. W. Press, University of Utah Press, Salt Lake City.

Jee, W. S. S. and Arnold, J. S. (1962) *Health Phys.*, **8**, 709–12.

Jowsey, J. (1956) The localization of yttrium in bone, in *Rare Earths in Biochemical and Medical Research: A Conference ORINS-12* (eds. G. C. Kyker and E. B. Anderson), Oak Ridge Institute of Nuclear Studies, Oak Ridge, TN, pp. 311–22.

Jowsey, J., Rowland, R. E., and Marshall, J. H. (1958) *Radiat. Res.*, **8**, 490–501.

Kappel, M. J., Nitsche, H., and Raymond, K. N. (1985) *Inorg. Chem.*, **24**, 605–11.

Katz, J. H. (1970) Transferrin and its functions in the regulation of iron metabolism, in *Regulation of Hematopoiesis*, vol. I (ed. A. S. Gordon), Appleton-Century-Crofts, New York, pp. 539–77.

Katz, J. J., Seaborg, G. T., and Morss, L. R. (1986) Summary and comparative aspects of actinide elements, in *The Chemistry of Actinide Elements* (eds. J. J. Katz, G. T. Seaborg, and L. R. Morss), Chapman and Hall, London, pp. 1121–95.

Kirby, H. W. (1986a) Actinium, in *The Chemistry of the Actinide Elements* (eds. J. J. Katz, G. T. Seaborg,, and L. R. Morss), Chapman and Hall, London, pp. 14–40.

Kirby, H. W. (1986b) Protactinium, in *The Chemistry of the Actinide Elements* (eds. J. J. Katz, G. T. Seaborg, and L. R. Morss), Chapman and Hall, London, pp. 102–68.

Kirschbaum, B. B. (1982) *Toxicol. Appl. Pharmacol.*, **64**, 10–19.

Kirschbaum, B. B. and Oken, D. E. (1979) *Exp. Mol. Pathol.*, **31**, 101–12.

Kisieleski, W. E. and Woodruff, L. (1948) Studies on the distribution of plutonium in the rat, in *Quarterly Report, Biology Division, August 1947 to November 1947*, Argonne National Laboratory, ANL-4108, pp. 86–103.

Kornberg, and H. A. Norwood, W. D. (eds.) (1968) *Diagnosis and Treatment of Deposited Radionuclides*, Excerpta Medica Foundation, Amsterdam.

Kroll, H., Korman, S., Siegel, E., Hart, H. E., Rosoff, B., Spencer, H., and Laszlo, D. (1957) *Nature (Lond.)* **180**, 919–20.

Kyker, G. R. (1962) Rare earths, in *Mineral Metabolism*, vol. 2, Part B (eds. C. L. Comar and F. Bronner), Academic Press. New York, pp. 499–541.

Lanz, H., Scott, K. G., Crowley, J., and Hamilton, J. G. (1946) *The Metabolism of Thorium, Protactinium, and Neptunium in the Rat*, USAEC MDDC-648 (CH-3606).

Leboeuf, R. C., Tolson, D., and Heinecke, J. W. (1995) *J. Lab. Clin. Med.*, **126**, 128–36.

Leggett, R. W. (1985) *Health Phys.*, **49**, 1115–37.

Leggett, R. W. (1989) *Health Phys.*, **57**, 365–83.

Leggett, R. W. (1992a) *Health Phys.*, **62**, 288–310.

Leggett, R. W. (1992b) *Radiat. Protect. Dosim.*, **41**, 183–98.

Lehmann, M., Culig, H., and Taylor, D. M. (1983) *Int. J. Radiat. Biol.*, **44**, 65–74.

Lemire, R. J., Fuger, J., Nitsche, H., Potter, P., Rand, M. H., Rydberg, J., Spahiu, K., Sullivan, J. C., Ullman, W. J., Vitorge, P., and Wanner, H. (2001) *Chemical Thermodynamics of Neptunium and Plutonium*, Elsevier, Amsterdam.

Lipsztein, J. L. (1981) *An Improved Model for Uranium Metabolism in the Primate*, New York University.

Lloyd, E. and Marshall, J. H. (1972) Toxicity of $^{239}$Pu relative to $^{226}$Ra in man and dog, in *Radiobiology of Plutonium* (eds. B. J. Stover and W. S. S. Jee), The J. W. Press, University of Utah, pp. 377–84.

Lloyd, R. D., Mays, C. W., Taylor, G. N., and Atherton, D. R. (1970) *Health Phys.*, **18**, 149–56.

Lloyd, R. D., Mays, C. W., Taylor, G. N., and Williams, J. L. (1972a) *Health Phys.*, **22**, 667–73.

Lloyd, R. D., Jee, W. S. S., Ratherton, D., Taylor, G. N., and Mays, C. W. (1972b) Americium–241 in beagles: biological effects and skeletal distribution, in *Radiobiology of Plutonium* (eds. B. J. Stover and W. S. S. Jee), The J. W. Press, University of Utah, pp. 141–8.

Lloyd, R. D., Atherton, D. R., Mays, C. W., McFarland, S. S., and Williams, J. L. (1974) *Health Phys.*, **27**, 61–7.

Lloyd, R. D., Dockum, J. G., Atherton, D. R., Mays, C. W., and Williams, J. L. (1975) *Health Phys.*, **28**, 585–9.

Lloyd, R. D., Mays, C. W., McFarland, S. S., Atherton, D. R., and Williams, J. L. (1976) *Radiat Res.*, **65**, 462–73.

Lloyd, R. D., Jones, C. W., Mays, C. W., Atherton, D. R., Bruenger, F. W., and Taylor, G. N. (1984a) *Radiat. Res.*, **98**, 614–28.

Lloyd, R. D., Mays, C. W., Jones, C. W., Atherton, D. R., Bruenger, F. W., Shabestari, L. R., and Wrenn, M. E. (1984b) *Radiat. Res.*, **100**, 564–75.

Lloyd, R. D., Bruenger, F. W., Mays, C. W., Atherton, D. R., Jones, C. W., Taylor, G. N., Stevens, W., Durbin, P. W., Jeung, N., Jones, E. S., Kappel, M. S., Raymond, K. N., and Weitl F. L. (1984c) *Radiat. Res.*, **99**, 106–28.

Lloyd, R. D., Taylor, G. N., Angus, W., Bruenger, F. W., and Miller, S. C. (1993) *Health Phys.*, **64**, 45–51.

Lloyd, R. D., Miller, S. C., Taylor, G. N., Bruenger, F. W., Jee, W. S. S., and Angus, W. (1994) *Health Phys.*, **67**, 346–53.

Lo Sasso, T., Cohen, N., and Wrenn, M. E. (1981) *Radiat. Res.*, **85**, 173–83.

Loeb, W. F. and Quimby, F. W. (1999) *The Clinical Chemistry of Laboratory Animals*, Taylor and Francis, Philadelphia, PA.

Luckey, T. D. and Venugopal, B. (1977) *Metal Toxicity in Mammals*, vol. 1. *Physiologic and Chemical Basis for Metal Toxicity*, Plenum Press, New York.

Luk, C. K. (1971) *Biochemistry*, **10**, 2838–43.

Mahlum, D. D. and Clarke, W. J. (1966) *Health Phys.*, **12**, 7–13.

Martell, A. E. and Smith, R. M. (1977) *Critical Stability Constants*, vol. 3. *The Organic Ligands*, Plenum Press, New York.

Maynard, E. A. and Hodge, H. C. (1949) Studies of toxicity of various uranium compounds when fed to experimental animals, in *Pharmacology and Toxicology of Uranium Compounds*, vol. 1 (eds. C. Voegtlin and H. C. Hodge), McGraw-Hill, New York, pp. 309–76.

Mays, C. W., Jee, W. S. S., Lloyd, R. D., Stover, B. J., Dougherty, J. H., and Taylor, G. N. (eds.) (1969) *Delayed Effects of Bone-seeking Radionuclides*, The University of Utah Press, Salt Lake City.

McKay, L. R. (1972) *Health Phys.*, **22**, 633–40.

Métivier, H., Kaul, A., Menzel, H.-G., and Stather, J. W. (eds.) (1998) *Radiat. Protect. Dosim.*, **79**, 1–4.

Mewhinney, J. A., Brooks, A. L., and McClellan, R. O. (1972) *Health Phys.*, **22**, 695–700.

Miller, S. C., Bowman, B. M., and Rowland, H. G. (1980) Comparison of the autoradiographic localization of plutonium in the testes of rats and dogs, in *Research in Radiobiology*, University of Utah School of Medicine Report COO-119-264, pp. 91–101.

Miller, S. C., Smith, J. M., Rowland, H. G., Bowman, B. M., and Jee, W. S. S. (1982) The relationship of bone marrow microvasculature with plutonium incorporation into bone, in *Research in Radiobiology*, University of Utah School of Medicine Report COO-119-257, pp. 63–71.

Miller, S. C., Bruenger, F. W., Kuswik- Rabiega, G., Liu, G., and Lloyd, R. D. (1993) *J. Pharmacol. Exp. Ther.*, **267**, 548–54.

Moore, R. C., Holt, K., Zhao, H. T., Hasan, A., Awwad, N., Gasser, M., and Sanchez, C. (2003) *Radiochim. Acta*, **91**, 721–7.

Morin, M., Nenot, J. C., and Lafuma, J. (1973) *Health Phys.*, **24**, 311–15.

Moskalev, Y. I. (1972) *Health Phys.*, **22**, 723–9.

Moskalev, Y. I., Buldakov, L. A., Zhuravelova, A. K., Zalikin, G. A., Karpova, V. M., Kreslov, V. V., Levdik, T. I., Lemberg, V. K., Lyubchanskiy, E. R., Miushkacheva, G. S., Sevast'yanova, Yl. P., and Khalturin, G. V. (1979) *Toxicology and Radiobiology of Neptunium–237*, Atomizdat Publishers, Moscow (Eng. trans. ORNL-tr–4936).

Moskvin, A. I. (1971) *Radiokhimiya*, **13**, 230–8 (Engl. trans.).

Muntz, J. A. and Guzman-Barron, E. S. (1947) *Combination of Plutonium with Plasma Proteins*, USAEC MDDC-1268, pp. 1–23.

Muntz, J. A. and Guzman- Barron, E. S. (1951) The transport of uranium in the tissues, in *Toxicology of Uranium* (ed. A. Tannenbaum), McGraw-Hill, New York, pp. 182–98.

NBS Handbook 52. (1953) *Maximum Permissible Amounts of Radioisotopes in the Human Body and Maximum Permissible Concentrations in Air and Water*. U.S. Government Printing Office.

NCRP. (1980) *Management of Persons Accidentally Contaminated with Radionuclides*, NCRP Report No. 65. National Council on Radiation Protection and Measurements, Bethesda, MD.

NCRP. (1988) *Neptunium: Radiation Protection Guidelines*, NCRP Pub. 90. National Council on Radiation Protection, Bethesda, MD.

NCRP. (2001) *Liver Cancer Risk from Internally-deposited Radionuclides*, NCRP Report No. 135. National Council on Radiation Protection and Measurements, Bethesda, MD.

Nenot, J. C. and Stather, J. W. (1979) *The Toxicity of Plutonium, Americium, and Curium*, Pergamon Press, New York.

Neuman, W. F. (1949) The distribution and excretion of uranium, in *Pharmacology and Toxicology of Uranium Compounds*, vol. 2 (eds. C. Voegtlin and H. C. Hodge), McGraw-Hill, New York, pp. 701–28.

Neuman, W. F. (1953) Deposition of uranium in bone, in *Pharmacology and Toxicology of Uranium Compounds*, vol. 4 (eds. C. Voegtlin and H. C. Hodge), McGraw-Hill, New York, pp. 1911–91.

Neuman, W. F. and Neuman, M. W. (1958) *The Chemical Dynamics of Bone Mineral*, University of Chicago Press, Chicago.

Painter, E., Russell, E., Prosser, C. L., Swift, M. N., Kisieleski, W., and Sacher, G. (1946) *Clinical Physiology of Dogs Injected with Plutonium*, AECD-2042.

Paquet, F., Verry, M., Grillon, G., Landesman, C., Masse, R., and Taylor, D. M. (1995) *Radiat Res.*, **143**, 214–18.

Paquet, F., Ramounet, B., Metivier, H., and Taylor, D. M. (1996) *Radiat. Res.*, **146**, 306–12.

Paquet, F., Metivier, H., Poncy, J. L., Burgada, R., and Bailly, T. (1997) *Int. J. Radiat. Biol.*, **71**, 613–21.

Paquet, F., Ramounet, B., Metivier, H., and Taylor, D. M. (1998) *J. Alloys Compds.*, **271–273**, 85–8.

Paquet, F., Montegue, B., Ansoborlo, E., Henge- Napoli, M. H., Houpert, P., Durbin, P. W., and Raymond, K. N. (2000) *Int. J. Radiat. Biol.* **76**, 113–17.

Passow, H., Rothstein, A., and Clarkson, T. W. (1961) *Pharmacol. Rev.*, **13**, 185–224.

Pearse, A. G. E. (1961) *Histochemistry, Theoretical and Applied.* Little, Brown, Boston, MA.

Pecher, C. (1942) *Univ. Calif. Pub. Pharmacol.*, **2**, 117–39.

Pecoraro, V. L., Harris, W. R., Carrano, C. J., and Raymond, K. N. (1981) *Biochemistry*, **20**, 7033–9.

Peter, E. and Lehmann, M. (1981) *Int. J. Radiat. Biol.*, **40**, 445–50.

Planas-Bohne, F. and Duffield, J. (1988) *Int. J. Radiat. Biol.*, **53**, 489–500.

Planas-Bohne, F. and Rau, W. (1990) *Hum. Exp. Toxicol.*, **9**, 17–24.

Planas-Bohne, F., Jung, W., and Neu-Muller, M. (1985) *Int. J. Radiat. Biol.*, **48**, 797–805.

Planas-Bohne, F., Kampmann, G., and Olinger, H. (1989) *Sci. Total Environ.*, **83**, 263–71.

Polig, E., Smith, J. M., and Jee, W. S. (1984) *Int. J. Radiat. Biol.*, **46**, 143–60.

Popplewell, D. S. and Boocock, G. (1968) Distribution of some actinides in blood serum proteins, in *Diagnosis and Treatment of Deposited Radionuclides* (eds. H. A. Kornberg and W. D. Norwood), Excerpta Medica Foundation. Richland, WA, pp. 45–55.

Popplewell, D. S., Stradling, G. N., and Ham, G. J. (1975) *Radiat. Res.*, **62**, 513–19.

Priest, N. D. and Giannola, S. J. (1980) *Int. J. Radiat. Biol.*, **37**, 281–98.

Priest, N. D., Howells, G. R., Green, D., and Haines, J. W. (1982) *Hum. Toxicol.*, **1**, 97–114.

Priest, N. D., Howells, G., Green, D., and Haines, J. W. (1983) *Hum. Toxicol.*, **2**, 101–20.

Ralston, L. G., Cohen, N., Bhattacharyya, M. H., Larsen, R. P., Ayres, L., Oldham, R. D., and Moretti, E. S. (1986) The metabolism and gastrointestinal absorption of neptunium and protactinium *n* adult baboons, in *Speciation of Fission and Activation Products in the Environment* (eds. R. A. Bulman and J. R. Cooper), Elsevier Applied Science, Oxford, p. 191.

Ramounet, B., Matton, S., Grillon, G., and Fritsch, P. (1998) *J. Alloys Compds.*, **271–273**, 103–5.

Raymond, K. N. and Smith, W. L. (1981) *Struct. Bond.*, **43**, 159–86.

Raymond, K. N., Harris, W. R., Carrano, C. J., and Weitl, F. L. (1980) The synthesis, thermodynamic behavior, and biological properties of metal-ion-specific sequestering agents for man and the actinides, in *Inorganic Chemistry in Biology*, (ed. A. E. Martell), ACS Symposium Series No. 140, pp. 313–32.

Rehfield, C. E., Blomquist, J. A., and Taylor, G. N. (1972) The beagles, in *Radiobiology of Plutonium* (eds. B. J. Stover and W. S. S. Jee), The J. W. Press, The University of Utah, pp. 47–58.

Robinson, B., Heid, K. R., Aldridge, T. L., and Glenn, R. D. (1983) *Health Phys.*, **45**, 911–22.

Rodgers, S. J. and Raymond, K. N. (1983) *J. Med. Chem.*, **26**, 439–42.

Rosenthal, M. W. (ed.) (1956) Therapy of radioelement poisoning, ANL-5584, Argonne National Laboratory.

Rosenthal, M. W. and Schubert, J. (1957) *Radiat. Res.*, **6**, 349–54.

Rothstein, A. (1961) *The Cell Membrane as the Site of Action of Heavy Metals*, University of Rochester, Atomic Energy Project, UR-549, pp. 2–36.

Rowland, R. E. and Farnham, J. E. (1969) *Health Phys.*, **17**, 139–44.

Scarrow, R. C., Riley, P. E., Abu–Dari, K., White, D., and Raymond, K. N. (1985) *Inorg. Chem.*, **24**, 954–67.

Schubert, J. (1955) *Ann. Rev. Nucl. Sci.*, **5**, 369–412.

Schubert, J., Finkel, M. P., White, M. R., and Hirsch, G. M. (1950) *J. Biol. Chem.*, **182**, 635–42.

Schuler, F. and Taylor, D. M. (1987) *Radiat. Res.*, **110**, 362–71.

Schuler, F., Csovcsics, C., and Taylor, D. M. (1987) *Int. J. Radiat. Biol*., **52**, 883–92.

Schuppler, U., Planas-Bohne, F., and Taylor, D. M. (1988) *Int. J. Radiat. Biol*. **53**, 457–66.

Schwartz, J. L. and Fien, M. (1973) Amino acids and proteins. The molecular framework and machinery of living systems, in *Best and Taylor's Physiologic Basis of Medical Practice*, 9th edn (ed. J. R. Brobeck), pp. 1-114–1-141.

Scott, K. G., Overstreet, R., Jacobson, L., Hamilton, J. G., Fisher, H., Crowley, J., Chaikoff, I. L., Entenman, C., Fishler, M., Barber, A. J., and Loomis, F. (1947a) *The Metabolism of Carrier-Free Fission Products in the Rat*, USAEC MDDC-1275.

Scott, K. G., Axelrod, D., Crowley, J., Lenz, H. C., Jr. and Hamilton, J. G. (1947b) *Studies on the Inhalation of Fissionable Materials and Fission Products and Their Subsequent Fate in Rats and Man*, USAEC MDDC-1276.

Scott, K. G., Copp, D. H., Axelrod, D. J., and Hamilton, J. G. (1948a) *J. Biol. Chem.*, **175**, 691–703.

Scott, K. G., Axelrod, D. J., Fisher, H., Crowley, J. F., and Hamilton, J. G. (1948b) *J. Biol. Chem.*, **176**, 283–93.

Scott, K. G., Axelrod, D., Crowley, J., and Hamilton, J. G. (1949a) *Arch. Pathol.*, **48**, 31–54.

Scott, K. G., Axelrod, D. J., and Hamilton, J. G. (1949b) *J. Biol. Chem.*, **177**, 325–35.

Seidel, A., Wiener, M., Kruger, E., Wirth, R., and Haffner, H. (1986) *Int. J. Rad. Appl. Instrum. B*, **13**, 515–18.

Seven, M. J. and Johnson, L. A. (eds.) (1959) *Metal Binding in Medicine*, J. B. Lippincott, Philadelphia, PA.

Shannon, R. D. (1976) *Acta Crystallog.*, **A32**, 751–67.

Sillen, L. G. and Martell, A. E. (1964) *Stability Constants of Metal-ion Complexes*, The Chemical Society, London, Special Publ. 17.

Sillen, L. G. and Martell, A. E. (1971) *Stability Constants of Metal-ion Complexes*, The Chemical Society, London, Suppl. 1. Special Publ. 25.

Simpson, M. E., Asling, C. W., and Evans, H. M. (1950) *Yale J. Biol. Med.*, **23**, 1–27.

Singer, T. P., Muntz, J. A., Meyer, J., Gasvoda, B., and Guzman-Barron, E. S. (1951) The reversible inhibition of enzymes by uranium, in *Toxicology of Uranium* (ed. A. Tannenbaum), McGraw-Hill, New York, pp. 208–45.

Smith, H. W. (1951) *The Kidney: Structure and Function in Health and Disease*, Oxford University Press, New York.

Smith, V. H. (1958) *Nature*, 1792–3.

Smith, V. H. (1972a) The biological disposition of $Es(NO_3)_3$ in rats after intravenous, intramuscular, subcutaneous, and transcutaneous administration, in *Pacific Northwest Laboratory Annual Report for 1971*, BNWL-1650 PT1, pp. 279–83.

Smith, V. H. (1972b) *Health Phys.*, **22**, 765–78.

Smith, R. M. and Martell, A. E. (1976) *Critical Stability Constants*, vol. 4. Inorganic Complexes, Plenum Press, New York.

Smith, R. M. and Martell, A. E. (1989) *Critical Stability Constants*, vol. 6. Second Supplement, Plenum Press, New York.

Sontag, W. (1993) *Int. J. Radiat. Biol.*, **63**, 383–93.

Spiers, F. W. (1968) *Radioisotopes in the Human Body: Physical and Biological Aspects.* Academic Press, New York.

Stannard, J. N. (1988) *Radioactivity and Health. A History*, Pacific Northwest Laboratory, Batelle Memorial Institute, Richland, WA.

Stather, J. W. and Karaoglou, A. (eds.) (1994). *Radiat. Protect. Dosim.*, **53**, 1–4.

Stather, J. W., Bailey, M. R., Harrison, J. D., Menze, H.-G., and Métivier, H., eds. (2003) Internal Dosimetry of Radionuclides: Occupational, Public and Medical Exposure. Radiat. Prot. Dosim. 105, Nos. 1–4, 1–662.

Stevens, W. and Bruenger, F. W. (1972) *Health Phys.*, **22**, 679–83.
Stevens, W., Bruenger, F. W., and Stover, B. J. (1965) *Radiat. Res.*, **26**, 114–23.
Stevens, W., Bruenger, F. W., and Stover, B. J. (1968) *Radiat. Res.*, **33**, 490–500.
Stevens, W., Stover, B. J., Bruenger, F. W., and Taylor, G. N. (1969) *Radiat. Res.*, **39**, 201–6.
Stevens, W., Stover, B. J., Atherton, D. R., and Bruenger, F. W. (1975) *Health Phys.*, **28**, 387–94.
Stevens, W., Bruenger, F. W., Atherton, D. R., Smith, J. M., and Taylor, G. N. (1980) *Radiat. Res.*, **83**, 109–26.
Stokinger, H. E., Rothstein, A., Roberts, E., Spiegl, C. J., Dygert, H. P., La Bille, C. W., and Sprague, J., G. F. (1949) Toxicity following inhalation, in *Pharmacology and Toxicology of Uranium Compounds*, vols 1 & 2 (eds. C. Voegtlin and H. C. Hodge), McGraw-Hill, New York, pp. 423–700.
Stone, R. S. (1951) *Industrial Medicine on the Plutonium Project*, McGraw-Hill, New York.
Stover, B. J. and Atherton, D. R. (1974) *Radiat. Res.*, **60**, 525–35.
Stover, B. J. and Jee, W. S. S. (eds.) (1972) *Radiobiology of Plutonium*, The J. W. Press, University of Utah.
Stover, B. J. and Stover, J. C. N. (1972) The laboratory for radiobiology at the University of Utah, in *Radiobiology of Plutonium* (eds. B. J. Stover and W. S. S. Jee), The J. W. Press, University of Utah, pp. 29–46.
Stover, B. J., Atherton, D. R., and Keller, N. (1959) *Radiat. Res.*, **10**, 130–47.
Stover, B. J., Atherton, D. R., Keller, N., and Buster, D. S. (1960) *Radiat. Res.*, **12**, 657–71.
Stover, B. J., Atherton, D. R., Bruenger, F. W., and Buster, D. S. (1962) *Health Phys.*, **8**, 589–97.
Stover, B. J., Bruenger, F. W., and Stevens, W. (1968a) *Radiat. Res.*, **33**, 381–94.
Stover, B. J., Atherton, D. R., Bruenger, F. W., and Buster, D. S. (1968b) *Health Phys.*, **14**, 193–7.
Stover, B. J., Bruenger, F. W., and Stevens, W. (1970) *Radiat. Res.*, **43**, 173–86.
Stover, B. J., Atherton, D. R., and Buster, D. S. (1971) *Health Phys.*, **20**, 369–74.
Stover, B. J., Atherton, D. R., and Buster, D. S. (1972) Retention of $^{239}$Pu(IV) in the beagle, in *Radiobiology of Plutonium* (eds. B. J. Stover and W. S. S. Jee), The J. W. Press, University of Utah, Salt Lake City, p. 149.
Stradling, G. N., Popplewell, D. S., and Ham, G. J. (1976) *Health Phys.*, **31**, 517–19.
Stradling, G. N., Stather, J. W., Ellender, M., Sumner, S. A., Moody, J. C., Towndrow, C. G., Hodgson, A., Sedgwick, D., and Cooke, N. (1985a) *Hum. Toxicol.*, **4**, 563–72.
Stradling, G. N., Stather, J. W., Strong, J. C., Sumner, S. A., Towndrow, C. G., Moody, J. C., Lennox, A., Sedgwick, D., and Cooke, N. (1985b) *Hum. Toxicol.*, **4**, 159–68.
Stradling, G. N., Stather, J. W., Gray, S. A., Moody, J. C., Ellender, M., and Hodgson, A. (1986) *Hum. Toxicol.*, **5**, 77–84.
Stradling, G. N., Stather, J. W., Gray, S. A., Moody, J. C., Ellender, M., Hodgson, A., Sedgwick, D., and Cooke, N. (1987) *Hum. Toxicol.*, **6**, 385–93.
Stradling, G. N., Stather, J. W., Gray, S. A., Moody, J. C., Hodgson, A., Sedgwick, D., and Cooke, N. (1988) *Hum. Toxicol.*, **7**, 133–9.
Stradling, G. N., Stather, J. W., Gray, S. A., Moody, J. C., Ellender, M., Hodgson, A., Volf, V., Taylor, D. M., Wirth, P., and Gaskin, P. W. (1989) *Int. J. Radiat. Biol.*, **56**, 503–14.

Stradling, G. N., Gray, S. A., Moody, J. C., Hodgson, A., Raymond, K. N., Durbin, P. W., Rodgers, S. J., White, D. L., and Turowski, P. N. (1991) *Int. J. Radiat. Biol.*, **59**, 1269–77.

Stradling, G. N., Gray, S. A., Ellender, M., Moody, J. C., Hodgson, A., Pearce, M., Wilson, I., Burgada, R., Bailly, T., Leroux, Y. G., El Manouni, Raymond, K. N., and Durbin, P. N. (1992) *Int. J. Radiat. Biol.*, **62**, 487–97.

Stradling, G. N., Gray, S. A., Moody, J. C., Pearce, M. J., Wilson, I., Burgada, R., Bailly, T., Leroux, Y., Raymond, K. N., and Durbin, P. W. (1993) *Int. J. Radiat. Biol.*, **64**, 133–40.

Stradling, G. N., Gray, S. A., Pearce, M. J., Wilson, I., Moody, J. C., Burgada, R., Durbin, P. W., and Raymond, K. N. (1995a) *Hum. Exper. Toxicol.*, **14**, 165–9.

Stradling, G. N., Gray, S. A., Pearce, M. J., Wilson, I., Moody, J. C., Hodgson, A., and Raymond, K. N. (1995b) *Efficacy of TREN-(Me-3,2-HOPO), 5-LI-(Me-3,2-HOPO) and DTPA for Removing Plutonium and Americium from the Rat after Inhalation and Wound Contamination as Nitrates: Comparison with 3,4,3-LI(1,2-HOPO) NRPB-M534.* National Radiological Protection Board, Chilton, Didcot.

Stradling, G. N., Henge-Napoli, M. H., Paquet, F., Poncy, J. L., Fritsch, P., and Taylor, D. M. (2000a) *Radiat. Protect. Dosim.*, **87**, 19–27.

Stradling, G. N., Henge-Napoli, M. H., Paquet, F., Poncy, J. L., Fritsch, P., and Taylor, D. M. (2000b) *Radiat. Protect. Dosim.*, **87**, 29–40.

Sutterlin, U., Thies, W. G., Haffner, H., and Seidel, A. (1984) *Radiat. Res.*, **98**, 293–306.

Talbot, R. J., Knight, D. A., and Morgan, A. (1990) *Health Phys.*, **59**, 183–7.

Talbot, R. J., Newton, D., and Warner, A. J. (1993) *Health Phys.*, **65**, 41–6.

Tannenbaum, A. (1951a) Reversible inhibition of enzymes by uranium, in *Toxicology of Uranium* (ed. A. Tannenbaum), McGraw-Hill, New York, pp. 236–44.

Tannenbaum, A. (ed.) (1951b) *Toxicology of Uranium*, McGraw-Hill, New York.

Taylor, D. M. (1962) *Health Phys.*, **8**, 673–7.

Taylor, D. M. (1967) *Health Phys.*, **13**, 135–40.

Taylor, D. M. (1969) *Br. J. Radiol.*, **42**, 44–50.

Taylor, D. M. (1970) *Health Phys.*, **19**, 411–18.

Taylor, D. M. (1972) *Health Phys.*, **22**, 575–81.

Taylor, D. M. (1973a) Chemical and physical properties of plutonium, in *Uranium, Plutonium, Transplutonic Elements* (eds. H. C. Hodge, J. N. Stannard, and J. B. Hursh), Springer-Verlag, New York, pp. 323–48.

Taylor, D. M. (1973b) Chemical and physical properties of the transplutonium elements, in *Uranium, Plutonium, Transplutonic Elements* (eds. H. C. Hodge, J. N. Stannard, and J. B. Hursh), Springer-Verlag, New York, pp. 717–38.

Taylor, D. M. (1991) Acceleration of the natural rate of elimination of transuranium elements from the mammalian body, in *Handbook on the Physics and Chemistry of the Actinides*, (eds. A. J. Freeman and C. Keller), vol. 6 , North-Holland, Amsterdam, pp. 533–49.

Taylor, D. M. (1998) *J. Alloys Compds.*, **271–273**, 6–10.

Taylor, D. M. and Bensted, J. P. M. (1969) Long-term biological damage from plutonium-239 and americium-241 in rats, in *Delayed Effects of Bone-seeking Radionuclides* (ed. C. W. Mays), The University of Utah Press, Salt Lake City, pp. 357–70.

Taylor, D. M. and Farrow, L. C. (1987) *Int. J. Rad. Appl. Instrum. B*, **14**, 27–31.

Taylor, D. M., Sowby, F. D., and Kember, N. F. (1961) *Phys. Med. Biol.*, **6**, 73–86.

Taylor, G. N., Jee, W. S., Dockum, N., and Hromyk, E. (1969a) *Health Phys.*, **17**, 723–5.

Taylor, G. N., Jee, W. S. S., Williams, J. L., Burggraft, B., and Angus, W. (1969b) Microscopic distribution of $^{241}$Am in the beagle, in *Research in Radiobiology. University of Utah School of Medicine Annual Report COO-119-240*, pp. 97–118.

Taylor, G. N., Jee, W. S., Mays, C. W., Dell, R. B., Williams, J. L., and Shabestari, L. (1972a) *Health Phys.*, **22**, 691–3.

Taylor, G. N., Jee, W. S. S., Williams, J. L., and Shabestari, L. (1972b) Hepatic changes induced by $^{239}$Pu, in *Radiobiology of Plutonium* (eds. B. J. Stover and W. S. S. Jee), The J. W. Press, University of Utah. Salt Lake City, p. 105.

Thompson, R. C. (ed.) (1962) *Proceedings of the Hanford Symposium on the Biology of the Transuranic Elements, Health Phys.*, 8, 561–780.

Thompson, R. C. (1982) *Radiat. Res.*, **90**, 1–32.

Thompson, R. C. (1989) *Life Span Effects of Ionizing Radiation in the Beagle Dog.* USDOE, Pacific Northwest Laboratory, Richland, WA.

Thompson, R. C., Bair, W. J. (eds.) (1972) *Proceedings of the Hanford Symposium on the Biological Implications of the Transuranium Elements, Health Phys.*, 22, 6.

Thomson, B. M., Smith, C. L., Busch, R. D., Siegel, M. D., and Baldwin, C. (2003) *J. Environ. Eng.-ASCE*, **129**, 492–9.

Turner, G. A. and Taylor, D. M. (1968a) *Phys. Med. Biol.*, **13**, 535–46.

Turner, G. A. and Taylor, D. M. (1968b) *Radiat. Res.*, **36**, 22–30.

Van Middlesworth, L. (1947) *Study of Plutonium Metabolism in Bone MDDC-1022*. USAEC Oak Ridge, TN.

Van Rossum, J. P. and Schamhart, D. H. (1991) *Exp. Gerontol.*, **26**, 37–43.

Van Wagenen, G. and Asling, C. W. (1958) *Am. J. Anat.*, **103**, 163–186.

Vaughan, J., Bleaney, B., and Taylor, D. M. (1973) Distribution, excretion and effects of plutonium as bone-seekers, in *Uranium, Plutonium, Transplutonic Elements* (eds. H. C. Hodge, J. N. Stannard, and J. B. Hursh), Springer-Verlag, New York, pp. 349–502.

Veeck, A. C., White, D. J., Whisenhunt, D. W., Xu, J. D., Gorden, A. E. V., Romanovski, V., Hoffman, D. C., and Raymond, K. N. (2004) *Solv. Extract. Ion Exchange*, **22**, 1037–68.

Voegtlin, C. and Hodge, H. C. (eds.) (1949) *Pharmacology and Toxicology of Uranium Compounds*, vols 1 and 2, , McGraw-Hill, New York.

Voegtlin, C. and Hodge, H. C. (eds.) (1953) *Pharmacology and Toxicology of Uranium Compounds*, vols 3 and 4, , McGraw-Hill, New York.

Volf, V. (1975) *Health Phys.*, **29**, 61–8.

Volf, V. (1978) Treatment of incorporated transuranium elements, *IAEA Technical Report 184*.

Volf, V. (1986) *Int. J. Radiat. Biol.*, **49**, 449–62.

Volf, V. and Wirth, R. (1986) *Int. J. Radiat. Biol.*, **50**, 955–9.

Volf, V., Taylor, D. M., Brandau, W., and Schlenker, P. (1986) *Int. J. Radiat. Biol.*, **50**, 205–11.

Volf, V., Burgada, R., Raymond, K. N., and Durbin, P. W. (1993) *Int. J. Radiat. Biol.*, **63**, 785–93.

Volf, V., Burgada, R., Raymond, K. N., and Durbin, P. W. (1996a) *Int. J. Radiat. Biol.*, **70**, 765–72.

Volf, V., Burgada, R., Raymond, K. N., and Durbin, P. W. (1996b) *Int. J. Radiat. Biol.*, **70**, 109–14.
White, D. L., Durbin, P. W., Jeung, N., and Raymond, K. N. (1988) *J. Med. Chem.*, **31**, 11–18.
Williamson, M. and Vaughan, J. (1964) A preliminary report on the sites of deposition of Y, Am, and Pu in cortical bone and in the region of the epiphyeal cartiledge plate, in *Bone and Tooth* (ed. H. J. J. Blackwood), Pergamon Press, London.
Wills, J. H. (1949) Characteristics of uranium poisoning, in *Pharmacology and Toxicology of Uranium Compounds*, vol. 1 (eds. C. Voegtlin and H. C. Hodge), McGraw-Hill, New York, pp. 237–280.
Winter, R. and Seidel, A. (1982) *Radiat. Res.*, **89**, 113–23.
Wirth, R. and Volf, V. (1984) *Int. J. Radiat. Biol.*, **46**, 787–92.
Wirth, R., Taylor, D. M., and Duffield, J. (1985) *Int. J. Nucl. Med. Biol.*, **12**, 327–30.
Wong, N. L., Reitzik, M., and Quamme, G. A. (1986) *Renal Physiol.*, **9**, 29–37.
Wood, R., Sharp, C., Gourmelon, P., Le Guen, B., Stradling, G. N., Taylor, D. M., and Hengé-Napoli, M.-H. (2000) *Radiat. Protect. Dosim.*, **87**, 51–6.
Wrenn, M. E. (ed.) (1975) *Conference on Occupational Health Experience with Uranium*, ERDA Report 93.
Wrenn, M. E. (ed.) (1981) *Actinides in Man and Animals*, RD Press, University of Utah, Salt Lake City.
Wrenn, M. E., Durbin, P. W., Howard, B., Lipsztein, J., Rundo, J., Still, E. T., and Willis, D. L. (1985) *Health Phys.*, **48**, 601–33.
Wronski, T. J., Smith, J. M., and Jee, W. S. (1980) *Radiat. Res.*, **83**, 74–89.
Xu, J. D. and Raymond, K. N. (1999) *Inorg. Chem.*, **38**, 308–15.
Xu, J., Kullgren, B., Durbin, P. W., and Raymond, K. N. (1995) *J. Med. Chem.*, **38**, 2606–14.
Xu, J., Radkov, E., Ziegler, M., and Raymond, K. N. (2000) *Inorg. Chem.*, **39**, 4156–64.
Xu, J., Durbin, P. W., and Raymond, K. N. (2001) Actinide sequestering agents: design, structural, and biological evaluations, in *Nuclear Science – Evaluation of Speciation Technology – Workshop Proceedings Tokai-mura*, Ibaraki, Japan, 26-28 October 1999, OECD, pp. 247–54.
Xu, J., Durbin, P. W., Kullgren, B., Ebbe, S. N., Uhlir, L. C., and Raymond, K. N. (2002) *J. Med. Chem.*, **45**, 3963–71.
Xu, J. D., Whisenhunt, D. W., Veeck, A. C., Uhlir, L. C., and Raymond, K. N. (2003) *Inorg. Chem.*, **42**, 2665–74.
Youmans, W. B. and Siebens, A. A. (1973) 'Respiration' in Best and Taylor's Physiological Basis of Medical Practice, 9$^{th}$ edition, (Brobeck, J. R., ed.), pp. 6–1 to 6–90, The Williams and Wilkins Co., Baltimore.
Yuile, C. L. (1973) Animal experiments, in *Uranium, Plutonium, Transplutonic Elements* (eds. H. C. Hodge, J. N. Stannard, and J. B. Hursh), Springer-Verlag, New York, pp. 165–96.
Zak, O. and Aisen, P. (1988) *Biochemistry*, **27**, 1075–80.
Zhu, D.-H., Kappel, M. J., and Raymond, K. N. (1988) *Inorg. Chim. Acta*, **147**, 115–21.
Zirkle, R. E. (1947) *Radiology*, **49**, pp. 269–365.